2nd Stage Report of the Project

Methodology Development for Modelling the
Propagation of Pollutant Plume & Estimation of Futuristic Impact on
Coastal Ecology using Remote Sensing & GIS
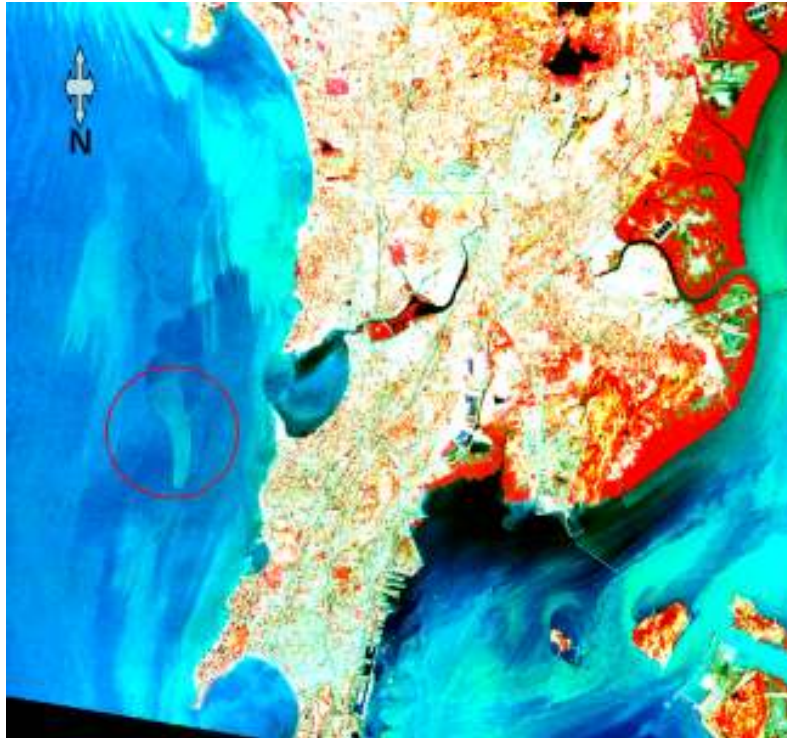
Submitted to

MMR Environment Improvement Society (MMR-EIS) of the

Mumbai Metropolitan Region Development Authority (MMRDA)

By

Centre of Studies in Resources Engineering

IIT Bombay

June, 2011

Team:

Prof. A. B. Inamdar
Mohor Bhattacharya
Yogesh Agarwadkar
Samee Azmi
Mugdha Apte

Acknowledgments

Besides the tireless efforts of the project team which has slogged it out for achieving various goals of this project, this scientific pursuit wouldn't have attained its present day form without selfless cooperation and help from individuals from several organizations that include MPCB, NIO, MCGM, DOD, ICMAM-PD, Indian Coast Guard, BPT, CMFRI, CIFE, Hindustan Construction Ltd., Indian Customs, Ferry Warf officials, Mumbai Police, ..the list goes on!

This report cannot be complete without expressing our gratitude to each and every individual who has directly or indirectly helped in collation of a wide variety of data needed for this project, as well as for those who offered useful suggestions and words of encouragement to us, specially all the officials and experts from the EIS-MMR committee, to go ahead despite several challenges faced during the course of this work.

- **Project Team**

Table of Contents

List of Figures

List of Tables

1 Introduction

The Mumbai Metropolitan Region (MMR) is spread over an area of 438 sq. km and supports a human population exceeding 15 million catering to a host of industries located in the region. Considering Mumbai's importance as the nerve center of country's trade, commerce and industry, the biggest challenge faced by the local authorities is that of providing necessary infrastructural facilities to its people to carry on with their multifarious activities. High population density of the region further makes it extremely difficult to deal with.

Solid and liquid waste disposal for the entire region is one such challenge of the MMR that keeps growing with the ever increasing population of the megacity. As per the recent statistics, every day, the city has to deal with solid waste and sewage to the tune of over 8000 tons and 2700 million litres, respectively. The enormity of the problem is further compounded by lack of space for processing / treating such waste anywhere in the coastal region, as it is either covered by CRZ-1 areas like eco-sensitive wetlands or thickly populated by people, thereby precluding such activities in its vicinity. Despite these constraints, there have been several attempts by the civic body to address the waste disposal problem of the region from various perspectives. As early as 1972, the Municipal Corporation of Greater Bombay (MCGM) (erstwhile Bombay Municipal Corporation) initiated preparation of a Master Plan for water supply and sewage disposal under the Colombo Plan, which was then followed by completion of the Sewage Master Plan in 1979 with a view to collect, convey and dispose off the sewage from Greater Bombay area. This plan was expected to cater to the city needs till 2005. Two later phases of the Integrated Project (Phase 1, 1975-1981 & Phase 2, 1979-1988) helped extend the sewage system to Mumbai suburbs. Taking it further, the Bombay Sewage Disposal Project (BSDP), on the basis of the operational directives of the World Bank and the EIA by NEERI (1993), suggested disposal of the sewage into the Arabian Sea and creeks through marine outfalls after preliminary treatment (Subodh Kumar & Parekh K.P., 1999). Design specifications of the 2 outfalls at Worli and Bandra as originally suggested by NEERI, are provided in the BSDP report (Table 1). The basic rationale behind this suggestion was to use the sea as a natural self purifying receiving water

body and take benefit of the available sunshine and infinite dilution offered by the sea, to achieve a better coastal environment. 2 Marine outfalls at Worli and Bandra, as well as leftover sewage work of Phase 2, were completed by December 2002 as a part of this project.

Table 1 Design Specification of Proposed Outfalls

			Worli Tunnel	Bandra Tunnel
(a)	Length of outfall	km	3.44	3.79
(b)	Diameter	m	3.5	3.5
(c)	Length of diffuser	m	250	250
(d)	Loss coeff at entry to outfall	m	0.5	0.5
(e)	Centerline depth of diffuser to MSL	m	47.48	46.38
(f)	Diffuser bed slope		0	0
(g)	No. of risers		10	10
(h)	Riser head		10 ports per riser	10 ports per riser
(i)	Riser diameter	m	1.0	1.0
(j)	Water depth at Ch 3000 m from sea bed to MSL	m	10.0	8.0
(k)	Roughness k, low flow	m	0.006	0.006
	high flow	m	0.002	0.002
(l)	Loss coeff in riser bend and multiport	m	5.0	5.0
(m)	Effluent density	kg/m³	1002	1002
(n)	Seawater density	kg/m³	1024	1024
(o)	Ambient current, minimum	m/s	0.07	0.21
	average	m/s	0.31	0.40
	maximum	m/s	0.74	0.72
(p)	Discharge (year 2005)	m³/s		
	Peak WWF		24.0	22.0
	Average DWF		16.9	17.4
	Minimum DWF		4.4	4.6
(q)	Discharge (75% of year 2005)	m³/s		
	Peak WWF		18.0	15.3
	Peak DWF		12.67	13.05
	Average DMF		6.6	6.9
	Minimum DWF		3.3	3.45
(r)	Available design head at pumping station		7.12	6.78

* *Metcalf and Eddy Report (1984;*

One of the main objectives of this effort was to improve the health and environmental conditions in coastal environment of Mumbai. As a part of this endeavour, 2 independent submarine tunnel outfalls of length of 3.7 km and 3.5 km With a diameter of 3.5 m and lined with precast cement concrete segments were

built at Bandra and Worli, respectively. The outfalls were constructed on firm rocky bed at 65 m below the mean sea level taking due care of the construction forces, soil load, erosion and possible earthquake impacts.

As per the environmental status studies carried out by NEERI during 1991-92 and 1997-98 condition of the Mumbai coast, beaches and seafronts was considered alarming. The water quality of several locations from these areas was found to be badly impaired in terms of physico-chemical and bacterial attributes as a result of the unhindered outflow of untreated sewage in the sea and leachates from the indiscriminate waste dumping practices followed around coastal areas. Further studies by NEERI on the hydrodynamic and water quality simulation models (Vyas L. and Vyas S., 2007) for the region indicated good chances of improvement of such physico-chemical and bacterial attributes after commissioning of marine outfalls of adequate lengths inside the Arabian Sea. Water quality status at 1 km, 3 km and 5 km from the shoreline was proposed to be assessed before commissioning of the outfalls and was also planned post outfall commission period to determine the outfall efficacy and to decide further options, if necessary. Studies carried out in accordance with this plan showed improvement in some and deterioration in several other water quality parameters. (S. C. Dhage et al, 2006) As per the observations of this exercise 'A comparison of baseline study with post-commissioning study status indicated improvement in DO, deterioration with respect to BOD, ammonical nitrogen and microbial parameters at beaches and seafronts. Coastal Water Quality showed low DO values close to the diffuser region during post-commissioning as compared to pre-commissioning phase. Depletion of DO near diffuser was observed as the tide recedes. Higher BOD values were observed after implementation of outfall at all the sampling locations in the coastal region. Maximum BOD observed at the diffuser was 5–7 mg/l during slack period of tide. Adverse impact of the sewage discharges was noticed at 1, 3 and 5 km distance with respect to ammonical nitrogen concentrations. Microbial water quality at 3 and 5 km had deteriorated due to wastewater discharge from Worli outfall (Annexure 1) and SW II and III standards for microbial parameters were not satisfied. No significant change in the heavy metal, nutrient and detergent concentrations had occurred after the commissioning of the outfall. About 50 to 70 times initial dilution was achieved as per modeling and tracer studies. The far field dilution up to 1 km ranged from 85 to 125 times. The modeling

exercise indicated possibility of fish toxicity due to higher concentration for ammonical nitrogen in the near-shore region.'

Aforementioned study coupled with the physical appearance and frequent foul odour of the Mumbai's coastal waters have raised serious doubts about the accrued environmental / ecological benefits from the recently commissioned outfalls and sufficiently justify the need for monitoring their behaviour.

Recent advancements in remote sensing and GIS technology have substantially widened the scope for supplementing sea truth data with that obtained from satellites. Useful clues are possible to be obtained about offshore advection of the pollutants transported by the marine outfalls with the help of various types of remotely sensed data ranging from visible to radar wavelength rages. Important water quality parameters like Chlorophyll-a, CDOM, TSS, sea surface temperature (SST) are possible to be quantified with reasonable accuracy from the oceanic water surfaces using recent remote sensing techniques and can serve as a powerful tool for efficient pollution monitoring. When used in conjunction with satellite synchronous in-situ observations it has become possible to derive ecological parameters like primary and secondary productivity from satellite borne data. Such repetitive observations can help estimate the changes and help us understand impacts as a result of any man made intervention like marine outfalls in a coastal setting. 3D GIS modelling techniques supported with depth-wise information from conventional as well as remotely sensed data sources, are further useful in tracing this impact to various depths and aid in visualizing the process of pollution dispersion in 3D, which can guide future course of action by decision makers, like never before (Clement-Colon P. and Pitchel W.G, 2006)

The current project was formulated with this background in mind and proposes to develop an effective methodology to model the pollution plumes from the 2 marine out falls from Bandra and Worli and goes on to estimate as well as predict their futuristic impact on an important ecological parameter like primary productivity in Mumbai's coastal waters.

The proposed plan of this project is broken into 3 main stages as follows:

Stage 1: Pre outfall scenario generation

- Base data generation and analysis
- Satellite data
- Mapping of ambient waters near the outfall prior to their installation

Stage 2: Post outfall installation scenario & impact

- Post installation mapping
- Simulation of ambient pollution without outfalls
- Impact on ecosystem (Primary productivity)

Stage 3: Futuristic impact prediction

- Plume propagation analysis
- Future propagation trend estimation
- Pollution impact predication

In addition to the task of studying the behaviour of marine outfalls at Worli and Bandra while evolving a methodology of pollution monitoring, an effort was made simultaneously (on the request of the MPCB) to assess the changes in Vashi and Mahul creek waters using Thermal Infra Red (TIR) data from available remotely sensed platforms, with a view to understand the changes in sea surface temperature due to natural as well as artificial reasons.

2 Study Area

The study area lies on the western coast of India, comprising of the coastal and offshore waters off the coast of Mumbai, roughly falling within the latitude-longitude coordinates: 19° 8' 23" N, 72° 39' 54" E and 18° 48' 26" N, 72° 58' 17"E. The area is predominantly hot and humid. The average annual rainfall is 1917.3 mm. About 94 per cent of the annual rainfall in Greater Mumbai District is received during the south-west monsoon months of June to September. The area is rich in natural resources, being a part of the Western Ghats of India, an area of great biological diversity. It is also very important from environmental point of view as it supports a vast area of mangrove forest besides flora and fauna at certain stretches. The study area has several major creeks and river systems. The Thane creek is a major source of silt in the area and a convenient disposal site for treated as well as untreated effluents.

Figure 1: Study area with field sampling locations shown on a Google Earth image

Apart from this, there are Mahul creek and Ulhas Estuary, which also contribute significantly to the localized turbid patches in the study area. Hence, the area has great variability in terms of water clarity within this small stretch of about 70 km.

3 Materials & Methods

This report presents the advancement in the work regarding field data collection for the calibration and validation of satellite images. The transect for field data collection was determined to cover maximum possible area on the short duration of the trips (10-12hrs) over the almost 40km long stretch while repeating the main sampling locations as shown in Figure 1. Also, several trips were planned to traverse long distances into the clear water patches away from the coast. However, for all the trips, three stations have been repeated without much spatial deviation, i.e., Colaba, Bandra and Worli outfall locations.

3.1 Sea-truth Data Collection

For this study, the most important requirement was sea-truth data (ship board measurement of water quality parameters) to validate the satellite image-derived algorithms. Details of the methodology to be followed for water sample collection and further chemical analysis are given below.

Most of the observations were carried out on-board mechanised fishing vessels. Surface water samples were collected using cleaned polythene buckets. Water from varied depths was collected using a sampler. Ambient water temperature was recorded by a centigrade thermometer.

Analytical methods followed for this project were as per the Standard Methods of the American Public health Association, 1998. The estimated water quality parameters can be classified, sensu lato, into three groups, i.e., physico-chemical parameters (Dissolved Oxygen, pH, and water temperature), biological parameters (photosynthetic pigments and primary productivity) and transparency parameters (SPM and light penetration).

3.1.1 Physico-chemical parameters

Dissolved Oxygen (DO)

Displacement water sampler was used to collect samples for the analysis of dissolved oxygen (DO) by Winkler's method. The value of DO in the sample was calculated with the help of the equation:

$$DO \ (mg/l) = \frac{(\text{Volume of sodium thio–sulphate – reagent blank}) \times 32000 \times \text{Strength of sodium thio–sulphate}}{4 \ (175-2)}$$

Where, a standard D.O. bottle capacity is 175 ml and 1 ml each of Winkler I & II reagent solutions has been used.

3.1.2 Biological parameters

Light harvesting pigments

For pigment analysis, sea water was filtered through a membrane filter of pore size 0.45μm previously soaked with magnesium carbonate suspension. The residue was transferred to a homogenizer containing 90% acetone. The contents were ground thoroughly in shaded light. The sample was kept at low temperature in complete darkness over night for complete extraction. Subsequently the sample was centrifuged at ~4000 rev/min for 10 min. The clear supernatant liquid was decanted and used to measure the absorbance at 750, 665, 645, 630 and 480 nm with the help of a VNIR Spectrophotometer. The detailed methodology is given below.

Spectrophotometric analysis of phytoplankton pigment:

Volume of sample is 1 litre. (2 litres when water has very low phytoplankton population, as determined by prior knowledge).

The samples were poured into clean bottles and stored in boxes packed with ice (Ambient temperature kept around ~4° C) for upto 8 hrs.

Samples were stored in dark at a lower temperature (~0° C) when longer periods of storage was needed.

Samples were filtered as soon as possible after sampling using 47 mm GF/F filter paper. The suction pressure was smaller than 0.5 atm.

A filtration assembly (conical flask of 1 litre volume, Gooch crucible, funnel, pump, tubing, and clamp) was used for filtration.

After filtration the filter papers were flooded with the 90% acetone and were kept for 24 hours in darkness in a fridge.

The tubes were shaken before centrifugation.

The extract was centrifuged (~4000 rev/min, 10 min).

Supernatant liquid was drained into clean test tubes, filled into one cm clean cuvettes for spectrophotometric analysis. The absorption spectra in the range 380-750nm are collected.

The equation used to estimate Chlorophyll a (Jeffrey and Humphrey, 1975)

Ca [mg m-3] = (11.85 (D663-665) - 1.54 D647 - 0.08 D630) v / V * 1

D663-665b - absorbance at 663-665nm, after correction by the cell-to-cell blank and subtraction of the cell-to-cell blank corrected absorbance at 750 nm, before acidification.

D663-665a - absorbance at 663-665nm, after correction by the cell-to-cell blank and subtraction of the cell-to-cell blank corrected absorbance at 750nrn, after acidification.

v - Volume of acetone [ml] 1-Cell (cuvette) length [cm]

V - Volume of filtered water [L]

Generation of optical properties

For the generation of optical properties of chlorophyll such as absorption (a) and scattering (b), the sample was analyzed through UV/VIS spectrophotometer using 1 cm cell (cuvette) The Optical Density (OD) was measured in the spectral range 380 to

750 nm with an interval of 1 nm against a cuvette containing 90% acetone as blank (Strickland and Parson, 1972). The OD at 750 nm was subtracted from the entire spectrum and converted to absorbance unit as,

$$a_c(\lambda) = 2.303 \, OD_c(\lambda) \, 100 \qquad [m^{-1}]$$

Primary productivity

Primary productivity was measured in situ using light and dark bottle method (Strickland and Parsons, 1968). Water samples were collected from surface by water samplers (Aqua-trap 2.5 litre non–metallic water sampler) and filtered through a nylon bolt net (150 μm) to eliminate zooplanktons, especially copepod predators. Water samples were incubated in situ (surface layer, 0–20 cm) for three hours in light (clear glass) and dark bottles (amber coloured to obstruct light) and one set was kept on board as control. D.O. content was measured in all sets after incubation period. The differences between the D.O. content in the dark bottle and the control bottle denotes the respiration. Since no light was available in the dark bottle, no photosynthesis was assumed to have occurred. The difference of D.O. in the light bottle and that of in the dark bottle (in terms of mg/litre) amounts to the Gross Primary Productivity (G. P. P.). Therefore, G. P. P. can be measured as:

$$\text{Gross Primary Productivity (mg C / m}^3\text{ / hr)} = \frac{12 \times (Lb - Db) \times 1000}{32 \times PQ \times t}$$

Where,

Db = D.O. in the dark bottle in mg / litre

Lb = D.O. in the light bottle in mg / litre

PQ = Photosynthetic quotient and

t = time of incubation in hours

PQ was the ratio of moles of oxygen released to moles of carbon fixed during photosynthesis; its value depends on whether nitrate or ammonia was available as a nitrogen source and varies from 1.0 to 1.3.

3.1.3 Transparency parameters

Light penetration (Secchi Disc Method)

Standard light intensity depths can be determined with a narrow band irradiance meter or a Secchi disc. On theoretical grounds, Secchi disc measurements may not be wholly related to the vertical attenuation of light (Tyler, 1968), but their use was endorsed in IBP handbook No. 12 (Vollen Weider, 1969) and use of Secchi disc has been suggested as the simplest and cheapest way to determine the light attenuation, especially while studying near shore environments. Again, a high correlation between Secchi depth and light transmission has been shown by several works.

Jones (2002) has reported the relationship:

E_d = 1% light depth (m)

    = 1.73 x Secchi depth (m),   with r^2 = 0.52;   (n = 681).

Scheffer (1998) also reported that the euphotic depth can be estimated as 1.7 times the Secchi depth. According to OECD (1982), Secchi disc reading (in meters) in which:

E_d = 2.5 × SD may be used though for coloured (dystrophic lakes), the factor was quite lower.

In contrast, measurements the Salton Sea, California, a highly saline body of water, found the 1% light depth = 4 × Secchi depth (Holdren, 2002).

National Institute of Oceanography, Goa uses a E_d = 2 × SD empirical relationship for the western coast of India (Suresh et al., 2006).

A Secchi disc of a diameter of 20 cm and painted alternately white and black in a radial manner was lowered and the depth at which it disappears was noted. Similarly, the depth at which it reappears was noted while it was being pulled up. Arithmetic mean of these two depths was considered as Secchi disc depth.

Extinction coefficient (k_t) of the water mass can be calculated using the formula:

$k_t = 1.44/ D$

Where, D was Secchi disc depth in metres, as applicable for turbid waters (Raymont, 1980). The Euphotic zone extends from the surface water to a depth called the euphotic depth or compensation depth, at which the rate of plant or algal respiration exactly balances the rate of photosynthesis. It was conventional to take this lower limit as occurring at a depth at which light was 1% of the surface irradiance, although in reality the limiting light can range between 0.1 and 20% of surface light. Accepting a limiting value of 1%, the depth of the euphotic zone, the euphotic depth (Ed)

$\ln (E_z/E_0) = -k_t . E_d$

That is, the euphotic depth, $E_d = (4.6) / k_t$ metres (Kirk, 1994).

Suspended particulate matter

For SPM concentration estimation, seawater samples were collected from undisturbed or temporarily disrupted area. A sample volume of 1 Litre was filtered through a pre-washed, pre-dried (at 103-105 °C) 0.45µm filter paper. This was dried and reweighed to calculate SPM in mg/L. SPM was calculated by using the equation below

SPM [mg/L] = ([A-B]*1000)/C

Where, A = final dried weight of the filter [mg],

B = Initial weight of the filter [mg],

C = Volume of water filtered [L].

3.1.4 In-situ sea-water analysis with the help of multi-sensor probes

Over the last few decades, several multi-sensor probes have come out for in-situ water quality analysis. These probes have multiple sensors attached to a main body which can be submerged in the water column to reveal various characteristics such as chlorophyll concentration, total suspended solids, turbidity, temperature, salinity,

pH, depth etc. These were very easy-to-use, while being designed for rough wear and protected against bio-fowling. Multi-sensor probes can be used for the on-board sea-water analysis, particularly when many sampling stations have to be covered within a short period of time, and also for corroboration of some of the wet-lab measurements of the water quality parameters. This may reduce the probability of error.

A multi-sensor probe (YSI Sonde 6600 V2-2) was acquired for the purpose of field measurement needed in this study. Several parameters were estimated with this probe, such as TDS, Temperature, pH, salinity and conductivity.

3.2 Satellite Data Collection

This study aims to analyse the satellite data through the forward way, i.e., atmospheric correction of the satellite data and retrieval of Ocean Colour Parameters and Sea Surface Temperature. For this purpose, satellite data was collected for trend generation, of which the details are given below.

Satellite data such as MODIS (36 bands ocean colour sensor on board Terra of NASA, highest resolution 250m), Sea-WiFS (8 bands, coarse resolution data), OCM (8 bands, medium resolution on board IRS-P4) and ASTER (high resolution, on-board Terra) have been collected. SeaWiFS data has been collected for chlorophyll and Suspended Particulate Matter (SPM) trend generation from 1996 till 2001.

MODIS data has been collected from 2005 till date, mainly for the pre-monsoon season a this time period is best for the study area (in terms of clear sky, low cloud cover and less SPM outflux from nearby coastal lands which happens during and after monsoon). The MODIS Level 1B dataset contains calibrated and geo-located at-aperture radiances for 36 discrete bands located in the 0.4 to 14.4 micron region of electro-magnetic spectrum. MODIS data is collected mainly for the purpose of long term trend analysis and ancillary parameter generation when needed, such as iPAR (instantaneous Photosynthetically Active Radiation), Aerosol Optical Depth, etc. Also, NOAA-AVHRR SST data was found to be of too coarse a resolution to be used for this project which is based on coastal waters. Hence, SST data was calculated from MODIS data only.

OCM data was procured from National Data Centre (NDC) for field synchronous days, to generate chlorophyll and SPM. The ASTER datasets were procured for a very high resolution (15, 30 and 90 m) imaging of the coastal plume features.

Table 2   **Satellite Data sources**

Satellite	Source of image
OCM	NRSC portal
ASTER	http://glcfapp.umiacs.umd.edu:8080/esdi/index.jsp
SeaWiFS	http://oceancolor.gsfc.nasa.gov/cgi/browse.pl
MODIS	ECHO-WIST web archive (https://wist.echo.nasa.gov/api/)

OCM images are 8 band 16 bit radiance data for specially designed for ocean colour, on-board IRS-P4 satellite. The important parameters for OCM data is given below:

Table 3   **Reflectance generation parameters of OCM images**

Band no.	Central wavelength (nm)	Conversion Factor (S)	Equivalent solar irradiance ($^-E0$)
1	414.21	1334	170.595
2	441.40	2275	186.805
3	485.70	2783	196.200
4	510.60	2972	187.275
5	556.40	3573	185.442
6	669.00	4647	153.978
7	768.60	9974	121.920
8	865.10	5979	97.6533

Table 4   **ASTER (VNIR & TIR) on-board Terra**

Band	Wavelength (μm)	Resolution (m)	Swath Width (km)	Revisit time (days)
Band 1 (VIS)	0.52 to 0.6	15	60	16
Band 2 (VIS)	0.63 to 0.69	15	60	16

Band 3n (NIR)	0.76 to 0.86	15	60	16
Band 3b (NIR)	0.76 to 0.86	15	60	16
Band 4 (SWIR)	1.6 to 1.7	30	60	16
Band 5 (SWIR)	2.145 to 2.185	30	60	16
Band 6 (SWIR)	2.185 to 2.225	30	60	16
Band 7 (SWIR)	2.235 to 2.285	30	60	16
Band 8 (SWIR)	2.295 to 2.365	30	60	16
Band 9 (SWIR)	2.36 to 2.43	30	60	16
Band 10 (TIR)	8.125 to 8.475	90	60	16
Band 11 (TIR)	8.475 to 8.825	90	60	16
Band 12 (TIR)	8.925 to 9.275	90	60	16
Band 13 (TIR)	10.25 to 10.95	90	60	16
Band 14 (TIR)	10.95 to 11.65	90	60	16

Table 5   Specifications of MODIS Terra/ Aqua Sensor

Central Wavelength (nm)	Resolution (m)	Revisit time (days)	Nominal Band Solar Irradiances mW/cm^2/μm
412	1000	2	171.18
443	1000	2	188.76
469	500	2	203.52
488	1000	2	194.18
531	1000	2	185.94
551	1000	2	187.00
555	500	2	183.76
645	250	2	158.74
667	1000	2	152.44
678	1000	2	148.14
748	1000	2	127.60
859	250	2	95.728
869	1000	2	94.874
1240	500	2	45.52
1640	500	2	22.99

Table 6   **Specifications of SeaWiFS sensor**

Band	Wavelength (µm)	Resolution (m)	Swath Width (km)	Revisit time (days)
Band 1 (VIS)	0.402 to 0.422	1100 (4500)	2801 (1502)	1
Band 2 (VIS)	0.433 to 0.453	1100 (4500)	2801 (1502)	1
Band 3 (VIS)	0.48 to 0.5	1100 (4500)	2801 (1502)	1
Band 4 (VIS)	0.5 to 0.52	1100 (4500)	2801 (1502)	1
Band 5 (VIS)	0.545 to 0.565	1100 (4500)	2801 (1502)	1
Band 6 (VIS)	0.66 to 0.68	1100 (4500)	2801 (1502)	1
Band 7 (VIS)	0.745 to 0.785	1100 (4500)	2801 (1502)	1
Band 8 (NIR)	0.845 to 0.885	1100 (4500)	2801 (1502)	1

3.3 Processing of Satellite Data

The datasets were imported, geo-referenced and subsetted using ENVI 4.2 software. A Bow-tie correction was applied to the MODIS images for correcting the swath distortion (which arises as the pixels towards the edges of the scan have increasingly larger coverage on the ground and the coverage of pixels from the subsequent mirror swaths partly overlaps). Dark pixel subtraction was applied to each image, band by band, for a basic atmospheric correction; assuming that the study area being small (around 70 km in length), the aerosol cover over it will not vary significantly on a particular day at a particular time (satellite imaging snapshot time). The method is given in details below.

3.3.1 Atmospheric Correction

Dark pixel subtraction was done for atmospherically correcting the satellite images. Dark pixel subtraction is a technique which determines the pixel in the image with the lowest brightness value. This pixel is assumed to have a zero ground reflectance such that its radiometric value represents the additive effect of the atmosphere (Crippen, 1987).

This method is also known as the histogram minimum method, based on the assumption that in the image there exists a pixel whose DN value is essentially zero, so that the radiance recorded by the sensor is solely due to path radiance. That is the

21

pixel of the lowest DN in each band in reality should be zero, and hence its radiometric value (DN) is the result of the atmospheric induced additive errors. In order to remove the path radiance, an area of shadow or a very dark object (such as clear deep sea water) is selected and the minimum pixel value is determined. The signatures are corrected by subtracting the minimum observed value, determined for each specific band, from all pixel values in each respective band. (Textbook of Remote Sensing and Geographical Information Systems, Kali Charan Sahu, Atlantic Publishers & Distributors, 2007)

Pixels with 2 lowest brightness values were identified in band 7 and band 8. These pixels were plotted on a log brightness value vs. wavelength graph. Best fitting line is passed through these plotted points which also passed through zero. This line is used as reference line for dark pixel subtraction, using which noise for other bands is analysed.
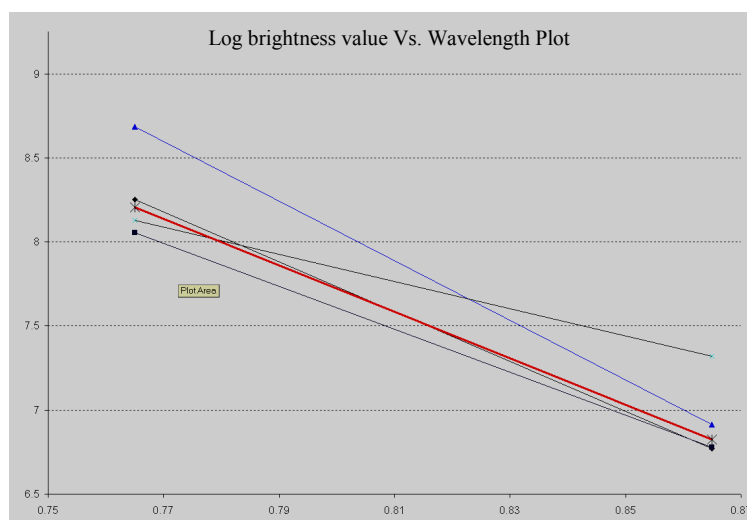
Figure 2 Trend Line of Dark Pixel Subtraction

3.3.2 Procesing of SeaWiFS data:

Data was downloaded from the GLCF portal. Data was downloaded in MLAC format, it's a LEVEL 1 data format. Downloaded data was then converted to software specific format. Dark pixel subtraction was done on these images. Chlorophyll algorithms were applied on these images.

3.3.3 Retrieval of Ocean Colour Parameters from Satellite Data

Radiance was calculated for each band of satellite data from the DN numbers using the formula

$L = DN/S$

Where, Ls = radiance, DN = recorded digital numbers and S = conversion factor (usually calculated from gain and bias provided in image ephemeris data).

The formula for calculating spectral reflectance from radiance is:

$\rho = \pi\, L / F_0 \cos\theta_0$

Where,

L was the upward radiance in the given viewing direction, F_0 was the extraterrestrial solar irradiance, and θ_0 was the solar zenith angle.

3.3.4 Estimation of Chlorophyll-a concentration

The chlorophyll-concentrations estimations were generated using one of the empirical algorithms available in literature. A brief description of the chlorophyll algorithms that can be applied in this study was provided below in table below.

Table 7   Structure of some semi-empirical bio-optical Chlorophyll retrieval algorithms

Algorithms	Type	Empirical equation	Band ratio (R)	Coefficients (a)
OC2 V. 4 (O'Reilly et. al., 2000)	Modified cubic	$C = 10\wedge(a_0 + a_1 \times R + a_2 \times R_2 + a_3 \times R_3) + a_4$	Log($R_{rs}490/R_{rs}555$)	[0.319, -2.336, 0.879, -0.135, -0.071]
OC4 V. 4 (O'Reilly et. al., 2000)	Modified cubic	$C = 10\wedge(a_0 + a_1 \times R + a_2 \times R_2 + a_3 \times R_3) + a_4$	log($R_{rs}443 > R_{rs}490 > R_{rs}510 /R_{rs}555$)	[0.366, -3.067, 1.93, 0.649, -0.532]
Chlor-MODIS (Clark, 1997)	Modified cubic	$C = 10\wedge((a_0 + a_1R + a_2 \times R_2 + a_3 \times R_3 + a_4)/e)$	log (LW[N]443+ LW[N]488)/ LW[N]551	Coefficients when R> 0.9866 are: a = [-2.8237, 4.7122, -3.9110,

				0.8904, 1] Coefficients when R<0.7368 are: a = [-8.1067, 12.0707, -6.0171, 0.8791, 1]
Chlor- a 2 (O'Reilly et. al., 2000)	Polynomial of order 4	$C= 10\wedge(a_0 + a_1 \times R + a_2 \times R_2 + a_3 \times R_3 + a_4 \times R_4)$	$\log[\max(r25, r35)]$ where $r25 = R_{rs}443/R_{rs}551$, $r35 = R_{rs}488/R_{rs}551$	[0.2830, −2.753, 1.457, 0.659, −1.403]
Chlor-a 3 (Carder et. al., 1999)	Quadratic	$C=10\wedge(a_0 + a_1 \times R + a_2 \times R_2)$	$\log(R_{rs}488/R_{rs}551)$	[0.289, -3.2, 1.2]

3.3.5 Calculation of SPM concentration

The SPM concentration in the coastal waters can be derived using the water leaving radiances in the wavelengths 490, 555 and 670 nm. The algorithm proposed by Tassan (1994) has been used for the purpose. It has the following mathematical form.

$$LogS = 1.82 + 1.23 (logXs)$$

Where S is the suspended particulate matter concentration in mg/l and Xs is the variable defined as

$$Xs = (Rrs555 + Rrs670)*(Rrs490/Rrs555)^{-0.5}$$

Where, Rrs is the spectral remote sensing reflectance in respective wavelengths.

Similar approach was maintained for calculation of reflectance from MODIS, OCM and ASTER data. However, as ASTER lacks a blue band which was required to estimate chlorophyll using the bio-optical algorithms given above, chlorophyll images were generated using the empirical formula given by Kallio et al., 2003, using ASTER bands 2 and 3. SPM was generated from ASTER using the algorithm suggested

by Babin, 2000. However, both of these algorithms require sea-truth data for establishing the relationship in the local waters.

3.3.6 Estimation of Yellow Substance (CDOM) Concentration

Remote sensing studies in which the competition of CDOM with phytoplankton pigments in absorption in the blue was important often employ 440 nm (Carder et al., 1989; Bowers et al., 2000).

aCDOM (λ) = aCDOM (440) exp[-s(λ-440)] [m-1]

Where, aCDOM (440) was the absorption measured at 440 nm and s was the slope coefficient which was calculated as the slope of the curve resulted by plotting logarithm of aCDOM against wavelength (λ). The magnitude of aCDOM (440) gives the concentration while the spectral slope (5) indicates its composition (Stedmon and Markager, 2003).

3.3.7 Estimation of Sea Surface Temperature from satellite data

The satellite measured SST provides both a synoptic view of the ocean and a high frequency of repeat views, allowing the examination of basin-wide upper ocean dynamics not possible with ships or buoys. NASA's (National Aeronautic and Space Administration) MODIS (Terra and Aqua) satellites have been providing global SST data since 2000. These gridded products are available with a one-day lag. However, these datasets come with binned 1 and 4 km resolution with coastal mixed pixels masked. Hence, for the purpose of this project, Sea Surface Temperature was calculated from MODIS data using the following formula:

L= 2 * h * c^2 * λ^{-5} / [$e^{(h * c / k*\lambda*T)}$ − 1]

Where, L=radiance(Watts/m2/steradian/m)

> h = Planck's constant (joule second)
> c = speed of light in vacuum (m/s)
> k = Boltzmann gas constant (joules/kelvin)
> λ =band or detector center wavelength (m)
> T = temperature (degree Kelvin)

This temperature is by theory surface skin temperature ranging from 5-10 micrometer depth. This parameter is generated from MODIS 1km microwave band data, which are first converted to radiance.

3.4 Processing of Ancillary Data

Ancillary data, mainly in the form of sea truth and other geophysical parameters were collected for this project from various governmental and other sources. These include data from Coastal Ocean Monitoring and Prediction System (COMAPS) Programme, undertaken by the Marine Area Management Project Directorate (ICMAM-PD). COMAPS has been monitoring the levels of marine pollution at several locations along the coastline of the country from the year 1991-92 onwards, under the umbrella of Ministry of Earth Sciences. The data collected have indicated clearly the levels of pollution at these locations. In general, the coastal waters along the east coast of India especially at the locations where monitoring programme is carried out indicate contamination of untreated sewage in the form of high levels of pathogenic bacteria. The main thrust of this programme is to collect and distribute marine pollution data over both east and west coast of India. (COMAPS 2009)

Other ancillary data has been collected from Indian Meteorological Department (IMD), Pune. Details of the ancillary data are given in the following sections.

3.4.1 COMAPS data

COMAPS data for the study area has been collected and integrated in GIS layers as given below (1996-2008). Data gap has been observed for the years 2002 and 2004.

- Water quality parameters (Chlorophyll, turbidity, D.O., B.O.D., nutrients etc.)
- Productivity data (primary productivity and zooplankton concentration)
- Physico-chemical parameters (SST, salinity, pH etc.)

The figure below shows the transect of COMAPS sea-truth data points which come under the extent of the present area of study. The labels in green denote the location of the points. The sampling points have been overlaid on an ASTER image of the study area for better understanding.
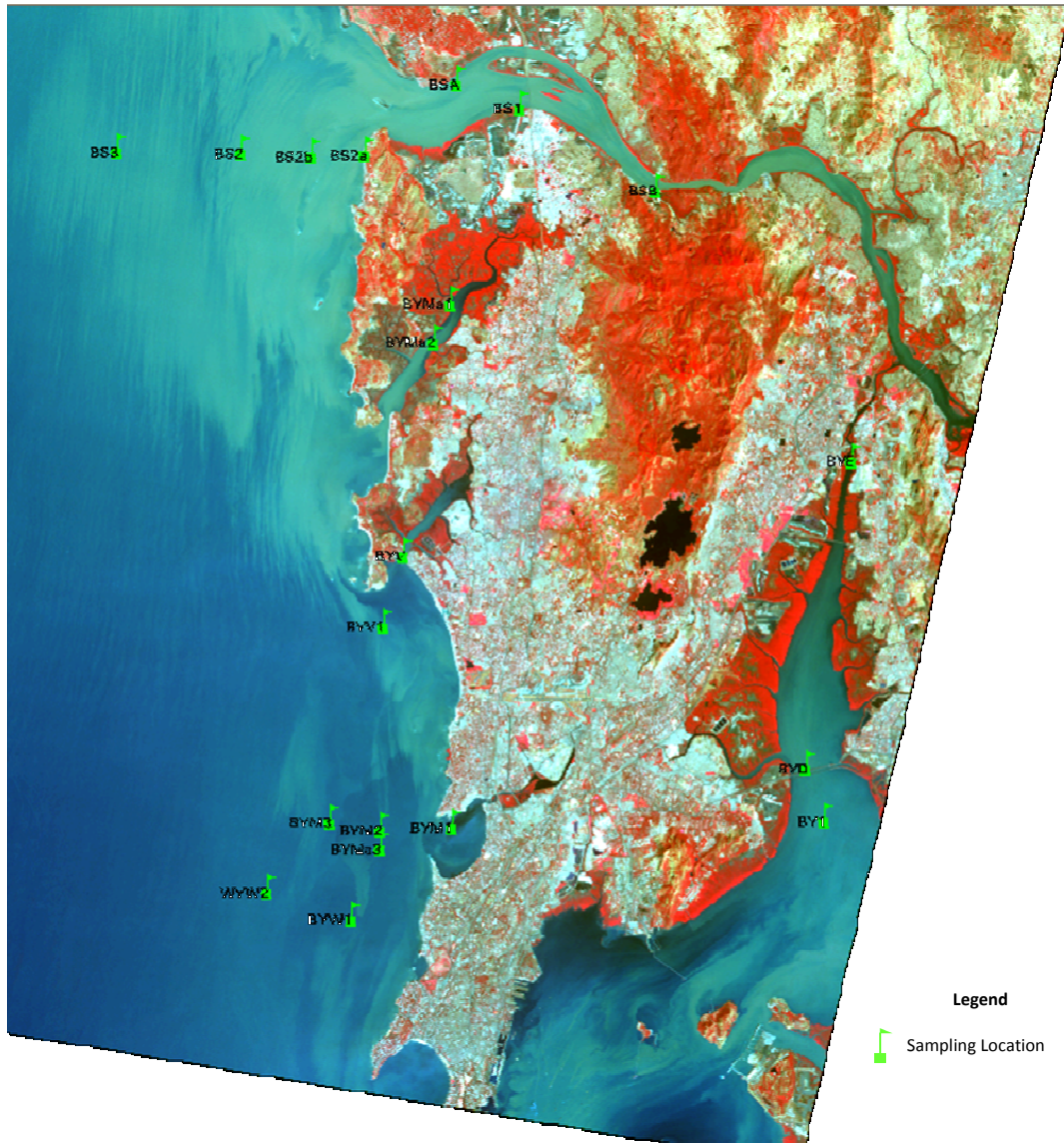
Figure 3 Location of COMAPS sea-truth survey points in the study area

3.4.2 Other ancillary data

Ancillary data such as sea-surface wind (direction and speed), precipitation, solar flux, wind driven wave (period and height), swell wave (period, height and direction), day-light period, sea-surface temperature has been obtained from Indian Meteorological Department (IMD), Pune. Basin bathymetry (Digital Elevation Map) has been generated fromb charts. Tidal data have been generated in the form of spreadsheets. Wave data from CWPRS has also been transformed into spreadsheets.

4 Results

4.1 Introduction

In this chapter, the results from the aforementioned exercises are given, with brief additional notes on methods to achieve specific project goals. According to the Project deliverables, there were three distinct goals during the this stage of the work, namely,

1. Post-installation plume mapping
2. Simulation of ambient pollution in a present day scenario without outfalls
3. Mapping of the impact on ecosystem

4.2 Post-installation plume mapping

The first goal during the second stage was to map the outfall plumes through remote sensing images using temporal data. This was envisioned to help observe and monitor the plume shape and structure from satellite data as they changed through the years after the Bandra and Worli marine outfall installation. The primary objectives were to assess the two different plumes on different days, with the help of snapshots taken from the satellite camera, as well as to map the pollution level near the outfall locations as understood from the changes observed in three water-quality parameters such as Chlorophyll_a, Suspended Particulate Matter and Yellow Substances, which have been described in this report before.

4.2.1 Methodology

To meet the requirement of the project goals, the post-installation plume mapping has been done in two steps:

a. Using ASTER data:

Snapshots of the plume shape and extent have been mapped through ASTER data which has very high spatial resolution of 15 m. This high resolution data helped to delineate the plume shape feature very clearly from year to year.

The level 2b ortho-rectified ASTER data was processed by stacking the visible and infra-red bands in a sequence; a PCA (principal component analysis) method was applied to the stacked data to find out the inherent correlation in the data in terms of spectral characteristics of the ambient waters. According to the theory of PCA, the first principal component is the least correlated part of the data, and as the number of the components increase, so does the correlation in them. As the spectral nature of the plumes is captured through the two visible (green and red) and the IR channels, maximum signature correlation is seen for the outfall plumes in 2nd and 3rd Principal components. It may however be cautioned that the colours and their intensity variation have little to do with the pollutants and their intensities.

b. Using MODIS Terra & Aqua data

Mapping of ambient pollution was done through MODIS-Terra and Aqua sensor data for long term trends from 2002 onwards. The parameters considered for long term trend determination were Chlorophyll_a, SPM and Yellow Substances.

4.2.2 Results using ASTER data

The results from ASTER data analysis are given below.
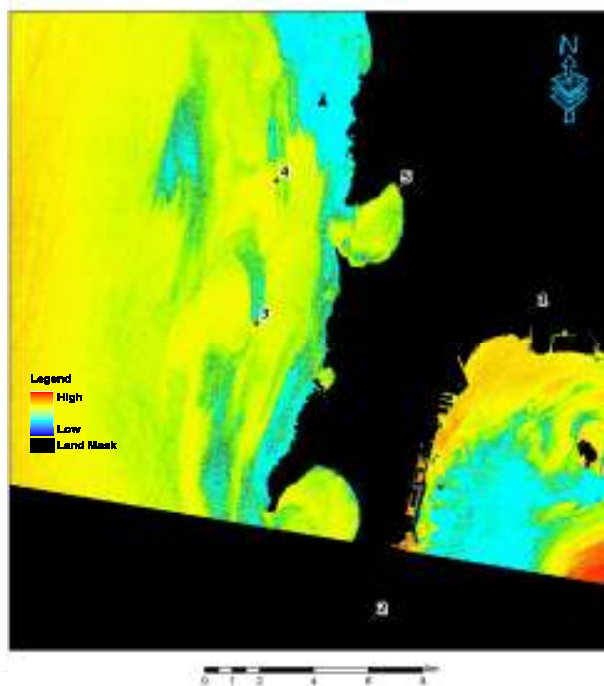
Point Number	Area
1	Mahul Creek
2	Colaba
3	Worli Outfall
4	Bandra Outfall
5	Mithi River Mouth

This is an ortho-rectified ASTER image of the study area dated 29th of January, 2002 from which the Second principal component image was obtained. The image shows a distinct tongue-shaped plume near the Worli outfall. The outfall flow direction appears to be North-ward. There is no presence of the Bandra outfall at this date. However, pollution outflow from the Mithi River as well from near Mahul creek is very prominent. [1]

---

[1] N.B: The color variation in the fig is to be viewed only for noting the shape of the outfall expression on the sea surface and are not related to pollution types and intensities
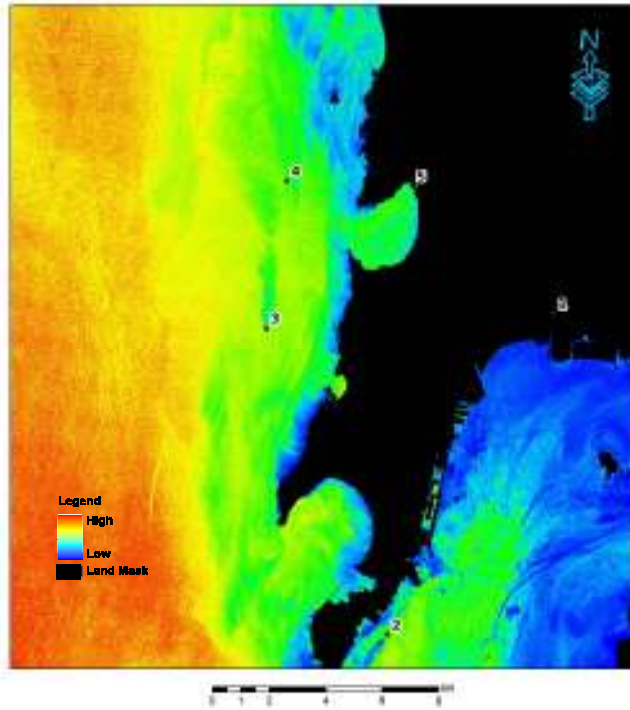
Point Number	Area
1	Mahul Creek
2	Colaba
3	Worli Outfall
4	Bandra Outfall
5	Mithi River Mouth

The ASTER image dated 27th of March, 2002, was acquired almost 2 months later. The 2nd principal component image still shows the single outfall plume in an extended tongue shape with a strong north-ward flow direction.

Figure 5: ASTER image dated 27/03/2002
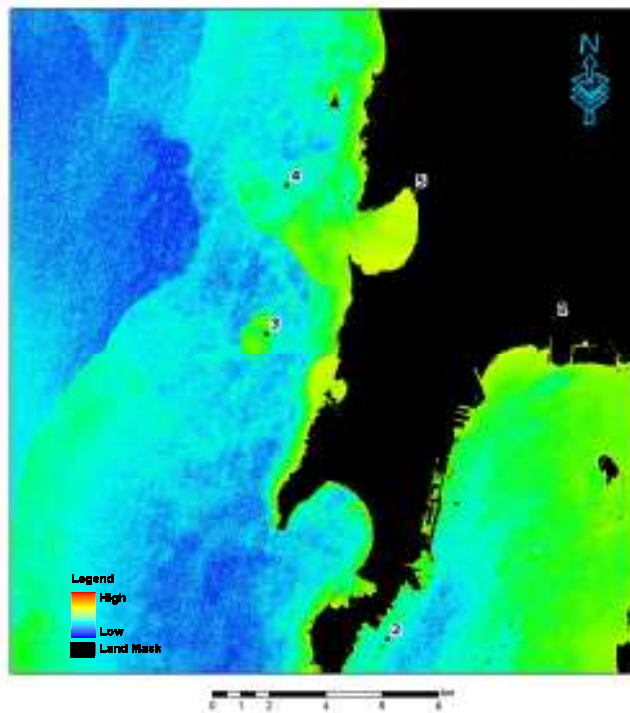
Point Number	Area
1	Mahul Creek
2	Colaba
3	Worli Outfall
4	Bandra Outfall
5	Mithi River Mouth

Almost a year later, the second principal component of the ASTER image dated 26th February 2003 shows a circular dispersion pattern of the Worli Outfall with a slight downward drift while several distinct fronts are seen. The level of pollution inside the Bandra bay area is found to have remained the same if not increased at this point of time.

Figure 6: ASTER image dated 26/02/2003
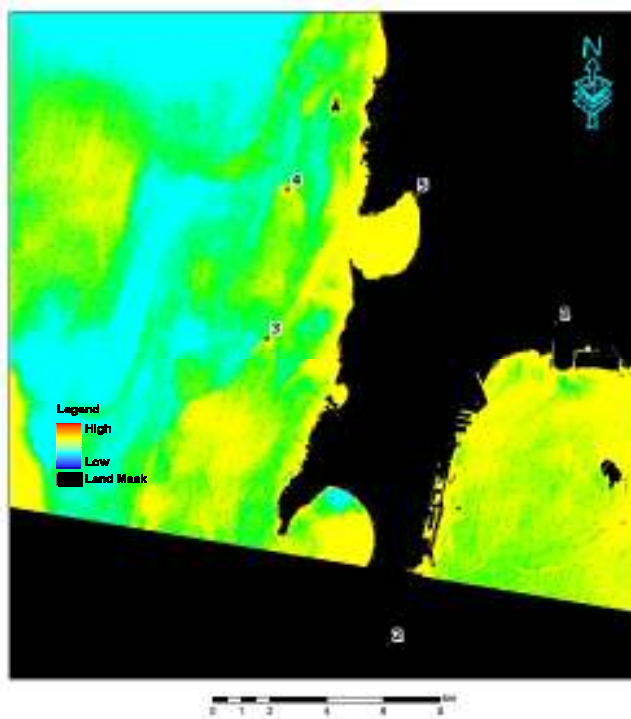
Point Number	Area
1	Mahul Creek
2	Colaba
3	Worli Outfall
4	Bandra Outfall
5	Mithi River Mouth

The above image was acquired on 18th of November, 2004 and by this date, both outfalls were functioning. While a general southward water flow direction is indicated from the picture, two distinct outfall plumes are seen at this stage. As this was the only available post-monsoon season image of the study area, it could not be inferred whether the predominant water movement during post-monsoon season is southwards.

Figure 7: ASTER image dated 18/11/2004
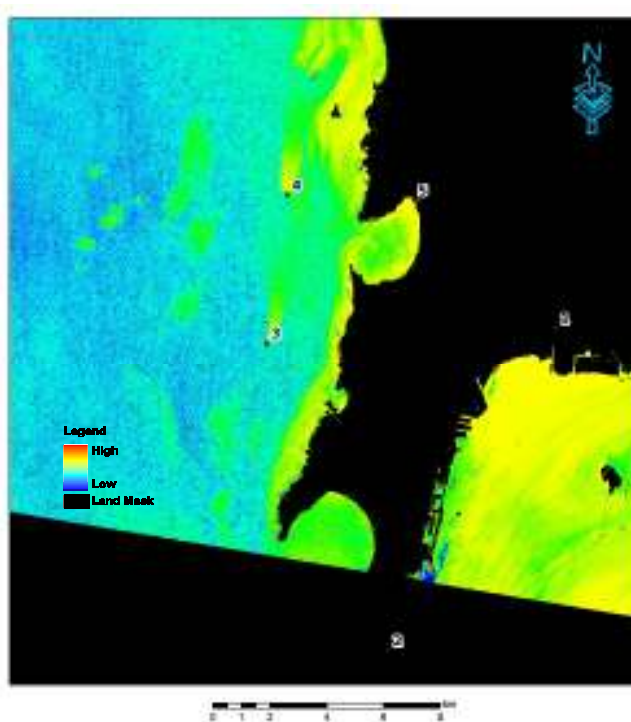
Point Number	Area
1	Mahul Creek
2	Colaba
3	Worli Outfall
4	Bandra Outfall
5	Mithi River Mouth

The above ASTER image is of 4th of June, 2007, showing distinct wind driven surface ripples on the west coast with a general North-ward trend. Both the Bandra and the Worli outfall plumes are seen as extended tongue shaped features in the image having a north-ward dispersing character. It is interesting to note that the plumes are very distinct in spectral characteristics from the strong long-shore sediment drifts in the study area.

Figure 8: ASTER image dated 04/06/2007

31

4.2.3 Conclusions

From the above ASTER PC-2 images, the plume structures are seen very clearly on the sea surface at the time of the satellite pass. As the images were acquired on different dates and seasons, the ambient sea state was different from day to day. In some, the prevalent wind direction is found to have been north-wards, resulting in extended tongue shaped plumes. Through none of these images, the sea surface expressions of the plumes are seen to be affecting or reaching the nearby shores or inside bay areas. Also, the plumes are found to be of different spectral texture and colour signature that is very different from the nearby sediment laden waters.

4.2.4 Results using MODIS data

The long term trends of the ocean colour parameters (Chlorophyll_a, SPM and Yellow Substances) are given below. The trends for the study area have been generated from MODIS Terra/ Aqua daily images from the September 2002 till April 2011 depending on data availability or product type changes from the data providers (International Space Agencies Such as NASA and ESA). The study region was between 70E-73E and17N-20N. Data of monsoon months have not been considered for the trend generation as the remotely sensed images had maximum cloud cover and were unusable. Data for the monsoonal period had to be interpolated from pre- and post-monsoon data trends. Daily images have been used to generate monthly mean and standard deviation images which are shown below. Two additional parameters are also shown here, such as Particulate Backscattering Coefficient and Diffuse Attenuation Coefficient at 490 nm. Both of these parameters are related to the amount of particulate and dissolved matter in the ambient waters (SPM and Yellow Substances) and have been calculated using standard algorithms given in MODIS Algorithm Theoretical Basis Document (ATBD) 18 and 19 respectively. The results are shown in a graphical form below.

Description
Variation in the monthly mean Chlorophyll_a concentration in mg/ m3 in the study area from 2002 to 2011. The data ranges from 0- 3.9 mg/ m3 with some abnormal spikes which may have occurred due to noise in the images.

Description
Monthly standard deviation in Chlorophyll_a concentration (mg/ m3) in the study area from 2002 to 2011.
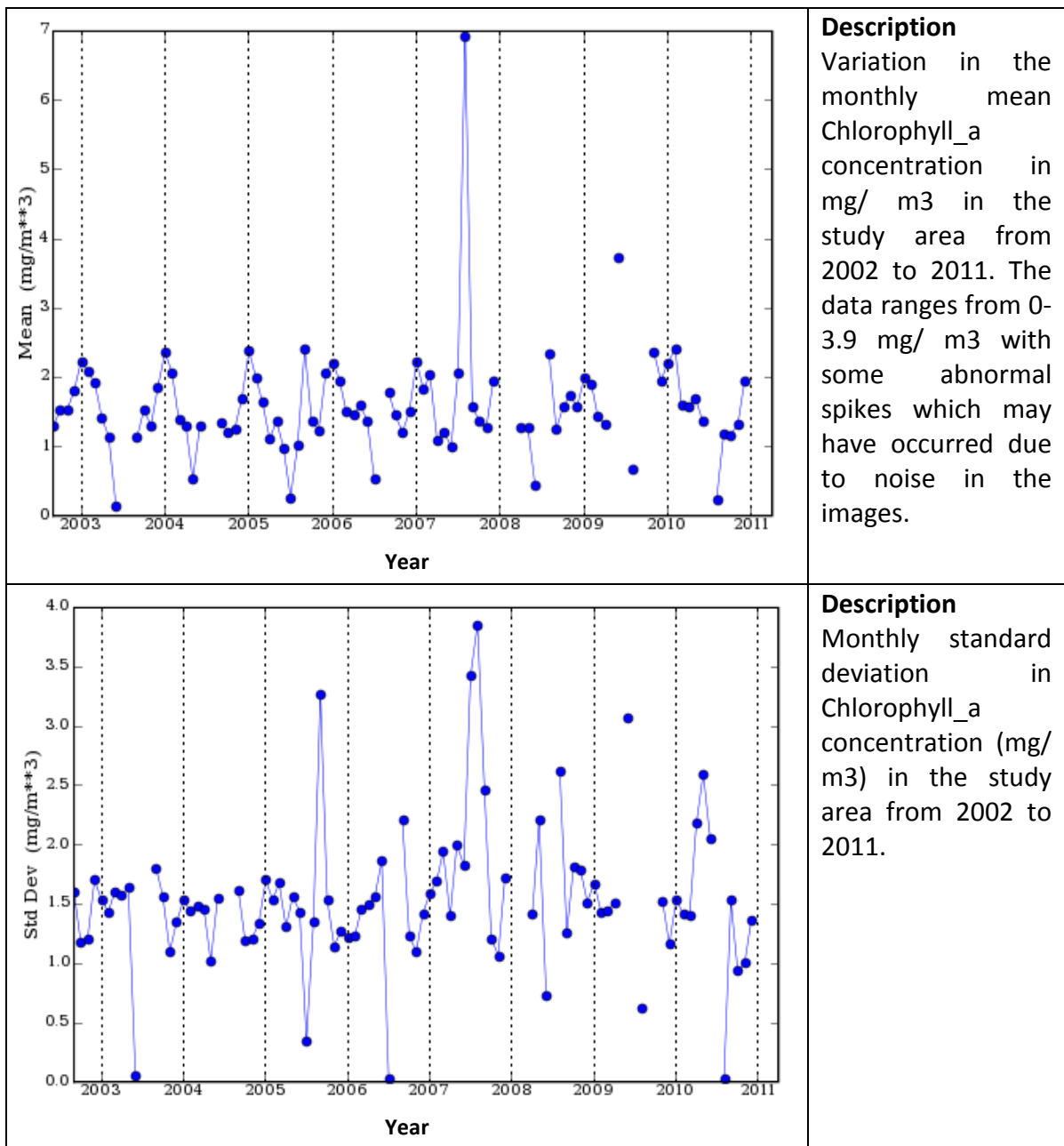
Figure 9: Mean and Standard deviation of Chlorophyll_a concentration from 2002 to 2011

	Description
	Description Variation in the monthly mean (SPM) Conc. in mg/m3 in the study area from 2002 to 2011. The data ranges from 0-68 mg/m3 with some abnormal spikes which may have occurred due to noise in the images.
	Description Variation in the monthly standard deviation in Particulate Backscattering Coefficient per meter in the study area from 2002 to 2010. The data ranges from 0-0.018 per meter.

Figure 10: Mean SPM Conc. & Standard deviation of Particulate Backscattering Coefficient from 2002 to 2011

	Description Variation in the monthly mean of Diffuse Attenuation Coefficient at 490 nm per meter in the study area from 2002 to 2011. The data ranges from 0.02-0.28 per meter. There are certain abnormal spikes in the data which may have occurred due to data noise.
	Description Variation in the monthly mean of Colored Dissolved Organic Material (Index) in the study area from 2002 to 2011. The data ranges from 1.6-6.2 per meter. There are certain abnormal spikes and data gaps which may have occurred due to data noise.

Figure 11: Mean Diffuse Attenuation Coefficient & Mean CDOM Index from 2002 to 2011
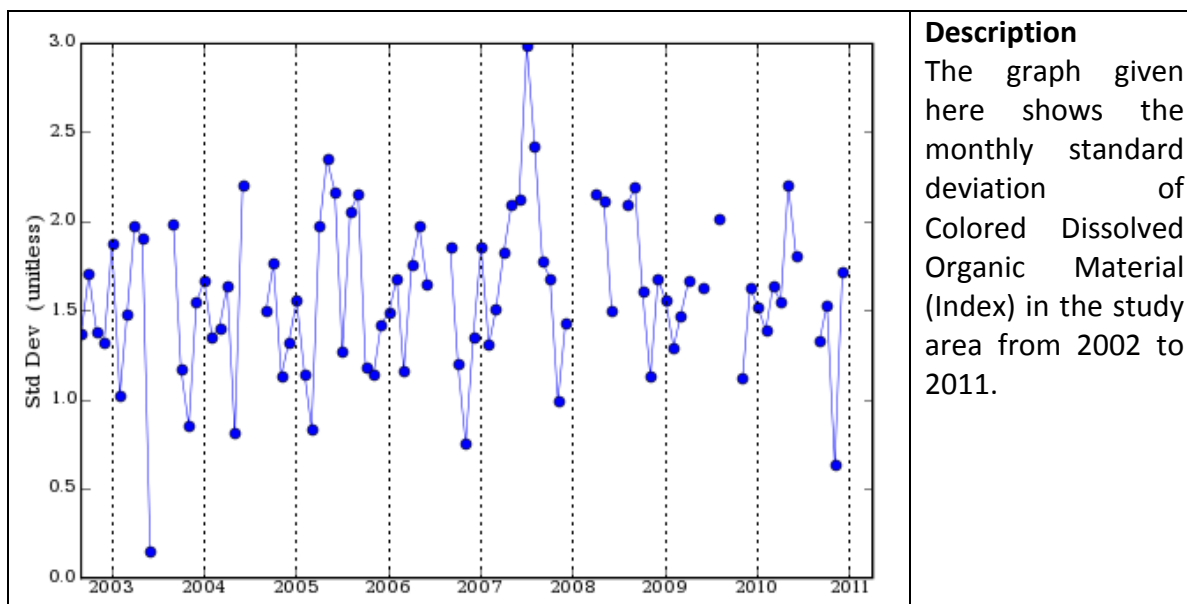
Description
The graph given here shows the monthly standard deviation of Colored Dissolved Organic Material (Index) in the study area from 2002 to 2011.

Figure 12: Standard deviation of CDOM Index from 2002to 2011

4.2.5 Conclusions

It was found from the trend results that 1) The study area shows more sudden changes during the pre-monsoon season than the post-monsoon season in terms of Chlorophyll concentration. 2) Chlorophyll trends show increase during the pre-monsoon period and a gradual decrease during the post-monsoon. 3) However, both SPM and Yellow substances (given as CDOM) show sharp decrease in pre-monsoon period; followed by a sharp increase in SPM during post-monsoon months. 4) The Particulate Backscattering Coefficient shows sharp peaks during the months of December and January, falling sharply during May-June. 5) The Diffuse Attenuation Coefficient at 490 nm (kd490) follows the same pattern as that of chlorophyll. 6) CDOM peaks are noted around October to February with high variation in between, with a sharp decline during April-May.

4.3 Simulation of ambient pollution in a present day scenario without outfalls

The goal of this exercise was to simulate the ambient water conditions at a present date assuming no outfall was commissioned back in 2002-2003. Pre and Post Monsoon SeaWiFS data was downloaded, processed and used for simulation for the years 1997 to March 2002. As there were no benchmark of historical water-quality

data of the area which could be correlated with the remotely sensed data, several chlorophyll_a estimation algorithms were applied on the Sea-WiFS data. The best suited algorithm was chosen with a later day validation of MODIS data with sea-truth data collected on satellite synchronous field visits (Bhattacharya et al, 2010).

Table 8: Pre and Post monsoon imagery dates used for simulation

Pre-Monsoon	Post-Monsoon
-	Nov 1997
Mar-1998	Nov-1998
Mar-1999	Nov-1999
Mar-2000	Nov-2000
Feb-2001	Nov-2001
Mar-2002	-

4.3.1 Processing of SeaWiFS data:

Data was downloaded from the GLCF portal. Data was downloaded in MLAC format; it's a LEVEL 1 data format. Downloaded data was then converted to software specific format. Dark pixel subtraction was done on these images to remove atmospheric errors. Chlorophyll algorithms were applied on these images. There were 5 algorithms that were applied viz. chlor_a2, chlor_a3, oc2_v4, oc4_v4 and aiken_p. For calculating SPM, Tassan's algorithm (1986) for Sea-WiFS data has been used.

The daily data contains certain null (no-data) values. It is because of the fact that data was not collected for those days. These pixels are causing extremity in results when extrapolated to get the future values. To reduce the errors in simulation it was decided to average out the daily values i.e. take the monthly average and then use it for extrapolation.

Results in the form of attribute distribution maps on a regional scale obtained from 2 best suited algorithms viz. Chl a 2 and Chl a 3 have been presented in the following pages. An area of approx. 70 km X 70 km comprising the main study region around Mumbai has been distinctly marked in each of these maps. Chlorophyll_a concentration values shown in the following maps were found to be between **Minimum 0 mg/m3 and Maximum 16 mg/m3 during pre-monsoon and minimum 0**

mg/m3 and Maximum 14 mg/m3. There are 6 sets of images below numbered (1a-1e) to (6a-6e). Each set is clubbed into two subsets of Pre and Post Monsoon images for the years 1998 – 2002.
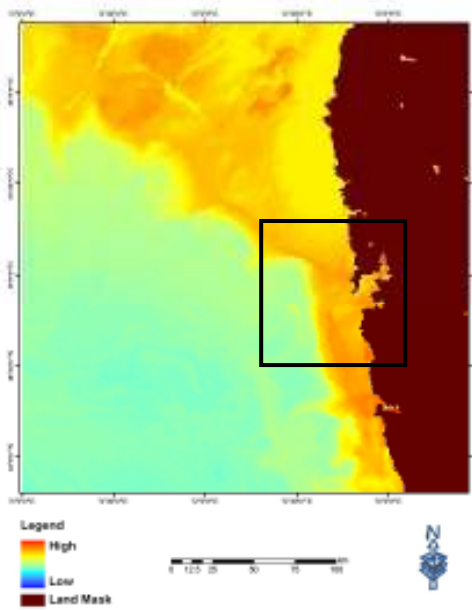
| **Pre monsoon** 1998 (1a)	Pre monsoon 1999 (1b)
Pre monsoon 2000 (1c)	Pre monsoon 2001 (1d)
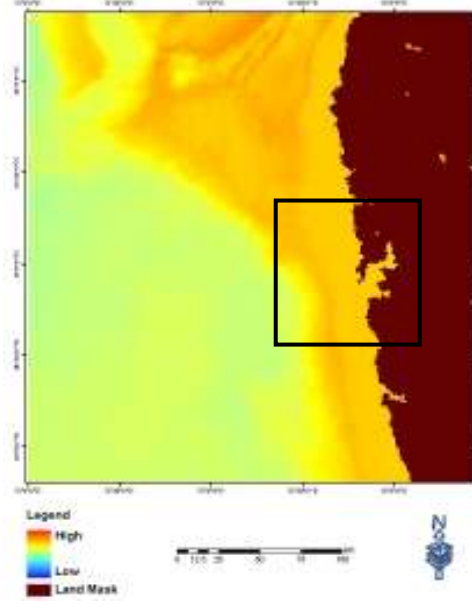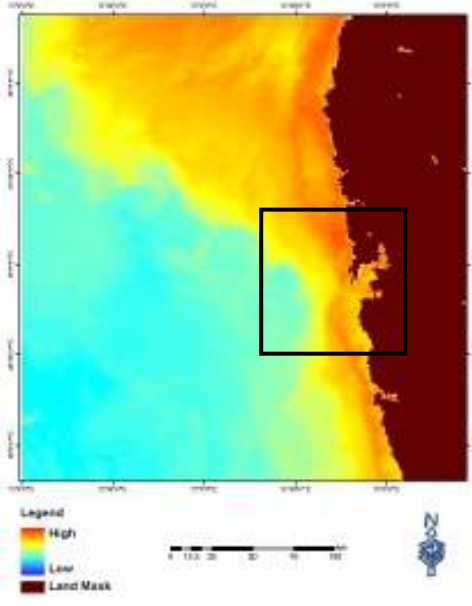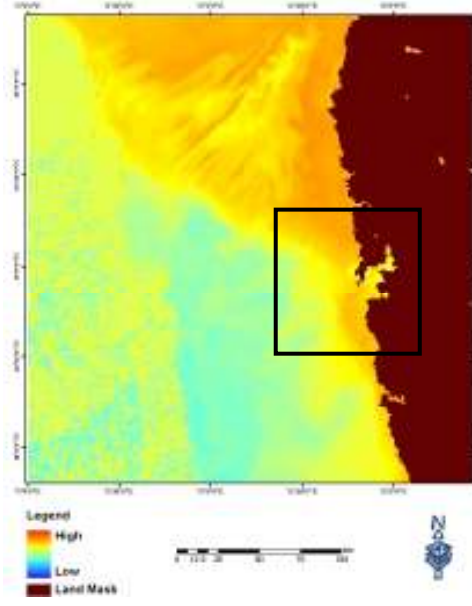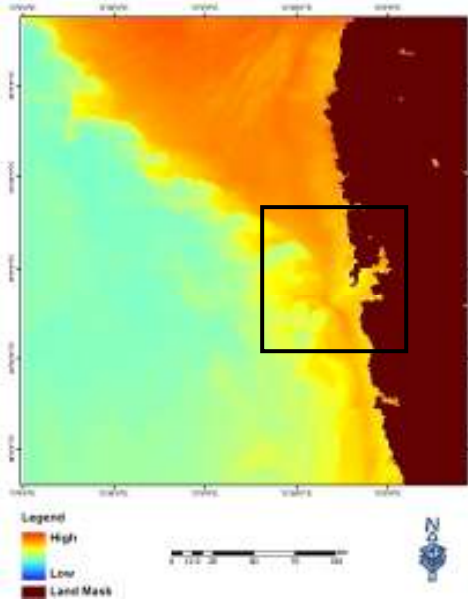
Pre monsoon 2002 (1e)	**Post Monsoon** 1997 (2a)
Post Monsoon 1998 (2b)	Post Monsoon 1999 (2c)
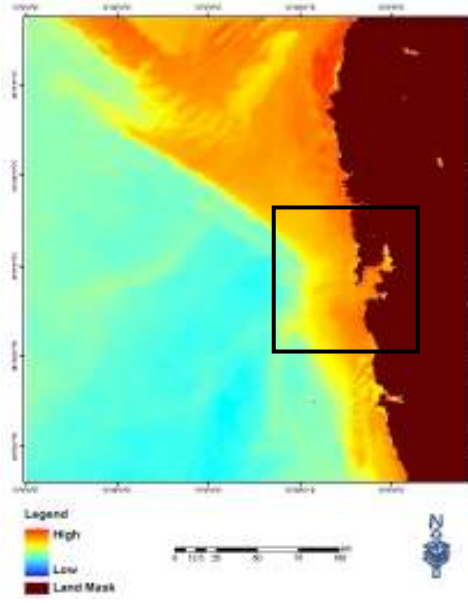
Post Monsoon 2000 (2d)
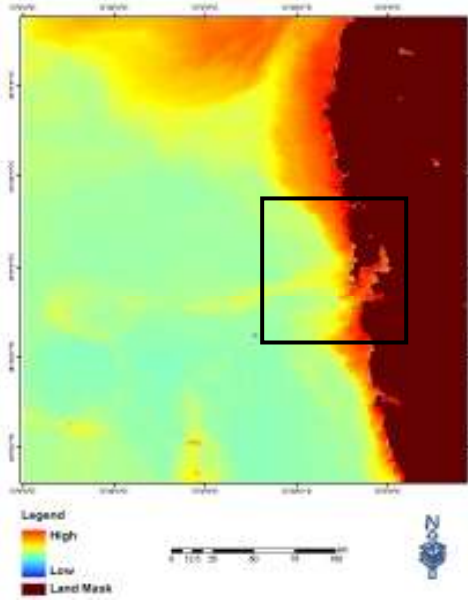
Post Monsoon 2001 (2e)
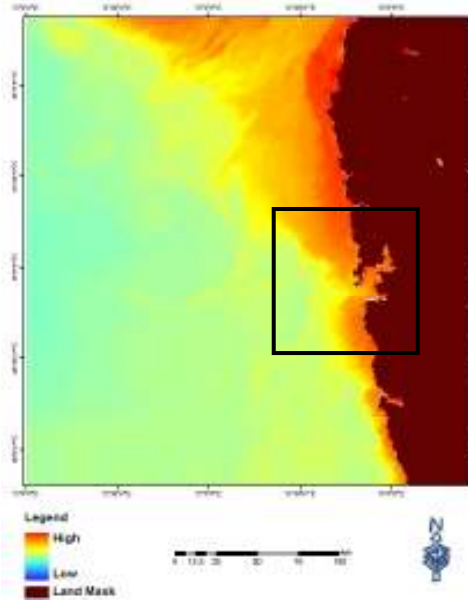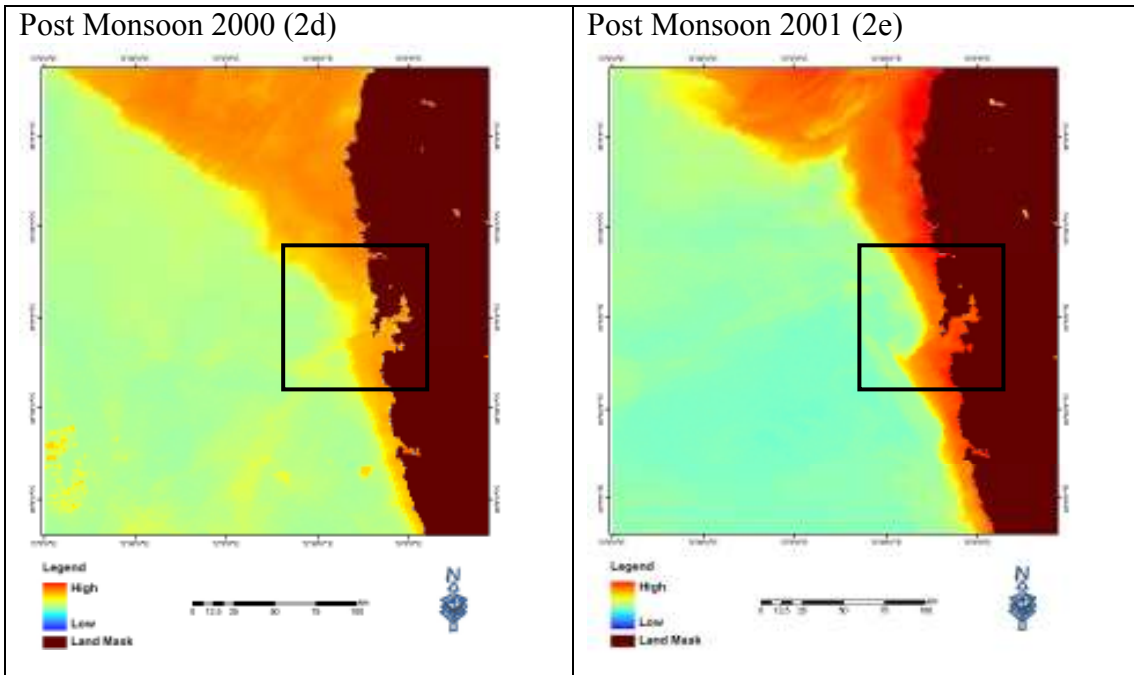
Figure 13: Figure numbered 1a – 2e are Chlorophyll_a conc. using Chlor_a_2 Pre and Post Monsoon Images (N.B: The images show variations in chl_a plumes of pre and post monsoon images)

Pre monsoon 1998 (3a)
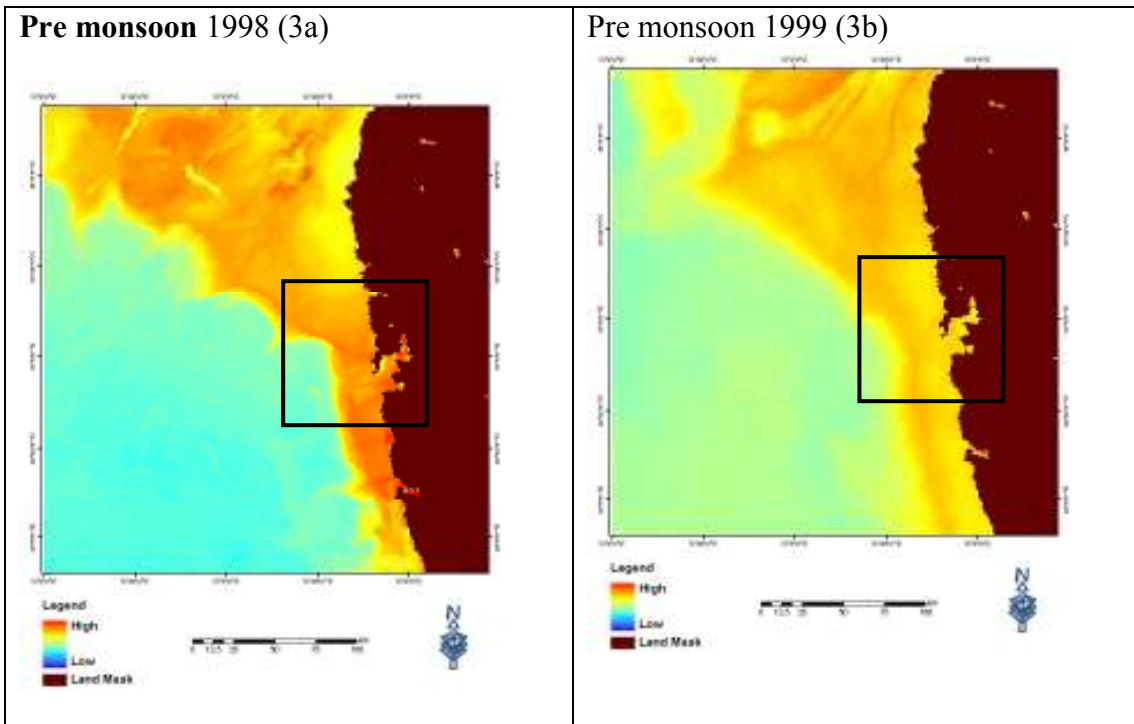
Pre monsoon 1999 (3b)
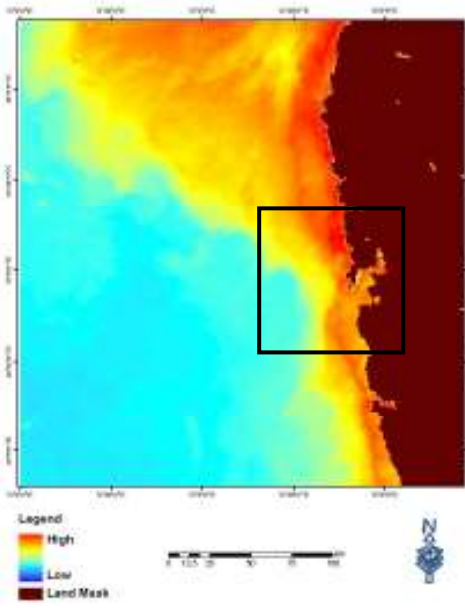
Pre monsoon 2000 (3c)	Pre monsoon 2001 (3d)
Pre monsoon 2002 (3e)	**Post Monsoon** 1997 (4a)
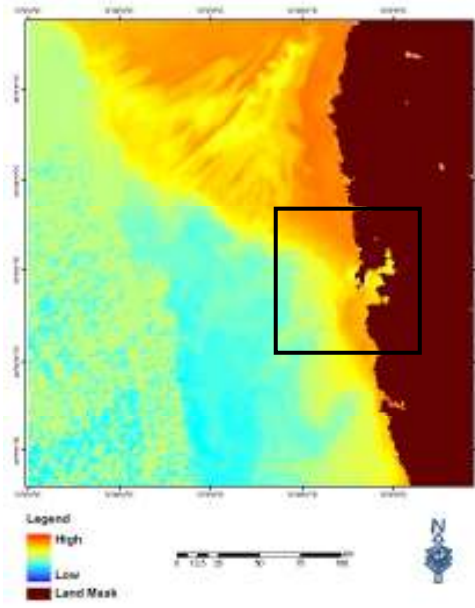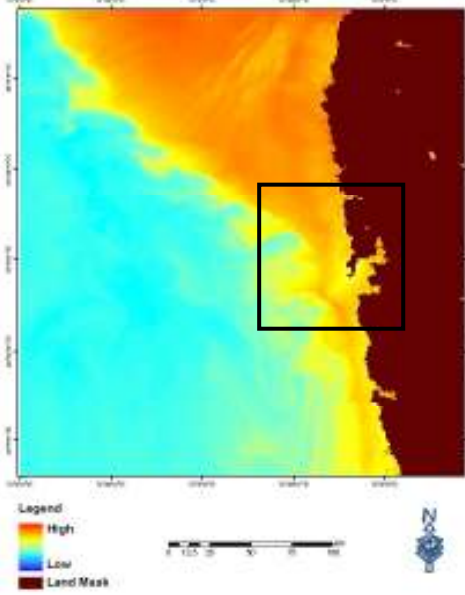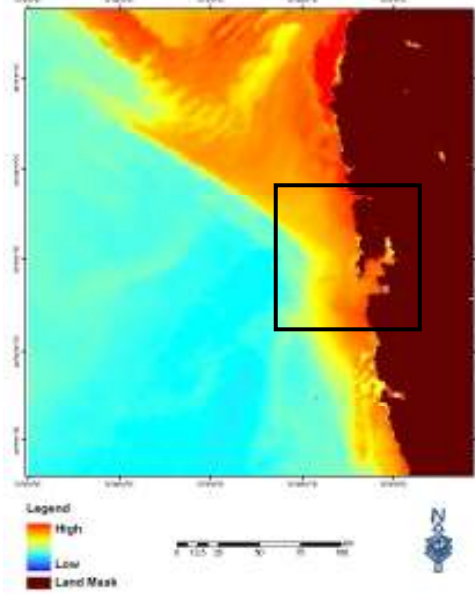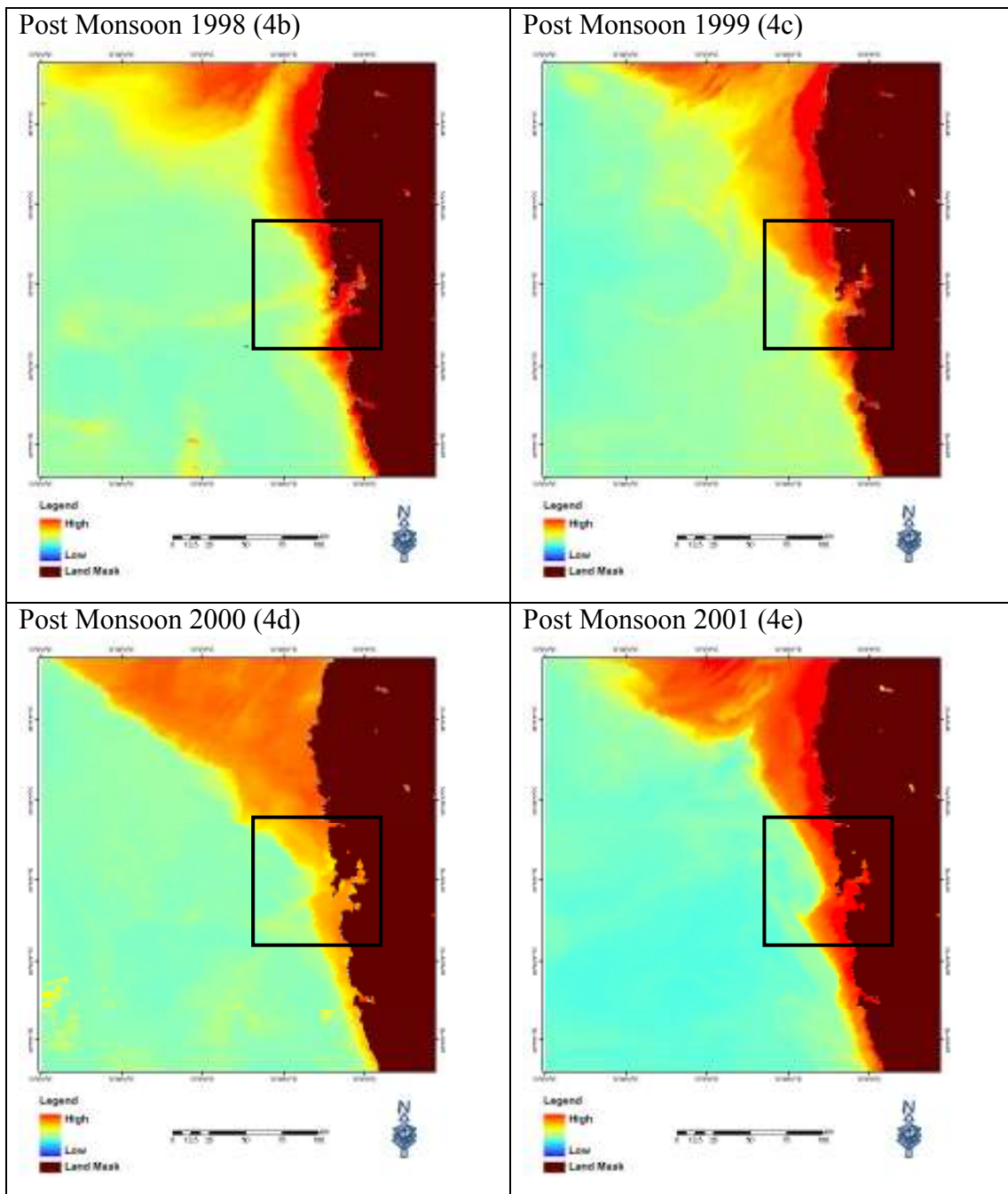
Figure 14: Figure numbered 3a – 4e are Chlorophyll_a conc. using Chlor_a_3 algorithm Pre and Post Monsoon Images (N.B.: The distinc differences between pre and post plume extent)
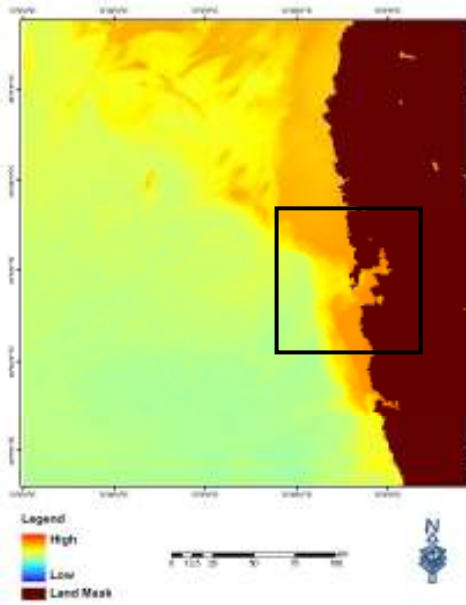
| Pre monsoon 1998 (5a)	Pre monsoon 1999 (5b)
Pre monsoon 2000 (5c)	Pre monsoon 2001 (5d)
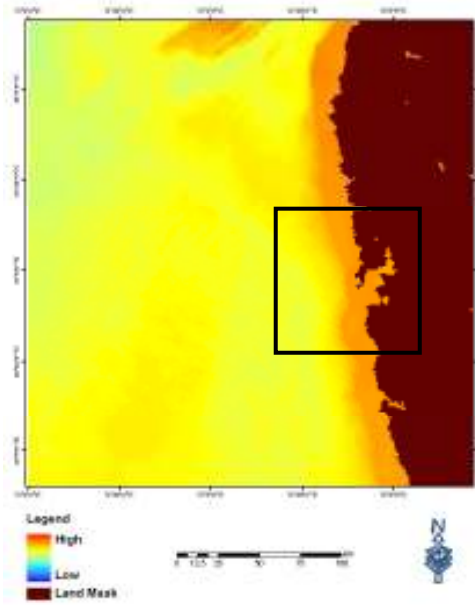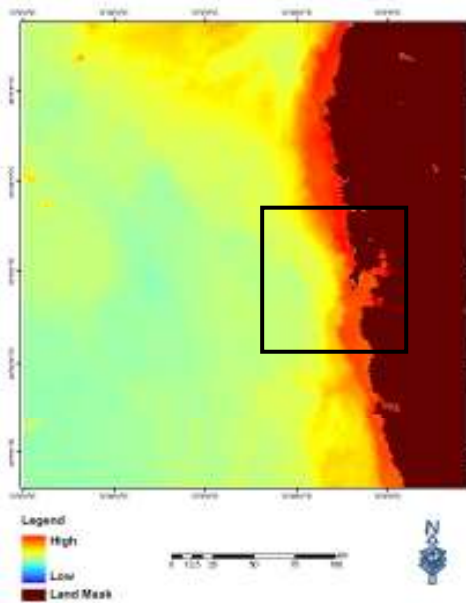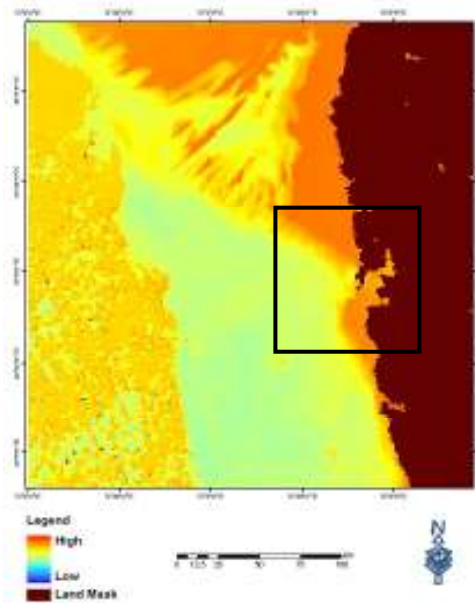
Pre monsoon 2002 (5e)
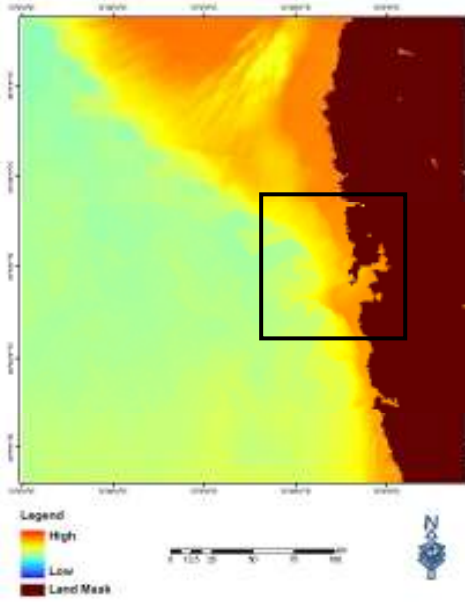
Post Monsoon 1997 (6a)
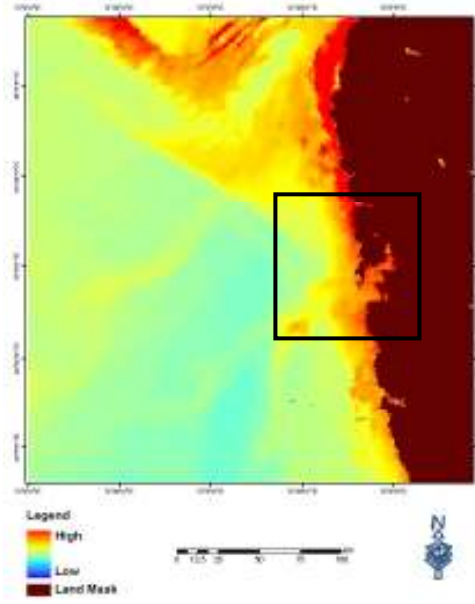
Post Monsoon 1998 (6b)
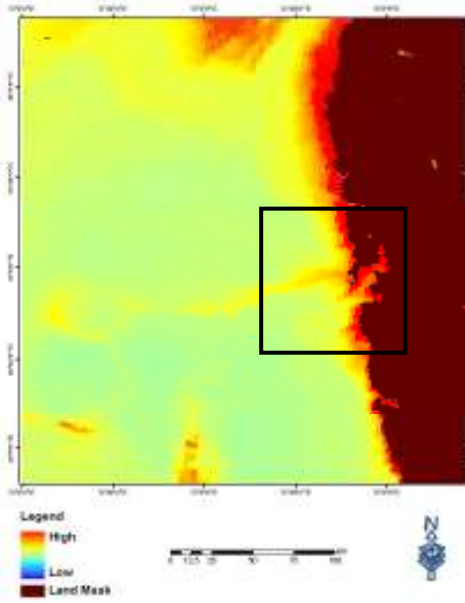
Post Monsoon 1999 (6c)
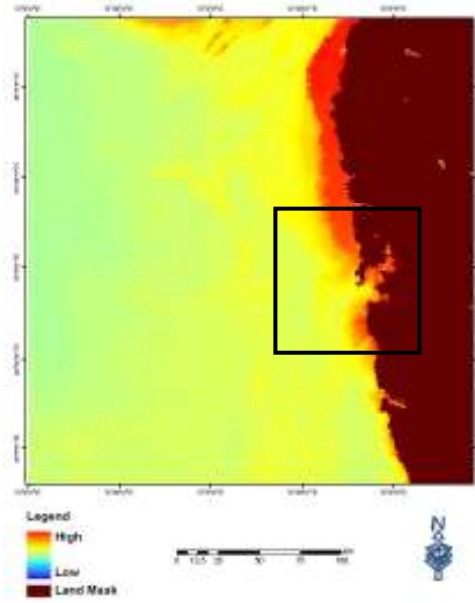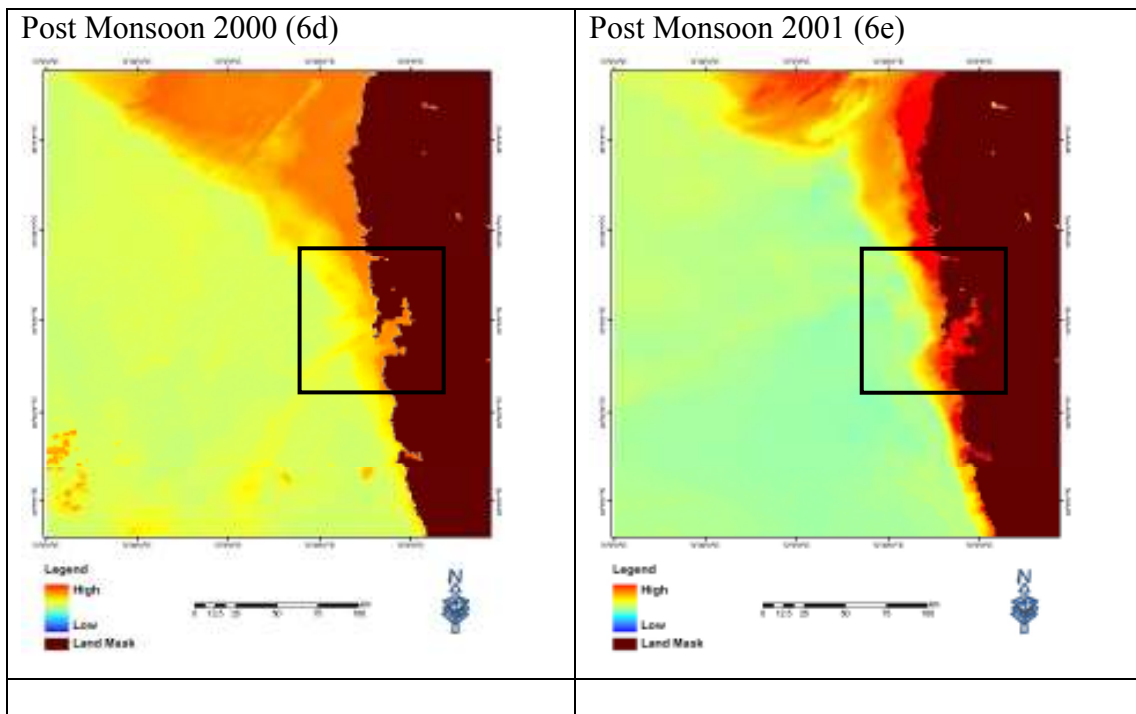
Figure 15: Figure numbered 5a – 6e are Suspended Particulate Matter (SPM) Pre monsoon and Post Monsoon Images Scenario Generation

The goal of this exercise was to generate a scenario of the outfall zone from extrapolation of pre-installation satellite data; to assess what could be the possible situation of the ambient waters of the study area in terms of the ocean colour parameters, if there were no outfalls installed in 2002-2003. This scenario has been generated using the data shown above. The data was linearly extrapolated to project the pre-monsoon and post-monsoon scenarios for ambient pollution in a present day scenario for the year 2009 and 2008 respectively.

Chlor-a2 Pre Monsoon 2009 (7a)
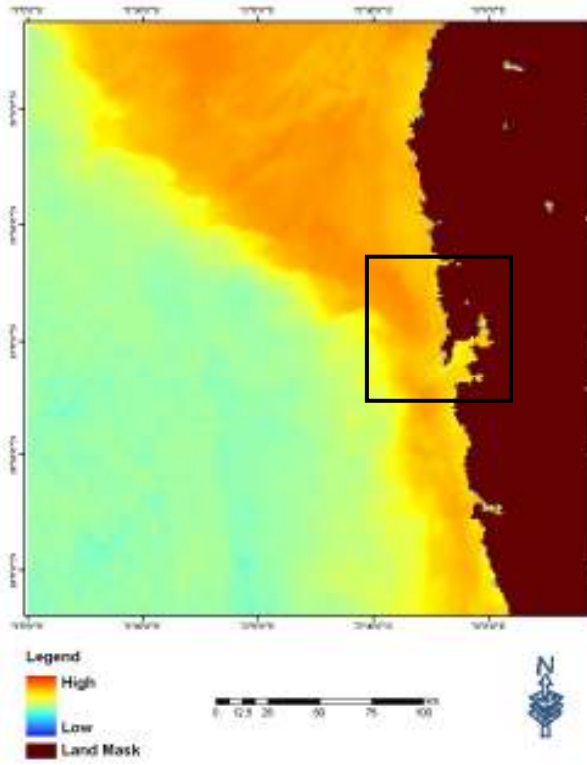
Chlor-a2 Post Monsoon 2008 (7b)
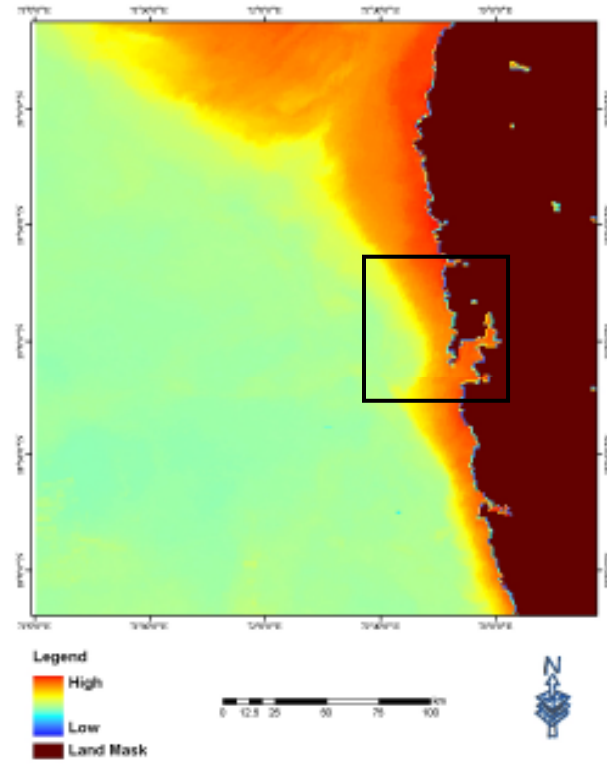
Chlor-a3 Pre Monsoon 2009 (7c)
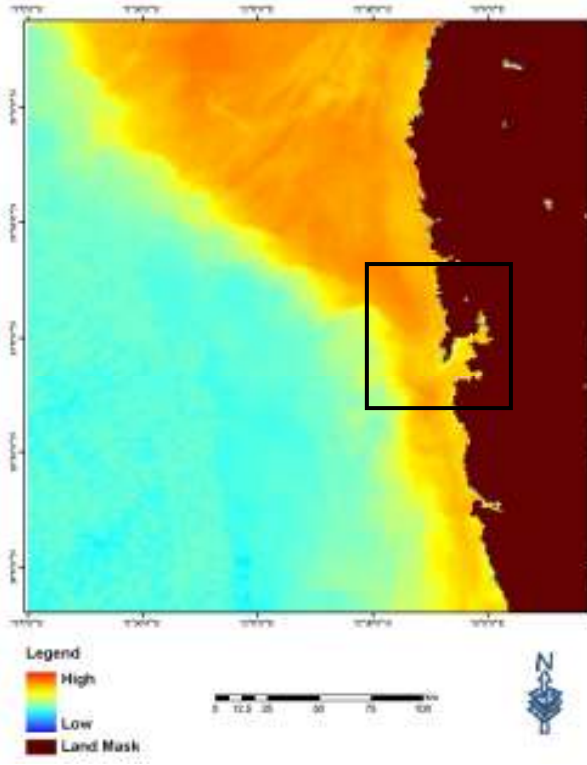
Chlor-a3 Post Monsoon 2008 (7d)
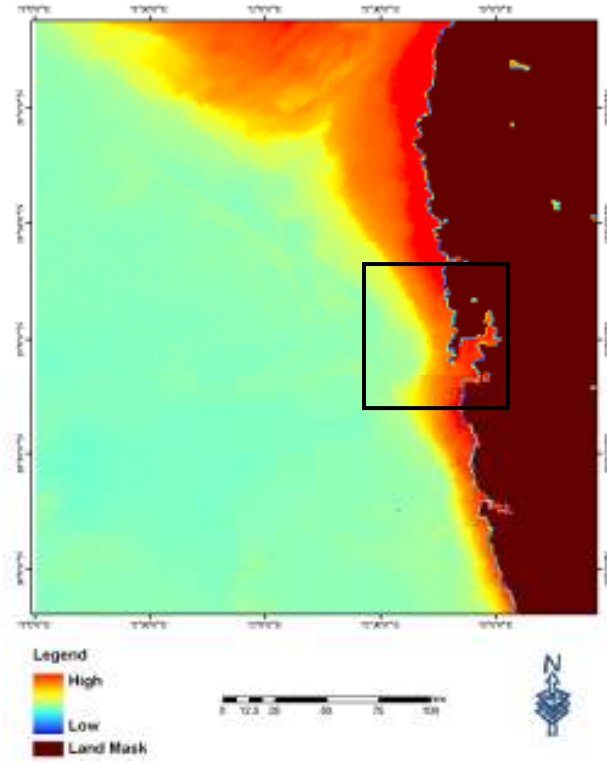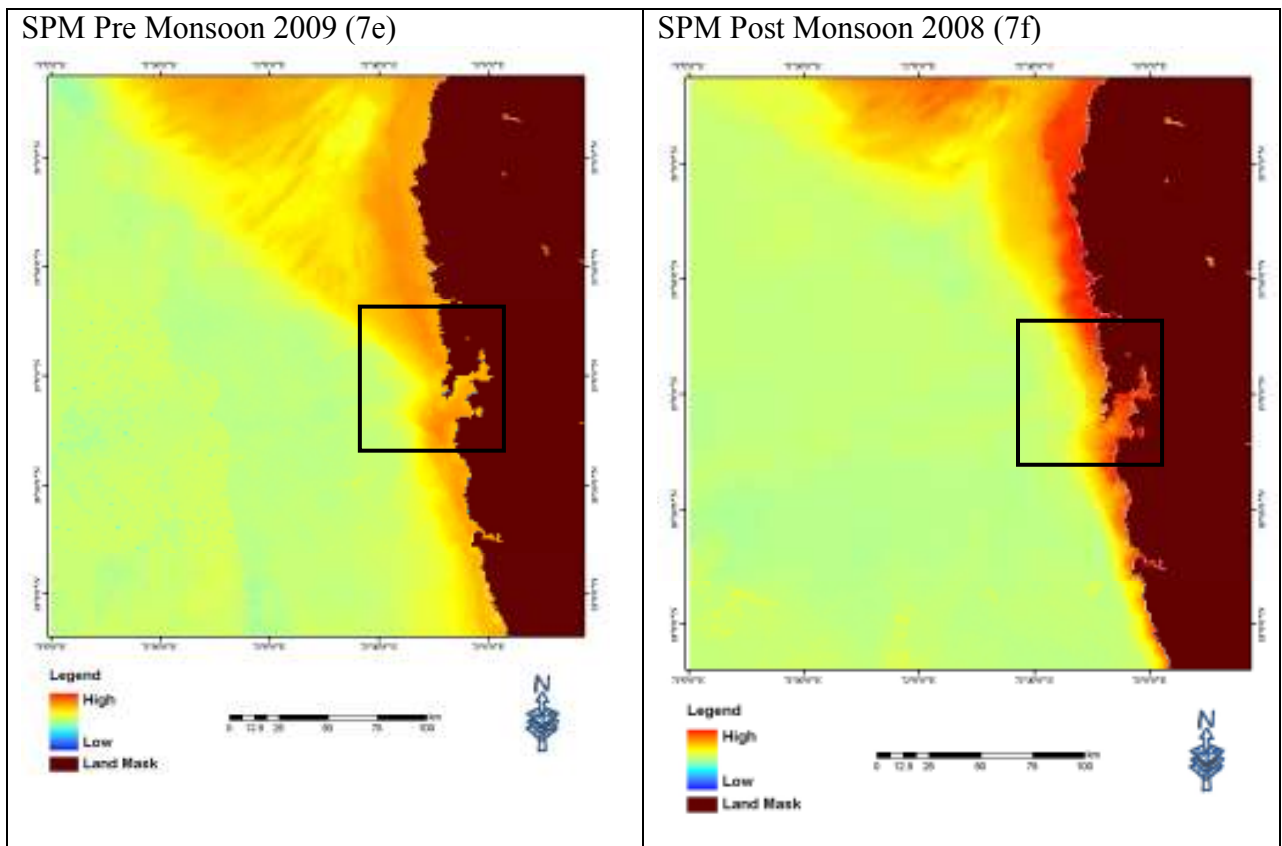
Figure 16: (figure 7a-7f) are Simulated Chlorophyll_a and SPM images for 2008 Post-Monsoon & 2009 Pre-Monsoon seasons.
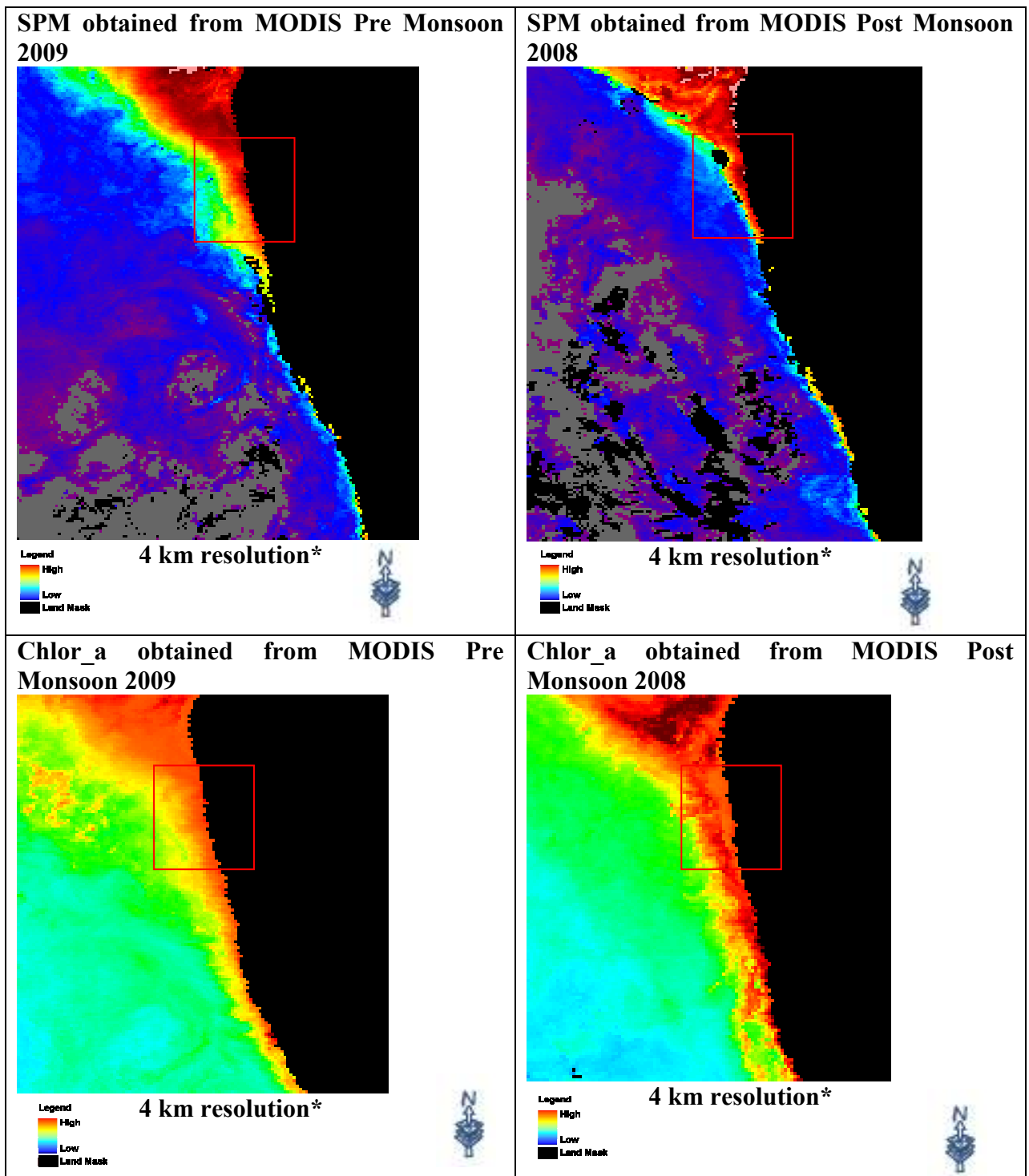
Figure 17: Actual Chlorophyll_a and SPM montly average images for 2008 Post-Monsoon & 2009 Pre-Monsoon seasons. (Note: The resolution of the these images are 4 km, The area marked in the red bounding box is the Bombay region. MODIS data is used for this comparision as the SeaWiFS data that is available is of a coarser resolution i.e. 9km)

4.3.2 Discussion

From the results shown above, several important observations can be made. The satellite data used for the work was mostly cloud free or with a cloud percentage below 10%. This, although lessening the noise level, generates a fair-weather bias in the data, which under the circumstances, is unavoidable. Also, data considered were mostly at the centre of the satellite swath, which removes most distortions due to satellite positioning and large swaths. This, along with bow-tie correction procedure applied in the data removed the geometric distortions to a great extent. But these measures also reduce the number of available datasets which could be used for the extrapolation of Chlorophyll-a concentration or SPM for later dates.

A comparison was made of the extrapolated data with actual later day images of 2008 and 2009 (daily data aggregated to monthly and seasonal averages), from MODIS sensor. The comparison was made from selecting points in the image far away in the open ocean, outside a 70 km radius buffer from the City of Mumbai, which was assumed to have undergone no significant changes in the last decade due to impact from the sewage disposal from the city. The results of these comparisons showed that the extrapolated data was 76% corroborated to the later day images, for the open ocean. Hence, the extrapolation results are taken to be valid for the study area.

4.4 Impact assessment on primary productivity

The aim of this exercise was to assess the impact of marine water quality changes happening over the years on ecological factors like Primary Productivity (PP) after the commissioning of the marine outfalls at Worli and Bandra. Using remotely sensed and field data, Vertically Generalized Production Model (VGPM) was generated to estimate PP in Mumbai waters over a period of 15 years and observations and conclusions based on this study have been presented below.

4.4.1 Behrenfeld-Falkowski Vertically Generalized Production Model (VGPM)

The Vertically Generalized Production Model (VGPM) described by Michael J. Behrenfeld and Paul G. Falkowski (1997), relates surface chlorophyll to depth-

integrated euphotic zone primary production. The form of the VGPM is that of many depth-integrated models (DIMs) which include a measure of depth-integrated phytoplankton biomass, estimated by the product of surface chlorophyll (C_{surf}) and euphotic depth (Z_{eu}), as well as inclusion of an irradiance dependent function [f (E_0)] and a photoadaptive yield term (P_{Bopt}) necessary to convert the estimated biomass into a photosynthetic rate (Behrenfeld and Falkowski, 1997). P_{Bopt}, the maximum carbon fixation rate within the water column, is the only model parameter that is neither relatable to sea surface chlorophyll, nor possible to be measure remotely. Attempts have been made to model this important photoadaptive parameter from sea surface temperature. Daylength (D_{irr}) is also included in the model, to scale observational data from hourly incubations to daily rates. The core equation of the VGPM is then:

$$\sum PP = 0.66125 \times E_0/ (E_0+4.1) \times P_{Bopt} \times C_{surf} \times Z_{eu} \times D_{irr} \ (mgC /m^2 /d)$$

Where:

PP: daily primary productivity in euphotic layer (unit: mgC / m^2 /day)

PBopt: the index shows optimum photosynthetic flux in euphotic layer

 (unit: g C/mg Chl / h)

E_0:   photosynthectically available radiation – PAR (unit: W/m2)

C_{surf} :   the surface chlorophyll content (unit: mg Chl/m3)

Z_{eu} :   euphotic depth (m)

D :   The daily photo period (h)

4.4.2 Data used and Method:

Both Sea-WiFS and MODIS-Terra sensor data have been used to generate long term trends of primary productivity in the study area. The data has been processed from the year 1997 till 2011, primarily chlorophyll-a concentration and Sea Surface Temperature derived from sensor emittive reflectance. The daily PAR values have been calculated from daily iPAR (instantaneous PAR) values obtained for MODIS

Aqua data from NASA ocean colour data archives and day light hours for the study area.

The VGPM model cited above was implemented and daily photo-period was taken directly from previous work on west coast of India (Suresh et al., 2006). The results are shown below.

4.4.3 Results and Discussion

The results of the exercise mainly consist of monthly mean estimates of primary productivity values (calculated from daily input images) for the study area, which were later aggregated into a standard deviation image for better understanding of the changes that the study area has undergone during the study period of 1997 to 2011 in terms of primary productivity rates. Each pixel in the image below represents the standard deviation in primary productivity values of that pixel and the images have been colour coded based on the level of standard deviation of each pixel. The minimum and maximum values of primary productivity observed in the study area from daily satellite images range from **0 to 240 mg carbon/ meter^2/ day.**
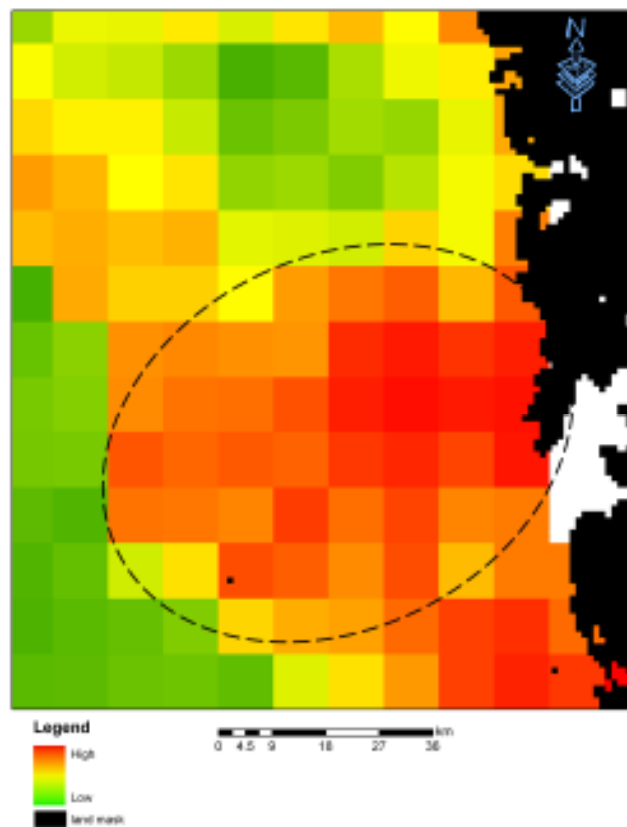
Figure 18: Aggregated Standard deviation in Primary Productivity (area bounded by the dashed line covers the highest level of standard deviation observed; referred to as "Plume" in the later section; the surrounding waters are referred to as "Non-Plume")

The area bounded by the dashed line shows the zone where highest amount of variation in primary productivity is found. As can be observed from the figure above, the zone undergoing maximum changes in the study area is also the zone most likely to have been influenced by the sewage discharge from the city of Mumbai. The white areas in the image are data gaps where data on was not available. It can also be observed that the surrounding areas of open ocean outside the area covered by the dashed line, are relatively undisturbed and mostly unaffected in the long term.

To better understand the nature of the changes in primary productivity in the area, the satellite images were further clumped into two seasonal groups,

- For pre-monsoon season (February to May)
- And for the post-monsoon season. (October to January)

Pre-monsoon
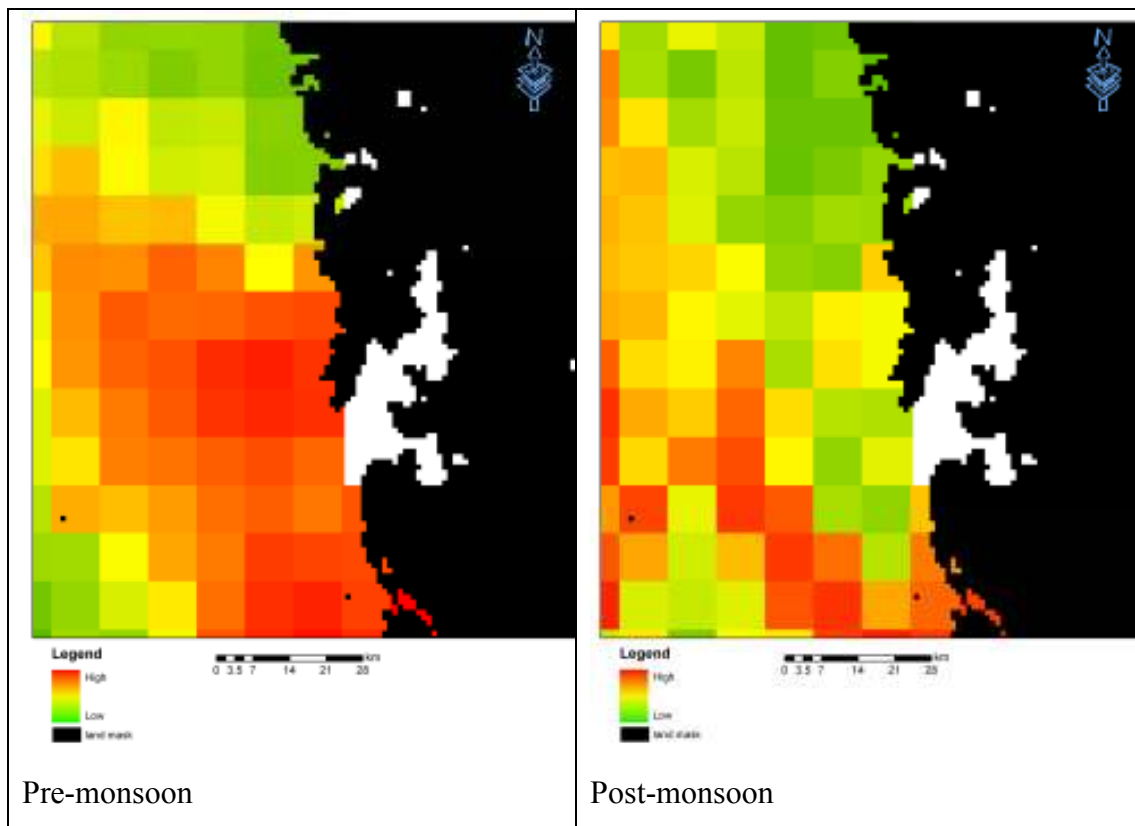
Post-monsoon

Figure 19: Pre- and Post- Monsoon primary productivity Image (Standard Deviation) (N.B.: Low 0 to High 240 mg carbon/ meter2/ day; Note that premonsoon variation is more compared to post mosnsson duration)

The figure above shows the standard deviation in primary productivity in the study area during the pre- and post-monsoon seasons. It can be seen from the images that the maximum amount of changes in primary productivity has taken place during the pre-monsoon season. This is very significant because the maximum amount of carbon fixation normally occurs during the pre-monsoon season in the Arabian Sea (Nagur et al, 2008).

Hence, the primary productivity values for the pre and post monsoon season have been plotted in a time series which are given below. For this purpose, monthly averages were calculated from daily data for two separate zones viz. area near the coast which is possibly affected by the sewage discharge from the city; and open ocean (referred to as 'Plume and 'Non-Plume', respectively, in figure no. 17, 19 and 20).
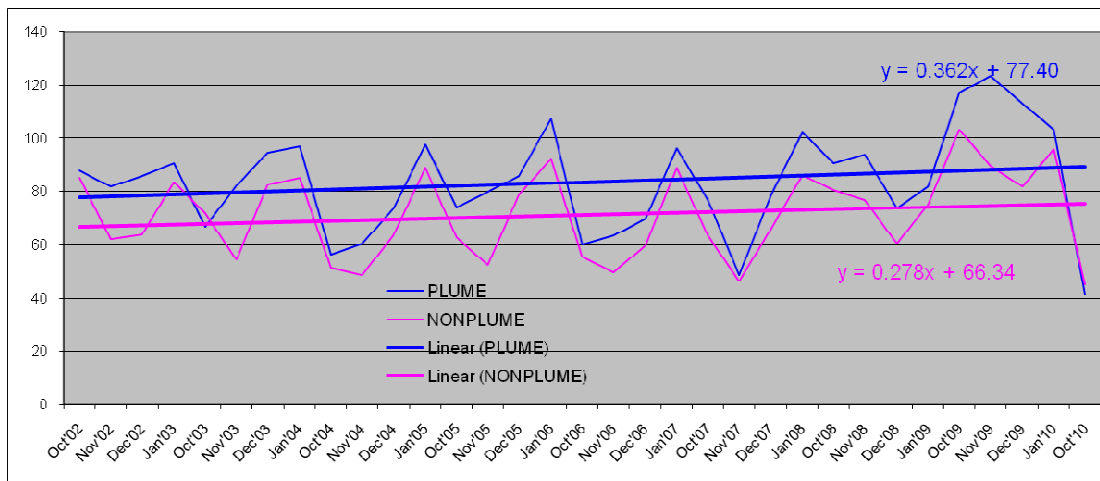
Figure 20: Post-monsoon Primary productivity trends for Plume & Non-plume areas (Area under the dashed line and Open Ocean, respectively, from figure 17).
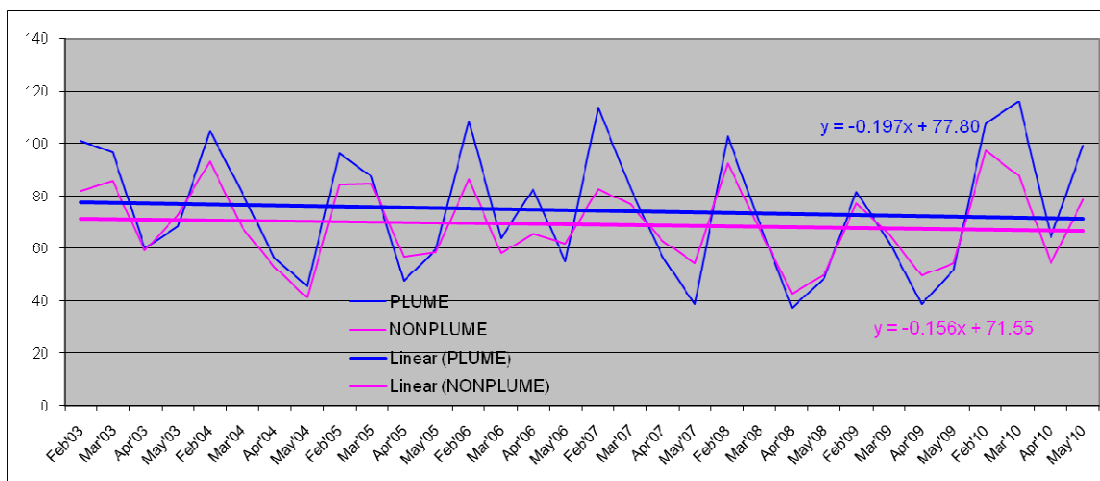
**Figure 21: Pre-monsoon Primary productivity trends for Plume & Non-plume areas (Area under the dashed line and Open Ocean, respectively, from figure 17)**
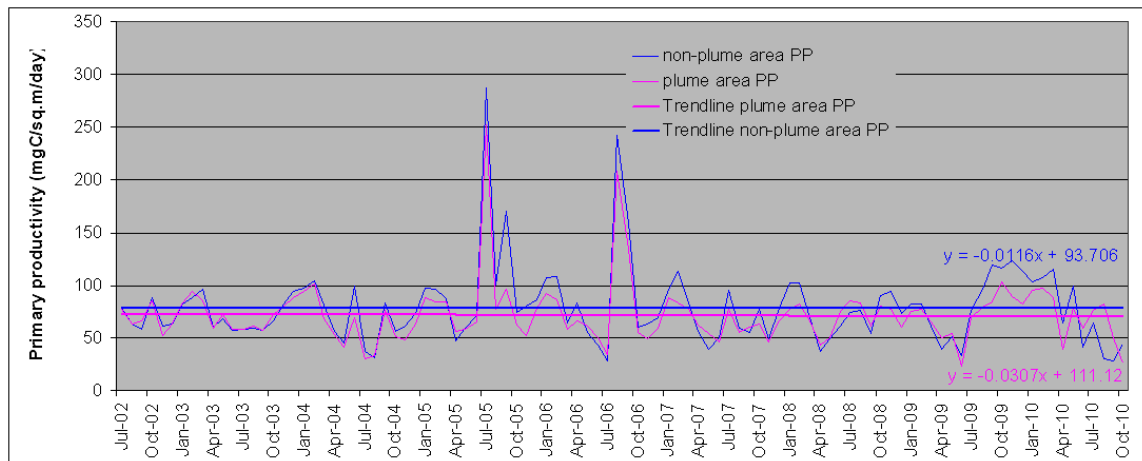
Figure 22: Primary productivity (over-all) trends for Plume & Non-plume areas (Area under the dashed line and Open Ocean, respectively, from figure 17).

As seen from the graphs above, primary production rates in the study area seem to be declining in the pre-monsoon season whereas they appear to be increasing slightly during the post-monsoon season. Also, during the pre-monsoon season, the amount and variability in the primary production rates are very close to each other for the plume area and Open Ocean; while during post-monsoon season, there are large variances between these two zones. From both these graphs, it can be observed that the most productive period for both the open ocean and the neritic zones over the years are months from December to February, which are the relatively colder months for the study area. The impact of a possible climatic warming of the area could be the reason behind the decrease in Primary production during these months; however, this possibility needs to be investigated in details with similar long term Sea Surface Temperature trends of the study area.

4.4.4 Conclusions:

There are several significant conclusions that were derived from the work detailed above.

1. Primary productivity rates show a high relative variance within the study area as revealed from long term standard deviation calculations for each pixel.
2. The variation is significantly more for an area which is possibly affected by the sewage disposal from the City of Mumbai, than the surrounding pelagic or open ocean waters.

55

3. The rate of primary production is found to be decreasing during the pre-monsoon season for the long term monthly average over the years 2002 to 2010.

4. Contrarily, primary productivity is found to increase slightly during the post-monsoon season in the study area.

5. Productivity appears to be highest during the colder months, December to February in the study area.

6. There is an overall decline in Primary Productivity during the past decade in the study area.

5 Discussion on the Model generation for propagation trend and futuristic impact assessment

The future goal of the project is to develop a model which would describe the flow propagation pattern and trends in a realistic three-dimensional manner, with the help of satellite data in a broad GIS based time-frame. Here, a general discussion including a short description of similar models and software developed or employed elsewhere in the world is given along with the rationale of the model being developed, is presented.

5.1 A comparison of existing models and software for similar work:

DESCAR Software:

DESCAR is a software for wastewater dispersion analysis. The program calculates the pollutant concentration in each point of the water considering each one of the pollutant sources and the conditions of the water. The system of simulation of processes of dispersion that DESCAR 3.2 has, offers to the beginner and the expert programmer, a quick and practical system to evaluate the dispersion of pollutants in the water. The program is based on the operating system Microsoft WINDOWS where one works intensively with the mouse and the graphic windows. We can say, with certainty that the software DESCAR 3.2 is one of the best tools, to carry out numeric simulations of water pollution processes.

FMS (Flexible Modeling System):

FMS is a software framework for supporting the efficient development, construction, execution, and scientific interpretation of atmospheric, oceanic and climate system models. FMS comprises the following:

- A software infrastructure for constructing and running atmospheric, oceanic and climate system models. This infrastructure includes software to handle parallelization, input and output, time management, data exchange between various model grids, make files, and simple sample run scripts. This

infrastructure should largely insulate FMS users from machine-specific details.

- A standardization of the interfaces between various component models.

- Software for standardizing, coordinating and improving diagnostic calculations of FMS-based models, and input data preparation for such models. Common preprocessing and post-processing software are included to the extent that the needed functionality cannot be adequately provided by available third-party software.

- A rigorous software quality review and improvement process to assist in contributed component models. The development and initial testing of these component models is largely a scientific question, and would not fall under FMS. The quality review and improvement process includes consideration of

- Compliance with FMS interface and documentation standards to ensure portability and inter-operability

- Understandability (clarity and consistency of documentation, comments, interfaces, and code)

- General computational efficiency without algorithmic changes.

- A standardized technique for version control and dissemination of the software and documentation.

HYCOM (HYbrid Coordinate Ocean Model)

The hybrid coordinate is one that is isopycnal in the open, stratified ocean, but smoothly reverts to a terrain-following coordinate in shallow coastal regions, and to z-level coordinates in the mixed layer and/or unstratified seas. The hybrid coordinate extends the geographic range of applicability of traditional isopycnic coordinate circulation models (the basis of the present hybrid code), such as the Miami Isopycnic Coordinate Ocean Model (MICOM) and the Navy Layered Ocean Model (NLOM), toward shallow coastal seas and unstratified parts of the world ocean. The theoretical foundation for implementing such a coordinate was set forth in Bleck and Boudra (1981) and Bleck and Benjamin (1993). In HYCOM, each coordinate surface is assigned a reference isopycnal. The model continually checks whether or not grid points lie on their reference isopycnals and, if not, tries to move them vertically toward the latter. However, the grid points are not allowed to migrate when this

would lead to excessive crowding of coordinate surfaces. Thus, in shallow water, vertical grid points are geometrically constrained to remain at a fixed depth while being allowed to join and follow their reference isopycnals over the adjacent deep ocean.

In the mixed layer, grid points are placed vertically so that a smooth transition of each layer interface from an isopycnic to a constant-depth surface occurs where the interface outcrops into the mixed layer. HYCOM therefore behaves like a conventional sigma model in very shallow and/or unstratified oceanic regions, like a z-level coordinate model in the mixed layer or other unstratified regions, and like an isopycnic-coordinate model in stratified regions. In doing so, the model combines the advantages of the different types of coordinates in optimally simulating coastal and open-ocean circulation features. The present procedure of driving high-resolution coastal models (which invariably use fixed vertical grids) with output from a basin-scale isopycnic model can be streamlined, since HYCOM will be able to provide the required near-shore data at fixed depth intervals.

CORnell MIXixing zone model

CORMIX is a USEPA-approved methodology for simulation of turbulent buoyant jet mixing behavior which covers a majority of common discharge and environmental conditions. It classifies momentum and buoyancy of the discharge in relation to boundary interactions to accurately predict mixing behavior. Boundary interactions can be flow surface or bottom contact or terminal layer formation in density stratified ambients.

The hydrodynamic simulation system contains a collection of regional flow models based upon integral, length scale, and passive diffusion approaches to simulate the hydrodynamics of near-field and far-field mixing zones. Efficient computational algorithms provide simulation results in seconds for mixing zone problems with space scales of meters to kilometers and time scales of seconds to hours.

The CORMIX methodology contains systems to model submerged single-port and multiport diffuser discharges as well as surface discharge sources. Effluents considered may be conservative, non-conservative, heated, or contain suspended sediments. CORMIX can predict mixing behavior from diverse discharge types

ranging from power plant cooling waters, desalinization facility or drilling rig brines, municipal wastewater, or thermal atmospheric plumes. CORMIX can also be applied across a broad range of ambient conditions ranging from estuaries, deep oceans, swift shallow rivers, to density stratified reservoirs and lakes.

Some special hydrodynamic features of CORMIX include:

- Makes complete near-field and far-field plume trajectory, shape, concentration, and dilution predictions.
- Includes plume boundary interactions, including dynamic near-field attachments.
- Predicts density current behavior with buoyant upstream wedge intrusion and stagnation points.
- Models conservative, non-conservative, and heated pollutant types.
- Application to steady, unsteady ambient currents/tides, or stagnant ambient conditions.
- Predicts stratified atmospheric plumes with skewed wind velocity.

Flow and Solute Transport Model for Estuaries and Rivers

FASTER is a numerical hydrodynamic, solute and sediment transport model for unsteady and subcritical gradually varied flow in a one-dimensional well-mixed river or estuarine system. The unsteady gradually varied flow is solved through an implicit finite difference scheme with varying grid size over a space staggered grid. The solute and sediment transport part of the model is solved by a new implicit scheme, which is a combination between finite volume central scheme and the highly accurate ULTIMATE QUICKEST scheme. The model accommodates variable channel geometry and any number of interacting channel segments or reaches. There is complete flexibility in the specification of open boundary conditions, also the junction solutions are established by an influence line technique.

The fundamental notions and hypotheses used in the mathematical modeling of rivers are formalized in the equations of unsteady open channel flow. It is assumed that all the St. Venant hypotheses are valid. The basic assumptions are that the flow

is in one-dimension, the water is homogeneous and that hydrostatic pressure distributions and Coriolis accelerations may be neglected.

In the model, the cross sectional areas of the flow at the nodes are calculated by means of a divided channel method. According to this method the model divides each cross section into several subsections and it has been assumed that the whole discharge passing through the section is the summation of the discharges passing through all the subsections. Since the model is able to specify the dry and wet parts in the cross section, the cross sectional area, wetted perimeter, top width of flow and the other hydraulic parameters related to the cross sections can be calculated accurately.

FASTER was developed using the FORTRAN 77 programming language by Prof. R.A. Falconer, Halcrow Professor of Environmental Water Management, and Dr. S. Kashefipour, both of the Cardiff School of Engineering, Cardiff University, UK. FASTER is continually updated and improved by both Prof. Falconer's team in Cardiff University and the MarCon staff.

Princeton Ocean Model

POM is a three dimensional, sigma coordinate, hydrodynamic and thermodynamic model. POM was originally develop by Alan Blumberg and George Mellor in 1977 and applied to oceanographic problems in the Atmospheric and Oceanic Sciences Program of Princeton University and the Geophysical Fluid Dynamics Laboratory of NOAA. Published papers that describe the numerical model or applications of the numerical model may be found at the model website here.

The principle attributes of the POM model are:

- It contains an imbedded second moment turbulence closure sub-model to provide vertical mixing coefficients.
- It is a sigma coordinate model, in that the vertical coordinate is scaled over the water column depth.
- The horizontal grid uses curvilinear orthogonal coordinates or rectilinear coordinates and an 'Arakawa-C' differencing scheme.

- The horizontal time differencing is explicit whereas the vertical differencing is implicit.
- The model has a free surface and a split time step.
    - The external mode portion of the model is two dimensional and uses a short time step based on the Courant-Friedrichs-Levy (CFL) condition and the external wave speed.
    - The internal mode portion of the model is three dimensional and uses a long time-step based on the CFL condition and the internal wave speed.
- Complete thermodynamics have been included.

The equations governing the dynamics of coastal circulation contain fast moving external gravity waves and slow moving internal gravity waves. It is desirable in terms of computer economy to separate the vertically integrated equations (external mode) from the vertical structure equations (internal mode). This technique, known as mode splitting permits the calculation of the free surface elevation with little sacrifice in computational time by solving the velocity transport separately from the three dimensional calculation of the velocity and thermodynamic properties. The velocity transport, external mode equations are obtained by integrating the internal mode equations over the depth, thereby eliminating all vertical structure. The external mode calculations results in updates for surface elevation and vertically averaged velocities. The internal mode calculations result in updates for the sigma layer velocities, thermodynamics and turbulence quantities.

The Courant-Friedrichs-Levy, (CFL), computational stability condition on the vertically integrated, external mode, transport equations limits the time step according to a relationship based on water depth and maximum current velocity. There are other restrictions but the CFL is the most stringent. The model time-step is usually ~90% of the CFL limit. The internal mode has a much less stringent time-step constraint since the fast moving external mode effects have been eliminated. The computational stability criteria for the internal model limit the time-step according to a relationship based on the maximum internal gravity wave speed and the maximum advective speed. For typical coastal ocean conditions the ratio of the timesteps INT/EXT is often a factor of 50 - 80 or greater.

There is an extensive online POM users community, of which the MarCon staff are members, involved in the application, extension and modification of the POM source code and the discussion or various aspects of coastal and ocean modeling.

5.2   Scope for new model

The entire study area is divided into uniform 3D grid. The extent of dispersion of the sewage is estimated by taking into account the effect of bathymetry, tide, current, wind, sewage characteristics, and outfall characteristics.   The bathymetry is important as it can lead to change in the direction of the sewage flow. The direction and speed of the tide, current and wind have a great influence on the sewage flow direction. As waves are a result of currents and dominant wind flow, waves have not been considered as a primary parameter for the proposed model. With every time step the dispersion patterns of the sewage change according to the effect of external parameters. Satellite images have been used to generate SPM (Suspended Particulate Matter), primary productivity and wind data. The details of the satellite data used are listed below.

5.3   Satellite data used

QuikSCAT (till 2009) ASAT (2009 onwards)

The SeaWinds on QuikSCAT Level 2B data set consists of wind vector solutions for all four wind vector ambiguities as well as the Direction Interval Retrieval with Threshold Nudging (DIRTH) wind vector solution. Each Level 2B file contains data for one full orbital revolution of the spacecraft or rev. These data are grouped by rows of 25km wind vector cells (WVC). Each row contains a total of 76 WVC values and corresponds to a single cross-track cut of the SeaWinds swath. 1624 wind vector cell rows are required to complete a rev. Data are currently available in Hierarchical Data Format (HDF) and exist from 19 July 1999 to present. The Level 2B data are derived from QuikSCAT Level 2A sigma-0 measurements. When rain is present, the measurements of the ocean surface sigma-0 are affected in several ways. The radar signal may be scattered by the raindrops and never reach the ocean's surface. The radar signal may be attenuated by the rain as it travels to and from the earth's surface. The roughness of the sea surface due to the splashing of the raindrops may

also affect the sigma-0 measurement and thus the wind vector solution. In an effort to indicate the presence of rain, the Level 2B data include the Multidimensional Histogram Rain Flag SDS (mp_rain_probability) and the Normalized Objective Function Rain Flag SDS (nof_rain_index). In addition, wvc_quality_flag bit 13 indicates whether or not the rain flag algorithm indicates rain. These data are available via anonymous FTP. Documentation, read software, and further information may also be obtained from the PO.DAAC QuikSCAT Web site, http://podaac.jpl.nasa.gov/quikscat/

OSCAR

World Ocean Surface Currents (OSCAR - Ocean Surface Current Analyses - Real Time) (1993-present) Ocean Surface Currents Analysis Real-time (OSCAR) is the product of several years of collaborative effort between the NOAA/NESDIS Laboratory for Satellite Altimetry (LSA), NOAA/PMEL and Earth & Space Research (ESR, a non-profit research institution). OSCAR is a global ocean circulation data set based on NOAA and NASA satellite data (sea level altimetry, surface vector winds, and SST) and continuously updated every 5 days. The program has been supported by NOAA/NESDIS, originally through the National Ocean Partnerships Program (NOPP), then via a NOAA Congressional "Research to Operations" appropriation and financial support from the NOAA Office of Climate Observations (OCO). The climate record extends from 1993 to the present. The data are being served via the interactive website www.oscar.noaa.gov.

5.4 Rationale of model

The current model can be divided into two phases 1) flow model 2) validation and optimization using RS/GIS data integrated framework. The model hence derived can be used for futuristic estimation of plume propagation.

The model uses tide, current, wind, bathymetry as important geo-physical parameters along with sewage characteristics (mainly density, BOD and COD) and outfall design parameters. Mixing due to waves is not considered as separate / primary parameter for this model as waves are mainly generated due to wind, current and tides. These driving parameters for waves are considered separately for

the model. Mixing due to temperature is not considered due the fact that the vertical mixing is done thoroughly for entire water column depth (based on the field data collected).

References

Bowers, D. G., Harker, G. E. L., Smith, P. S. D., Tett, P., 2000. Optical properties of a region of freshwater influence (the Clyde Sea). Estuarine Coastal and Shelf Science, 50, 717 :.- 726.

Carder, K L., Steward, R. G., Harvey, G. R., Ortner, P. B. 1989. Marine humic and fulvic acids: their effects on remote sensing of ocean chlorophyll. Limnology and Oceanography, 34, 1, 68-81.

Clemente-Colon P. and Pitchel W.G. (2006), Remote Sensing of Marine Pollution, Chapter 7 in Remote Sensing of the Marine Environment , Manual of Remote Sensing 3rd Edition, Publisher ASPRS, USA, PP – 197-229

Green, S., Blough, N. 1994. Optical absorption and fluorescence properties of chomophoric dissolved organic matter in the natural waters. Limnology and Oceanography, 39, 1903 1916.

Kowalczuk. P., Kaczmark, S. 1996. Analysis of temporal and spatial variability of Yellow Substance absorption in the southern Baltic. Oceanologia, 3 - 32.

Lakshmi Vyas and Sapna Vyas (2007), Simulation Models for the dispersion of sewage outfalls along the west coast of Mumbai, India, in Proceeds. of the 7th WSEAS International Conference on Simulation, Modelling and Optimization, Beijing, China, September 15-17, 2007, pp. 502-507

NEERI (1995), Final Report – BSDP Marine Outfalls, EnvironmentalAssessment/ Analysis Reports (Report 2 of 4), India- BSDP, EA Category A, Report E0071, P – 161

S.S. Dhage *, A.A. Chandorkar, Rakesh Kumar, A. Srivastava, I. Gupta (2006), Marine water quality assessment at Mumbai West Coast in Environment International V.32, PP- 149-158

Stedmon, C. A., Markager, S. 2003. Behaviour of the optical properties of coloured dissolved organic matter under conservative mixing. Estuarine, Coastal and Shelf Science, 57, 1-7.

BMB, 1979, Recommendations on methods for marine biological studies in the Baltic Sea.

Subodh Kumar & Parekh K.P., (1999), Disposal of sewage through deep sea marine outfall into coastal marine envronment – A case study, in Proceeds. of Integrated Coastal Management Workshop, with Special Reference to Western Coast of India, Nov.29-30, 1999, P 1-5

Phytoplankton and chlorophyll, [Ed. L. Edler], BMB, 5

Gordon, H. R., Morel, A. 1983. Remote assessment for ocean colour for interpretation of satellite visible imagery - A review. Springer-Verlag, New York, 114.

Guideline for Baltic Monitoring Program, 1988, Baltic Marine Environment Protection Commision, Helsinki, 116.

Jeffrey S. W., Humphrey G. F., 1975, New spectrophotometric equation for determining chlorophyll a, b, c1 and c2, Biochem. Physiol. Pflanz., 167, 194-204

Lorenzen C. J., 1967, Determination of. chlorophyll and phaeopigments: spectrophotometric equations, Limnol. Oceanogr., 12

Mobley, C.D. 1994. Light and Water - Radiative Transfer in Natural Water. London Academic Press, 95 - 100.

Strickland and Parson, 1972 Strickland, J.D., Parson, T. R. 1972. A Practical handbook of Seawater Analysis. Bulletin of Fishery Research Board, Canada, 167 - 310.

Strickland J. D. H., Parsons T. R., 1968, A practical handbook of seawater analysis. Pigment analysis, Bull. Fish. Res. Bd. Canada, 167

UNESCO, 1966, Determinations of photosynthetic pigments in seawater, Rep. SCOR/UNESCO WG 17, UNESCO Monogr. Oceanogr. Methodol., 1, Paris

APHA. (1998). Standard methods for the examination of water and wastewater. 19th Edition.

American Public Health Association, American Water Works Association, Water Pollution Control Federation, Washington, DC.

Morel, A. 1988. Optical modeling of the upper ocean in relation to its biogenous matter content (case I waters). Journal of Geophysical Research, 93, C9, 10749 - 10768.

T. Suresh, P. Naik, M. Bandishte*, E. Desa, A. Mascaranahas, S.G. Prabhu Matondkar. 2006. Secchi Depth Analysis Using Bio-Optical Parameters Measured In The Arabian Sea. Remote Sensing of the Marine Environment, edited by Robert J. Frouin, Vijay K. Agarwal, Hiroshi Kawamura, Shailesh Nayak, Delu Pan, Proc. of SPIE Vol. 6406, 64061Q, 2006.

Annexure I: Thermal Monitoring of Thane (Vashi) Creek and Mahul Creek: Submitted to MPCB.

Introduction

India has over 6000 km of coastline. Its territorial seas alone come to about 0.13 million square km (with 12 nautical miles as limit). The exclusive economic zone (EEZ) covers an area of about 2.3 million square km including those around the islands. However, As far as coastal development and pollution are concerned only the territorial seas and brackish waters are of greater relevance. This long stretch of coastline consists of various types of lands like marshes, mangrove swamps, hilly or raised areas, rocky coasts, sandy coasts, cities and ports. These varied coastal environments are regularly used for ports and shipping, waste dumping from variety of industries, fishing, salt pans, aquaculture; recreation and water sports at the same time.

The Central Pollution Control Board (Government of India) has classified the entire coastal areas into five types based on evaluations of 'best-use-of-coastal segment' from traditional and organised uses and activities. They are:

- SW1 – salt pans, mariculture, contact water sports and ecologically sensitive areas,
- SW2 – fishing and noncontact recreation,
- SW3 – industrial cooling and aesthetics,
- SW4 – harbours and
- SW5 – navigation and coastal waste disposal.

According to this classification the central west coast of India including northern Karnataka, Goa and southern Maharashtra is grouped under SW1. Yet, off Mumbai, the coastal waters are hardly amenable to contact usage and are polluted enough to affect the fisheries. The main sources of pollution of the Mumbai coast are urban sewage, drilling and shipping of crude oil, industrial effluents like chemicals, heat etc.

Mahul and Vashi creeks, which are the main focus of this study receive a variety of pollutants from a variety of industries based in the Thane -Belapur industrial belt. The effluents that make their way to these creeks comprise chemicals, antropogenic waste as well as discharges from refineries and nuclear establishments. These sources keep degrading the coastal water bodies in many ways that can be classified into chemical, biological as well as physical. Temperature is one of the most important physical attributes amongst the physical type of pollution that governs the marine life, besides other things. Thermal pollution of rivers and coastal seas by heat released from coolants from the factories is a serious environmental problem causing destruction and imbalance of aquatic life. Many aquatic lives are very temperature sensitive. The warm waste water released into coastal seas raises the ambient temperature causing physiological and other problems to aquatic organisms. Standard guidelines exist for levels of permitted warming to avoid harm to aquatic life. In tropical regions 2°C rise can be harmful.

To monitor the sewage, river discharge and other sources of pollution regularly and synoptically is a challenge of the coastal environment management. Towards this purpose, one of the most important tools is remotely sensed satellite imagery and ancillary data analysis. Thermal sensors on some of the satellites (MODIS, AVHRR, etc) are most effective in assessing and monitoring the Sea Surface Temperature (SST) and were successfully utilized through this study of satellite images of last 6-7 years

Thane (Vashi) Creek and Mahul Creek

Thane Creek is part of the estuary of Ulhas River opening into Bombay Harbour. It has been recognized as an Important Area for bird watching by the Bombay Natural History Society, as it is home to flamingoes and several other migratory and wading birds.

Mahul Creek is a tidal creek in northwest Mumbai. It opens into the Thane Creek. The creek is surrounded by mangrove forests. When measured from the high tide line of one bank to another, the creek is over 350 metres (1,148 ft) wide at its mouth. The creek also serves as a source of discharge for excess rainwater in eastern suburban Mumbai. This creek is surrounded by industries like BPCL and Tata

refineries, RCF and BARC which are dependent on the sea water for their functioning. Migratory birds come to this creek every winter. Bordering the Mahul Creek on its west is the area around the village of Anik, which was reserved as coastal no-development zone, being largely salt-pans and lands flooded by the sea during very high tides and swamps populated by migratory birds. The Anik wetlands also act as sponges absorbing excessive surface runoffs

Sea-truth Data Collection

For this study, the most important requirement was sea-truth data (ship board measurement of water quality parameters) to validate the satellite image-derived algorithms. Details of the methodology to be followed for water sample collection and further chemical analysis are given below.

Most of the observations were carried out on-board mechanised fishing vessels. Surface water samples were collected using cleaned polythene buckets. Water from varied depths was collected using a sampler. Ambient water temperature was recorded by a centigrade thermometer.

Analytical methods followed for this project were as per the Standard Methods of the American Public health Association, 1998. The estimated water quality parameters can be classified, sensu lato, into three groups, i.e., physico-chemical parameters (Dissolved Oxygen, pH, and water temperature), biological parameters (photosynthetic pigments and during the rainy season.

Sea Surface Temperature (SST estimation) from MODIS data

SST has been estimated from daily MODIS (Terra) images which were cloud-free and had minimum positional distortion. Monthly average of SST were generated for every year from 2004 (December) to March (2010) for the months December, January and March, from the daily images. These three months have been analyzed as they showed the maximum variation with minimum cloud interference; December being the beginning of winter after the post-monsoon season, January is the coldest month of the study area and March is the transition period from cold to summer. These months show the major SST variation and reflect possible anthropogenic sources of increased heat in the waters.

Monthly averages then were aggregated to generate yearly month-wise averages (December, January and March averages for the year given above). Standard deviation was calculated for daily images and yearly averages for the above-mentioned months were calculated. To generate the regional SST trends, the 1 km pixel size images were resampled to a 5 x 5 km grid size and a land-mask has been applied to the images. Monthly average images for the month of December are shown below. Due to the global nature of the SST algorithm applied here, the estimated SST in the study area was found to be consistently lower by 7-8 degree Kelvin than the ground measurements. However, as this error is very continuous and not random, and as the study is more or less comparative than qualitative, no correction has been applied to the images. The correction is however applied when using the SST images as a parameter for Primary Productivity estimation at a later stage.
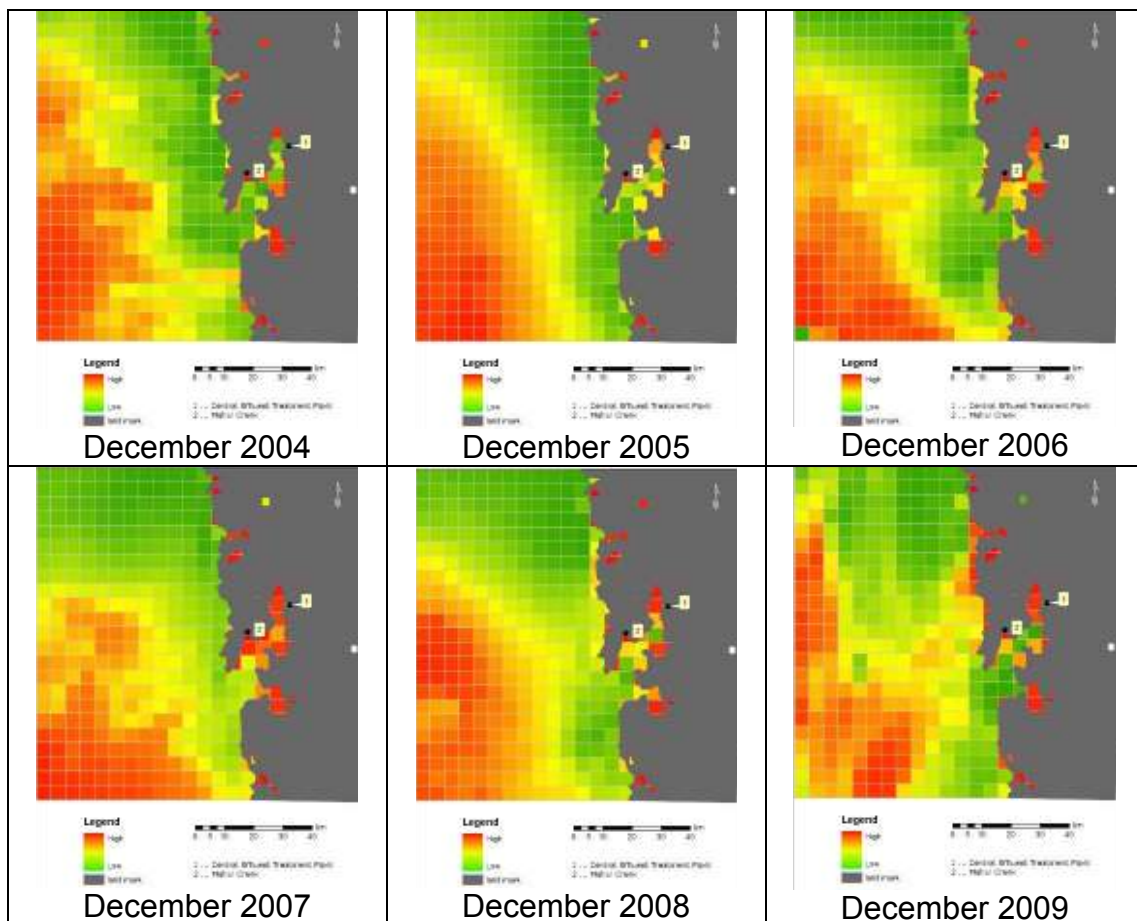
Figure 1: Monthly average SST for the month of December (2004-2010)

As seen in the figure 1, during December, warm water was found to occur at a distance of 30-40 km from the shoreline, every year. The standard deviation in SST in these areas shows a pretty stable condition during this month for every year of the study period. Hence it can be assumed that warm water is part of some eddy structure forming off the coast in the study area during the winter months. However, the water close to coast is not affected by this phenomenon and shows a large variation, as seen in the standard deviation SST image (Fig.2)
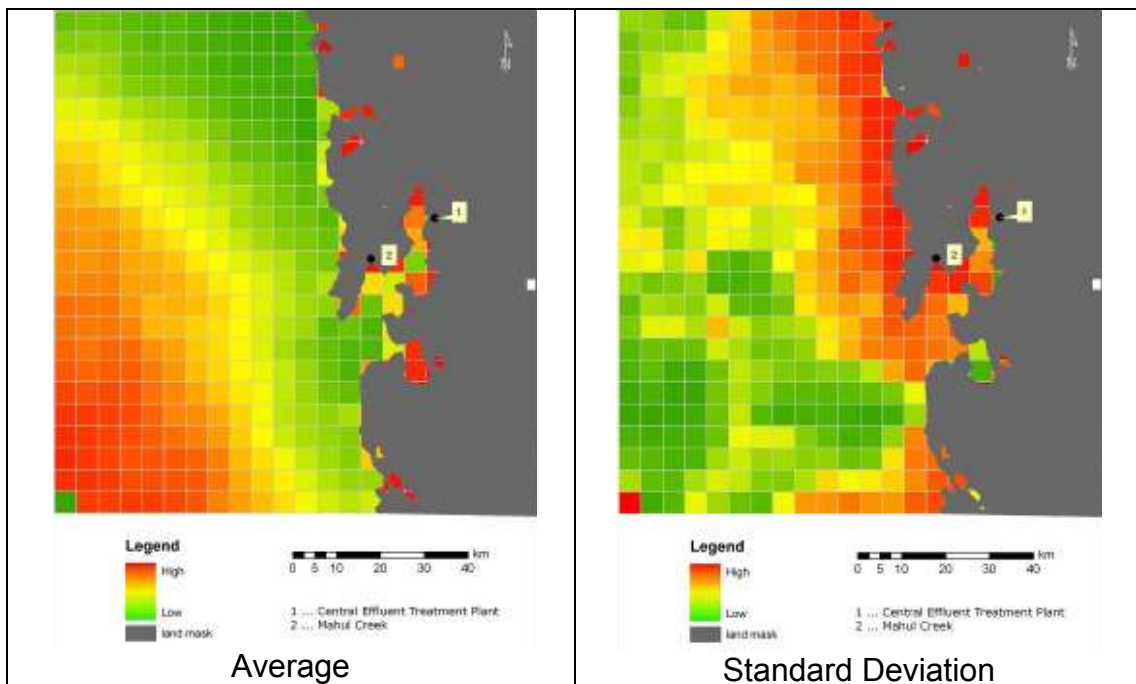
Figure 2: Monthly aggregated average and standard deviation images for December (2004-2010)

Average SST (December)
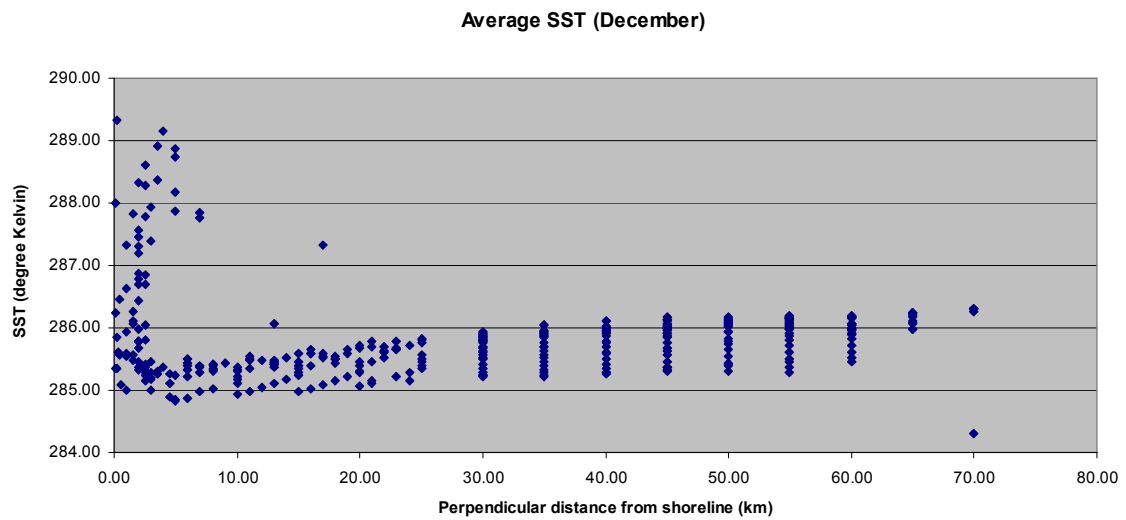
Figure 3: Relationship between average SST and perpendicular distance from shoreline (Note: the SST variation is maximum in coastal areas)

The variation in SST changes is found to decrease as distance increases from shoreline, that is, highest possible variation in SST is found near the coast. Away from the coastline the waters are pretty stable seasonally in terms of SST. The following two graphs demonstrate this aspect very well. Aggregated average SST for the month of December was found to be varying mostly near to the coastline within 5km perpendicular distance, as emphasized in Figure 4.

Standard Deviation in SST (December)
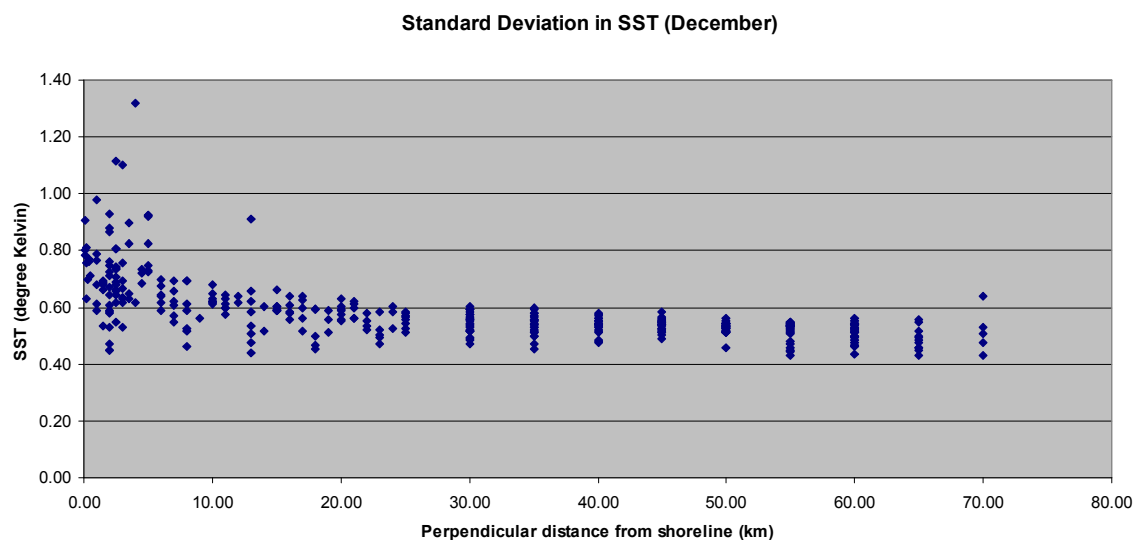
Figure 4: Relationship between SST standard deviation and perpendicular distance from shoreline

During the month of January, for most of the years, the warm eddy like structure just away from the coastline remained in place and intensified. Because of this meso-scale structure, the coastal waters were perturbed and have shown some random behaviour. However, it can be still seen that the maximum variation is still limited to the first 10 km stretch from the coastline.
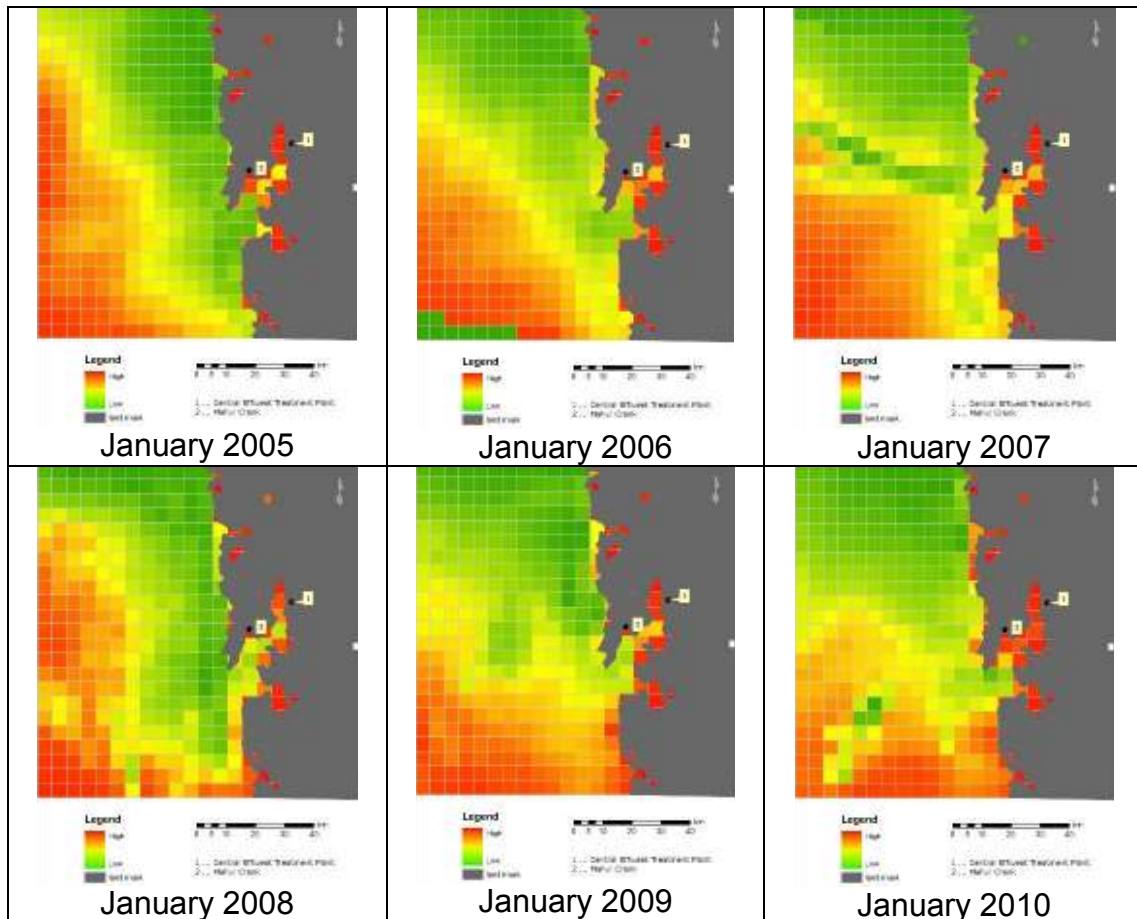

**Figure 5: Monthly average SST for the month of January (2005-2010)**
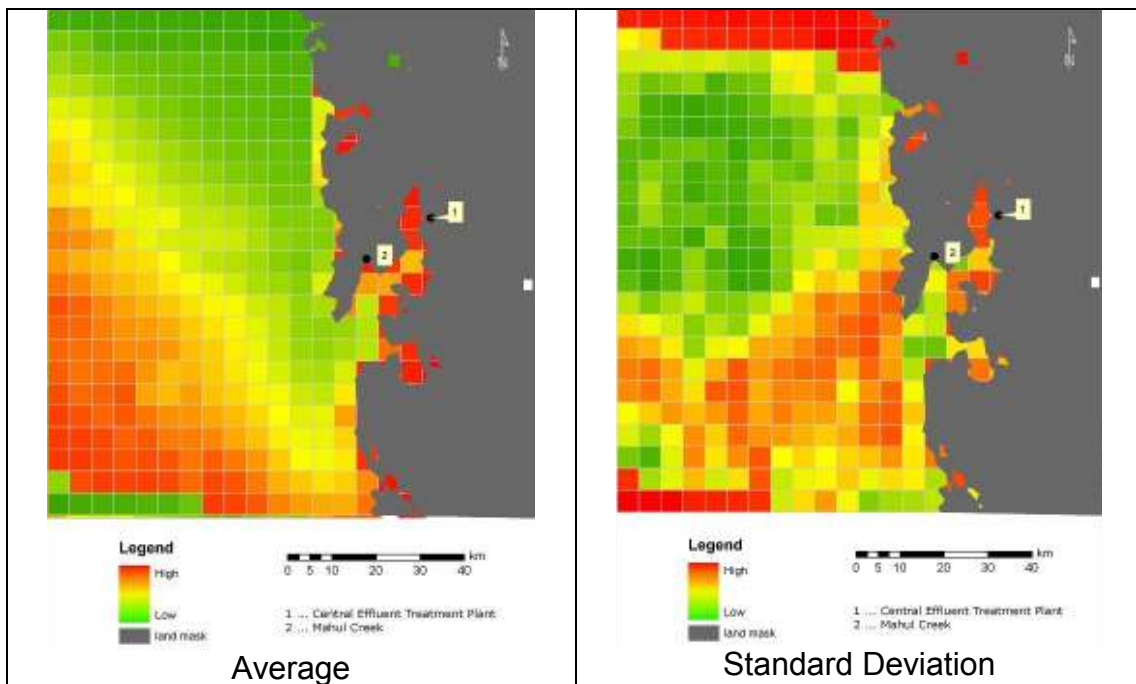
Figure 6: Monthly aggregated average and standard deviation images for January (2005-2010)
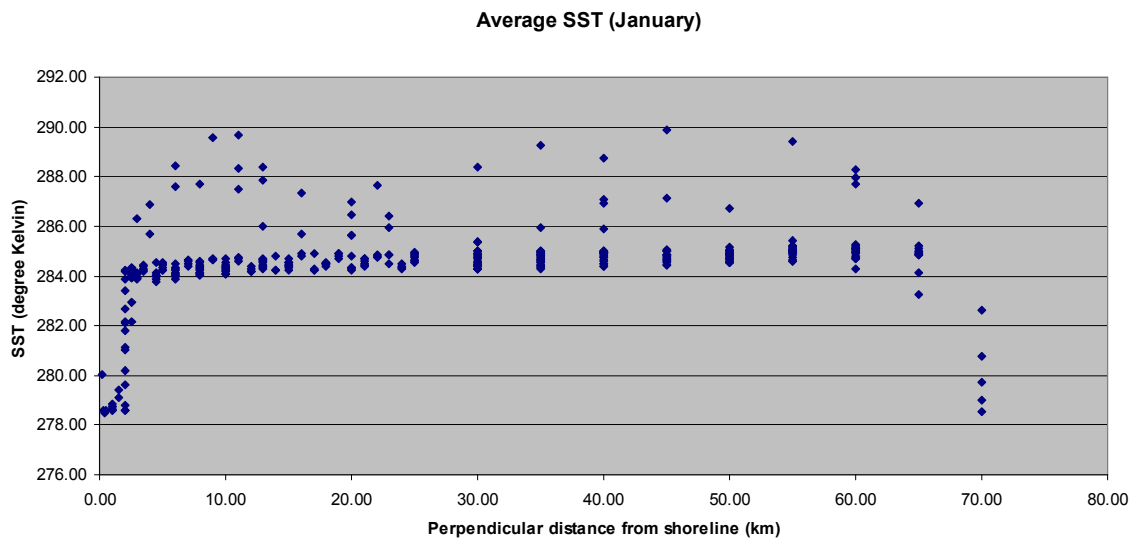
Figure 7: Relationship between Average SST and perpendicular distance from shoreline

**Standard Deviation in SST (January)**
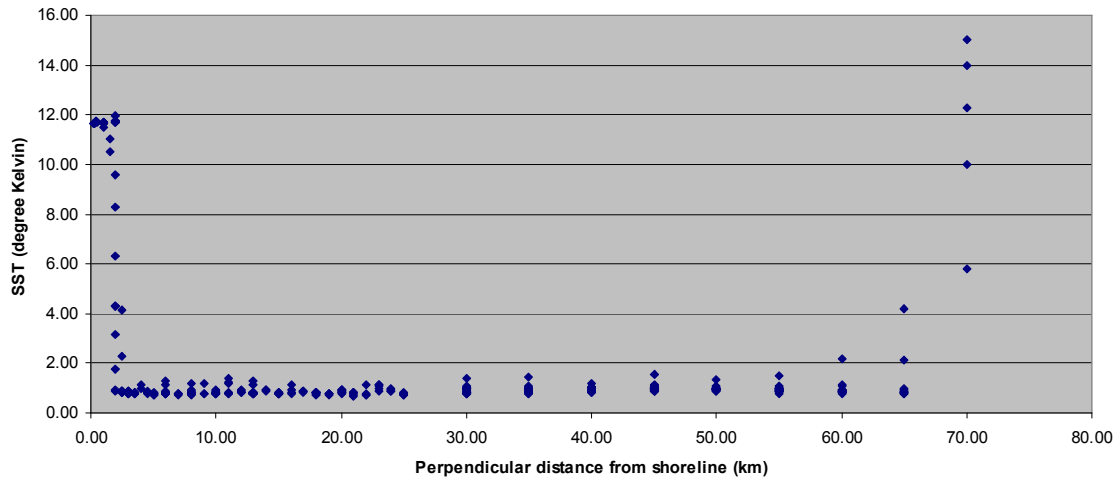
Figure 8: Relationship between SST standard deviation and perpendicular distance from shoreline

Since there were fewer data sets in the months of December and January for certain years, December and January data were also clumped together and trends were generated separately for the clumped data as well. These data comprise mainly information from end of December and entire month of January, the coldest season of the study area. The results are shown below.


December-January 2004 | December-January 2005 | December-January 2006

December-January 2007 | December-January 2008 | December-January 2009
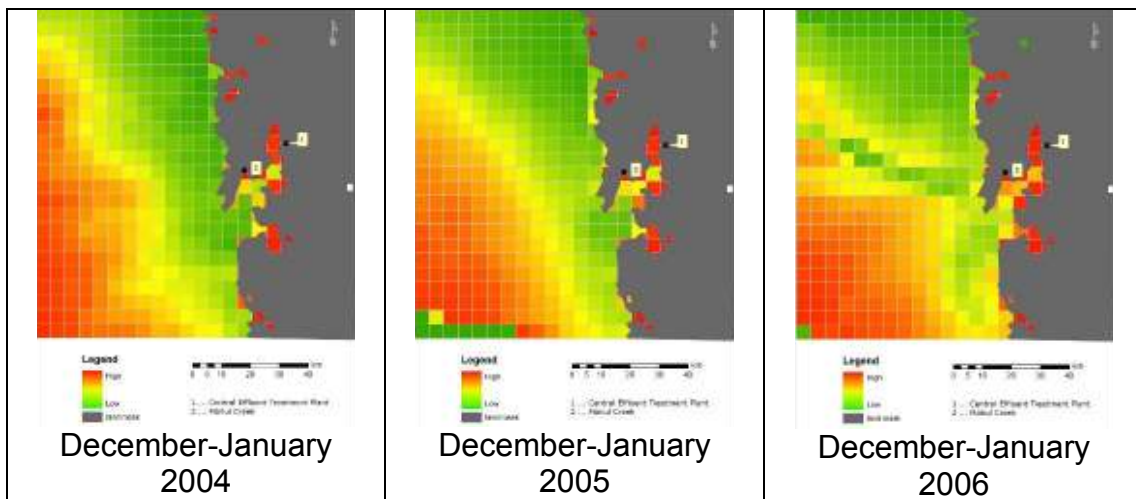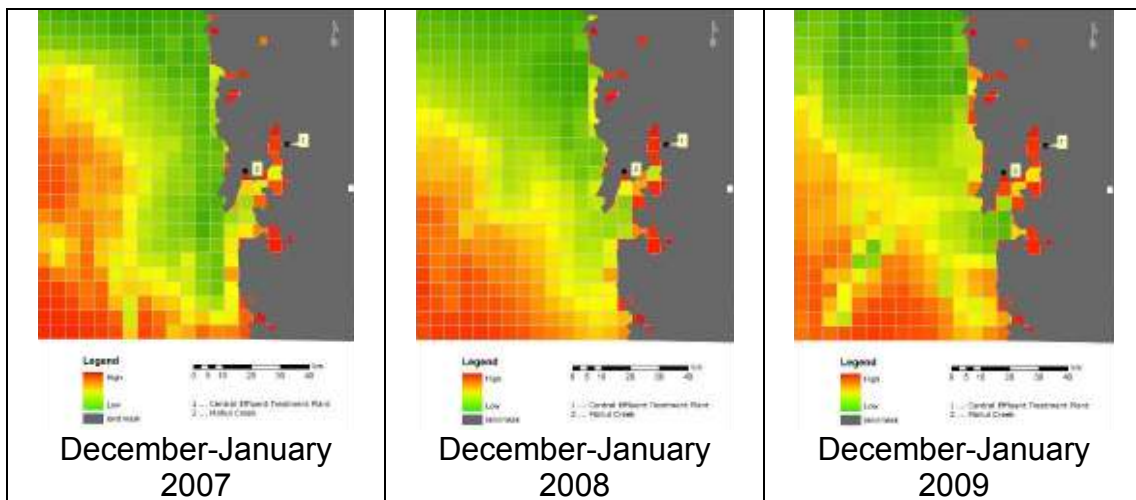
Figure 9: Monthly average SST for the month of December-January (2004-2010)

Average | Standard Deviation
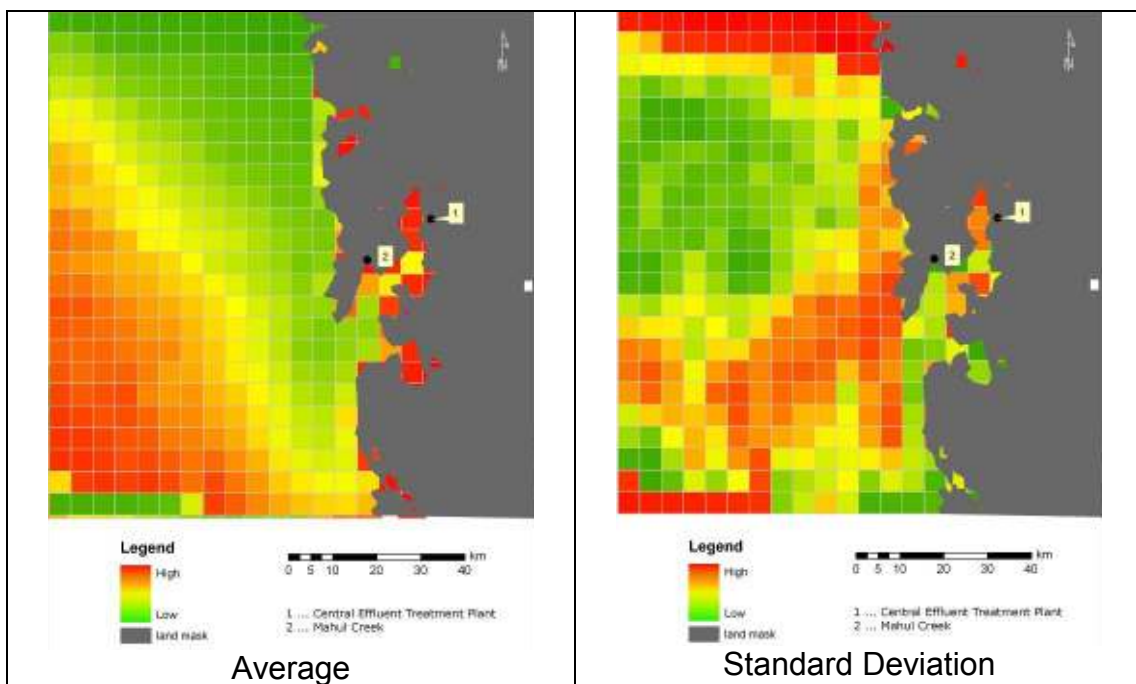
Figure 10: Monthly aggregated average and standard deviation images for Dec-Jan (2004-2010)

The clumped images reiterate the warm water structure offshore, while showing maximum variability in SST near to the coast. Ignoring the possible irregularity and noise in the satellite data, the trends, very steadily, show a temperature disturbance in the area which possibly indicates anthropogenic source/s of warm water in the area.
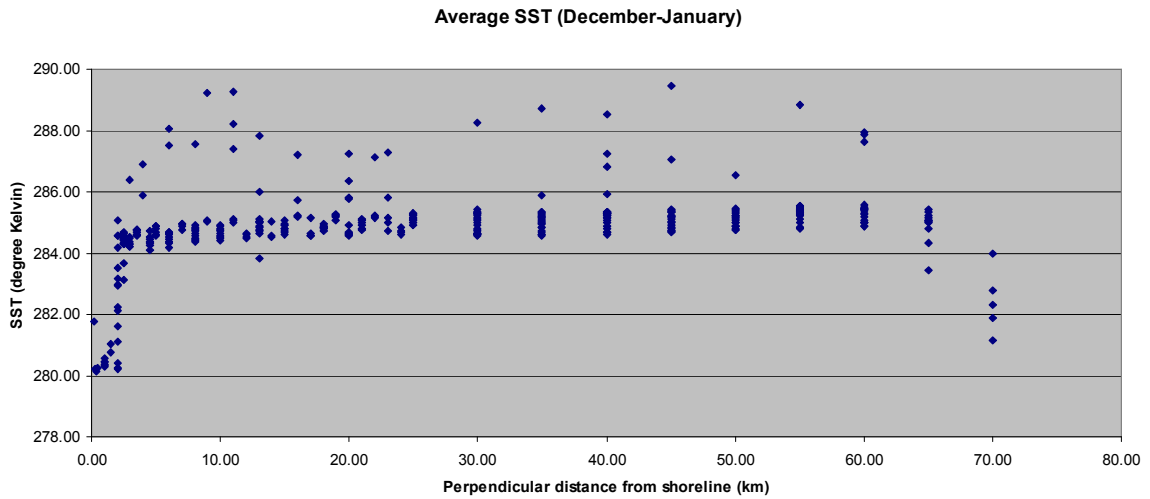
Figure 11: Relationship between average SST and perpendicular distance from shoreline

**Standard Deviation in SST (December-January)**
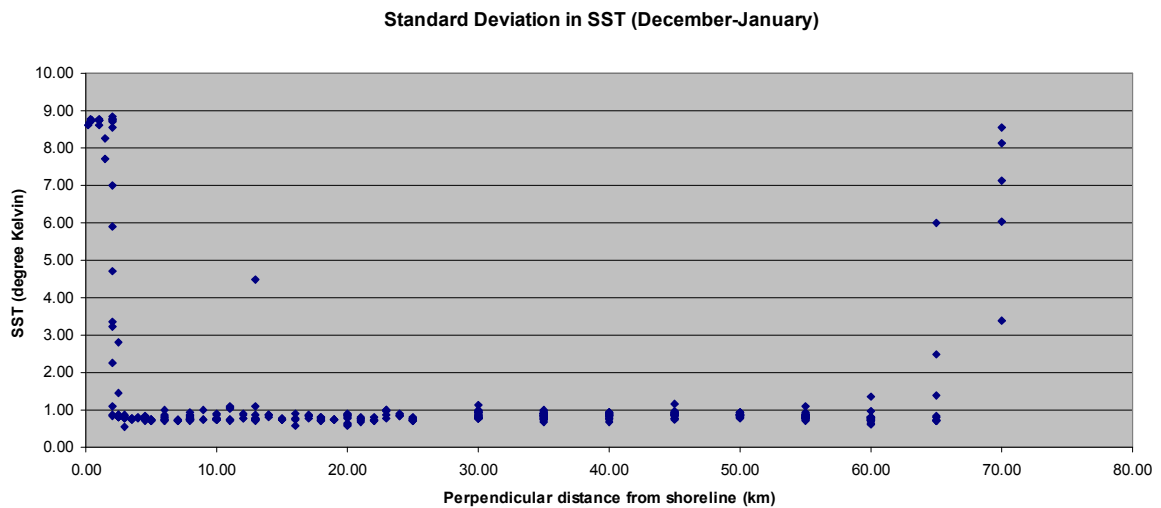
Figure12: Relation between SST standard deviation and perpendicular distance from shoreline

For the month of March, the open ocean scenario changed with the onset of summer. As seen from March images, the coastal waters are throughout warmer than the pelagic ocean zone. The warm water eddy-like structure was found to dissipate during this time as the coastal waters grow warmer. The coastal zone also shows the maximum variation within the study area (standard deviation in SST, figure 16).
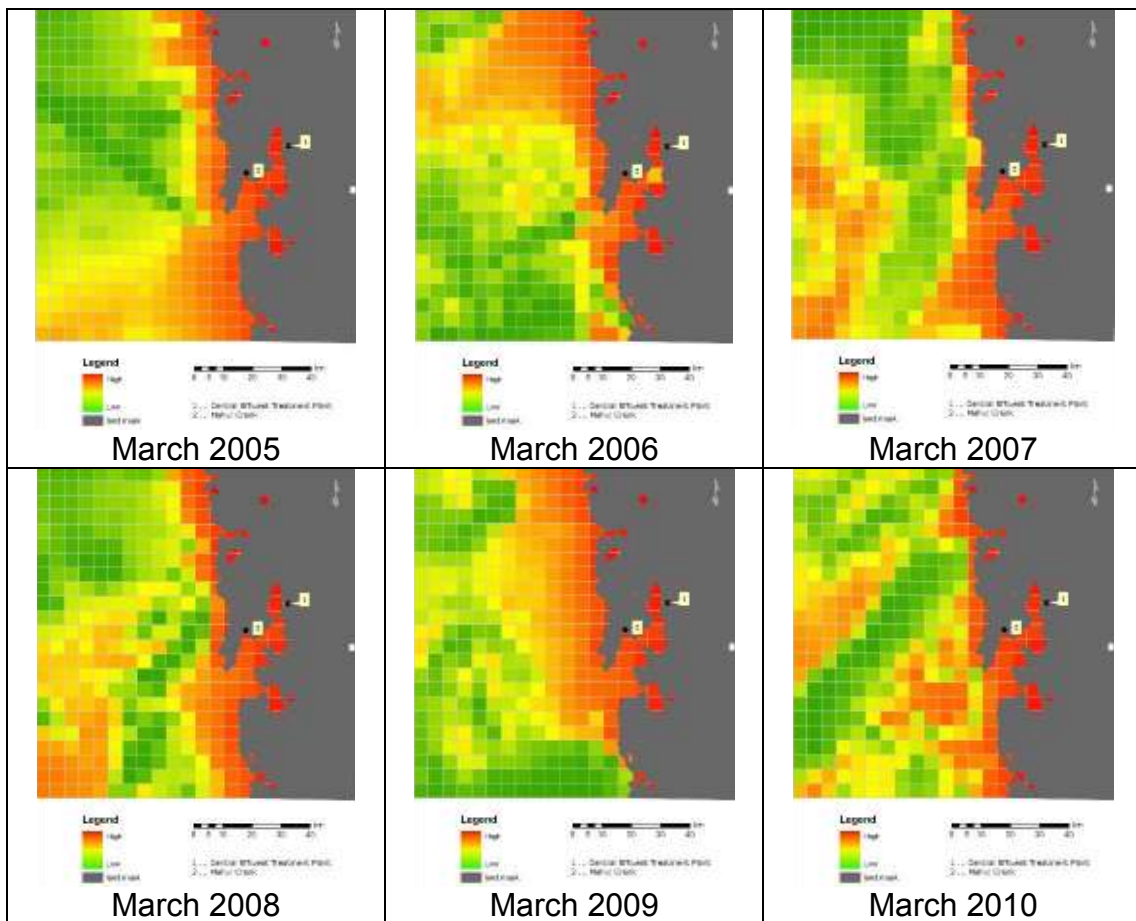
**Figure 13: Monthly average SST for the month of March (2005-2010)**
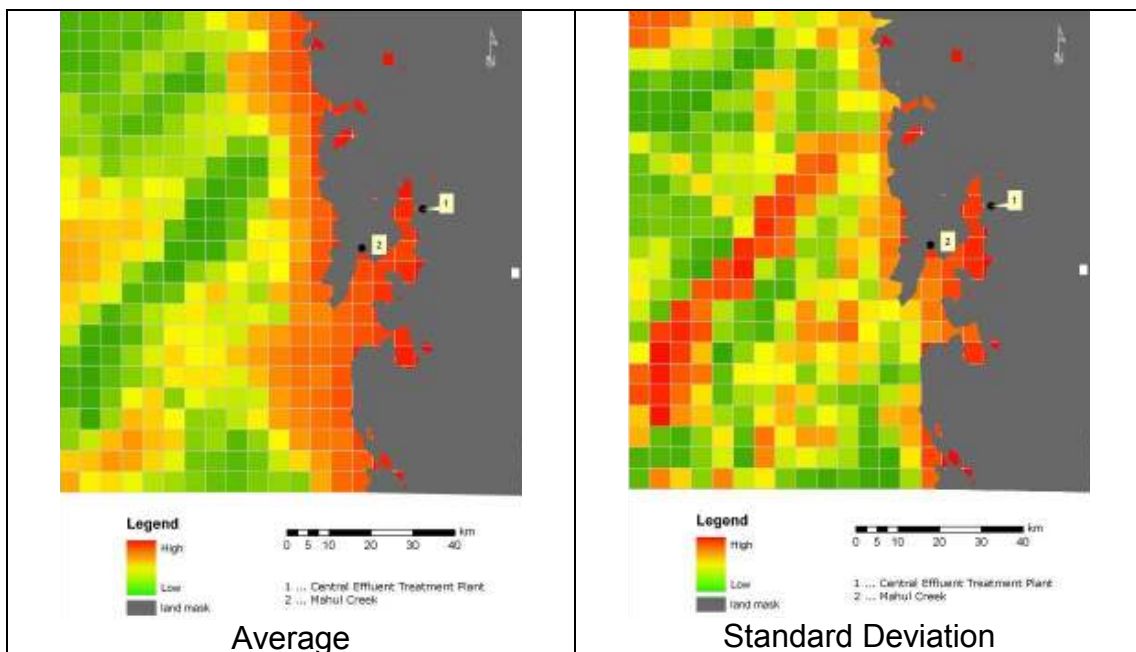
Figure 14: Monthly aggregated average and standard deviation images for March (2005-2010)

Average SST (March)
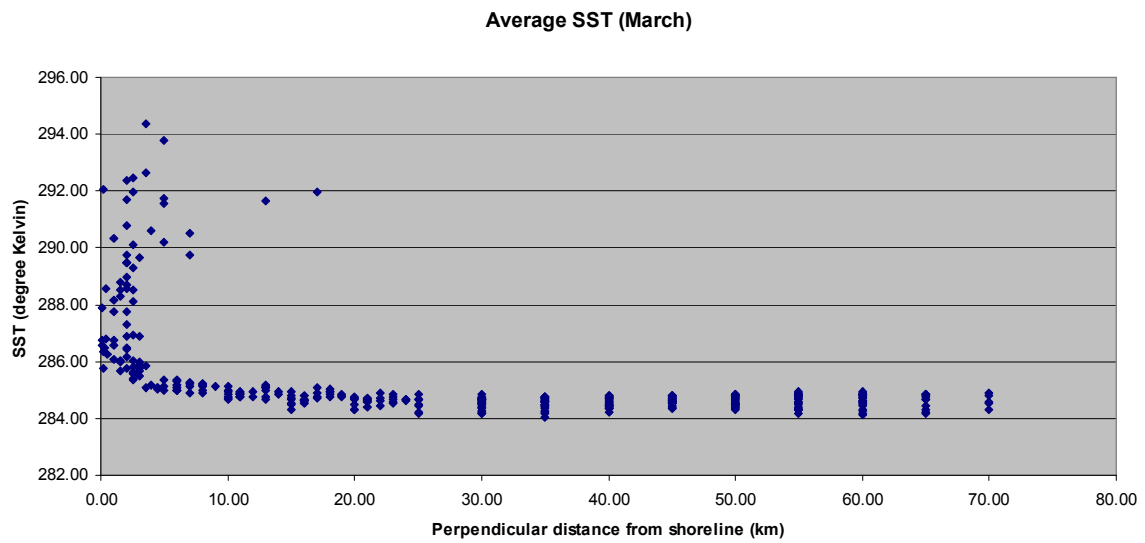
Figure 15: Relationship between average SST and perpendicular distance from shoreline

Standard Deviation in SST (March)
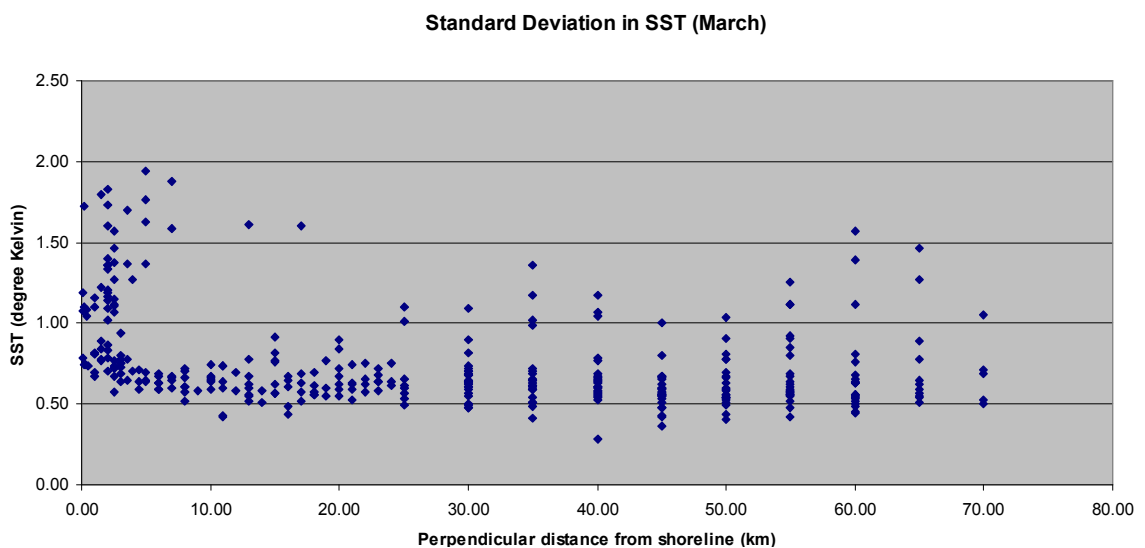
Figure 16: Relation between SST standard deviation and perpendicular distance from shoreline

In general, as found from the above standard deviation curves for all 3 months, SST deviations are highest in all the cases nearest to the shoreline. Since this study is particularly focused on Vashi and Mahul Creeks, SST variation trend has been generated for these two areas. The graphical representation is given below in the Figures 17 and 18.

December

January
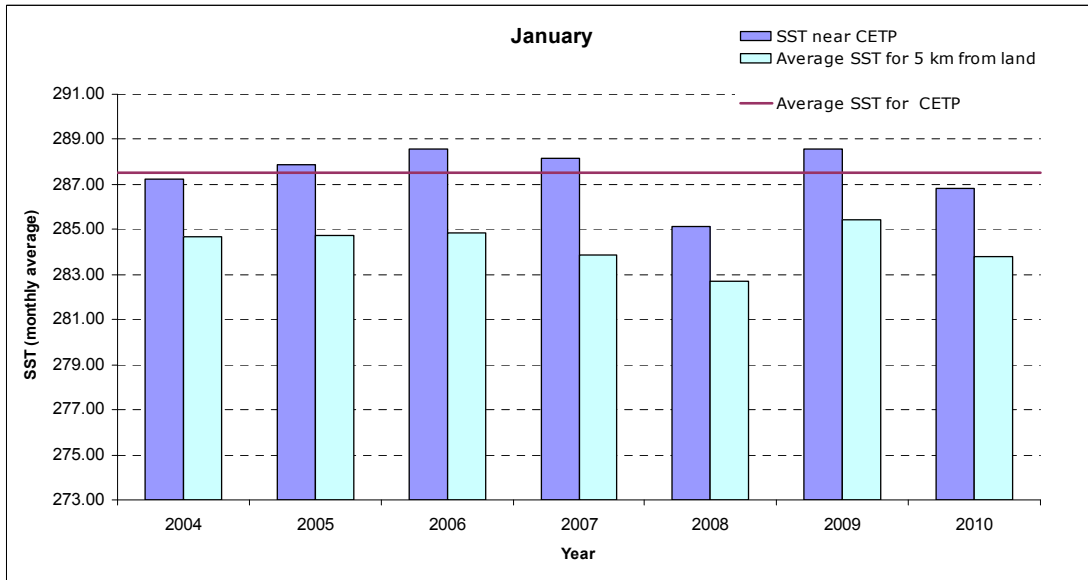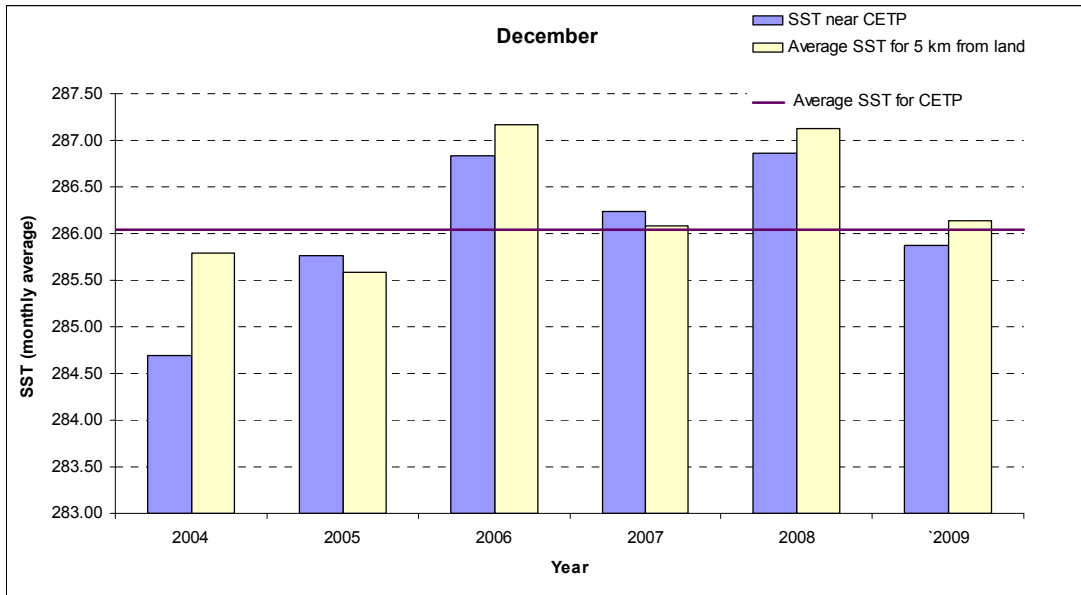
Note: The uniform high SST in 2006 matches the El-Nino event reported during this year
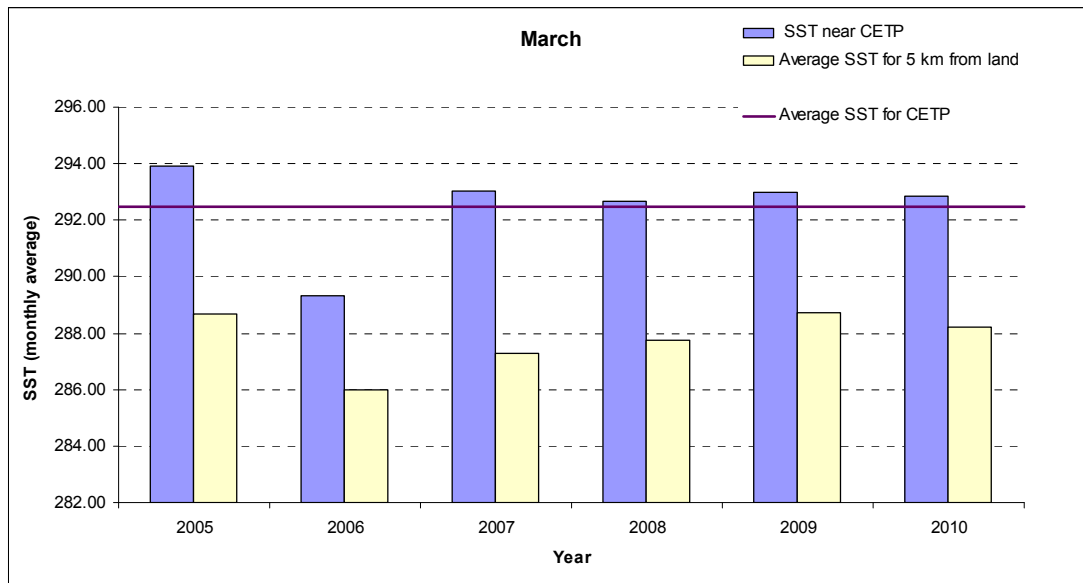
Figure 17: Comparative SST trend near Vashi (CETP) area with respect to the average SST 5 km away from shoreline for the study period. Aggregated average SST in degree Kelvin has been shown as a linear trend-line.

The anthropogenic nature of the warmer water in this area is very much obvious from these figures. For the month of December, the waters near Vashi Creek are found to be lesser than the waters 5 km off the coast. However, this may happen because of the warm water formation which was mentioned earlier. This warm water mass was forming every year very close to the creek mouth, thus masking the effect of any landward source of heat. However, as this warm water dissipated, from the colder month of January till the onset of summer in March, all through the study period of 2004-2010, the water of the Vashi creek remained warmer than the waters off a 5km buffer zone from shoreline. In the graphs above, the difference in SST of these two areas (random points near CETP location and random points 5 km away from shoreline) has been shown for each year. The average trend given for the area is the aggregated average for all the years. Similar trends have been generated for the Mahul Creek region.
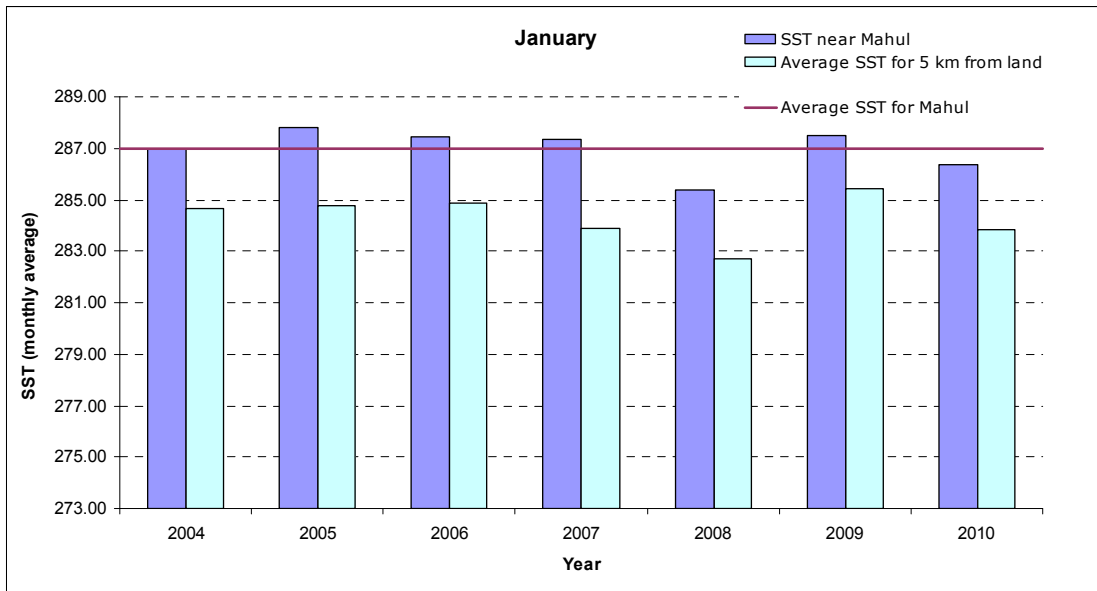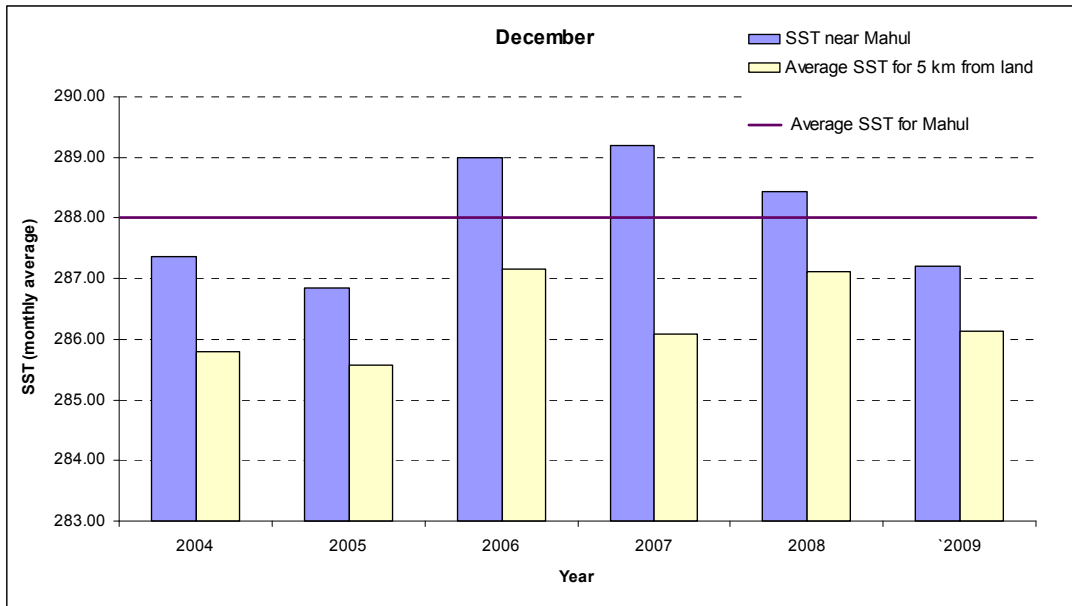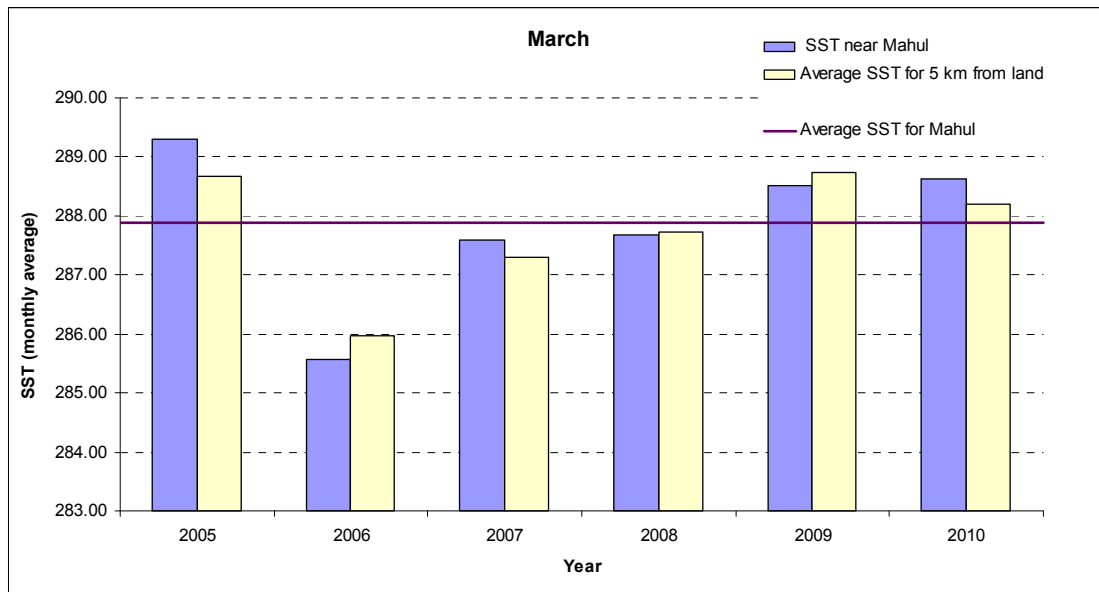
Figure 18: Comparative SST trend near Mahul Creek mouth with respect to the average SST 5 km away from shoreline for the study period. Aggregated average SST in degree Kelvin has been shown as a linear trend-line.

Mahul Creek, situated in a bay area which has lesser impact from the change in pelagic water-mass, consistently shows higher temperature than the 5 km off the coastline buffer. The surface temperature of these waters is consistently warmer than the offshore areas. Apart from this, a significant drop in overall temperature can be seen in the year 2006, very prominent in this area. This decrease is seen to be increasing from December, 2006 to March 2006. Coincidentally, the year 2006 happened to be a La Nina year (NASA, 2006). Because of this atmosphere-ocean coupled phenomenon, temperature in the Indian Ocean is known to go down by several degrees, which happens in a 3-5 year cycle. The effect is seen in the Vashi CETP area also during the month of March, when the climatologic phenomenon was in full sway.

Conclusions

There have been some important findings in this project, varying in scope and application. These can be grouped into three major parts. To address them properly, the observations can be put in relation to the objectives of the project. However, some general findings can be stated as follows:

85

- The 5 km buffer from land that has been taken in this study as reference to estimate the thermal anomaly in the near-shore waters has been derived from the over-all standard deviation pattern of SST in the study area. After the 5 km stretch, the waters are found to be quite stable in terms of monthly/ seasonal variability.

- During the months of January and December, warm water masses are seen to form consistently in the deep sea (~ 40 km away from land), having higher temperatures in all the years. This may be a part of some meso-scale eddy feature, or warm current offshoot parallel to the shore. This phenomenon could be related to the coastal winter-time upwelling and should be investigated further thorough temporal studies.

- Area near Vikhroli also shows high thermal anomaly with respect to the 5 km buffer specified before. This area is known to harbour a good growth of mangroves, and high temperature in the coastal waters could harm the vulnerable eco-system there. However, a detailed study of this area was not in the scope of this project. It is suggested that a detailed and in-depth investigation of this anomaly should be carried out. Similar SST anomaly is found throughout the study period near the Ulhas River mouth and upstream locations.

Further, observations according to the stated objectives are given below.

Objective 1) Monitoring & study of the sewage plumes near Mahul Creek area on the East Coast of Mumbai using visible and TIR range of Satellite Data.

Several sets of satellite data have been collected, pre-processed and analyzed to attain this objective. Results have shown consistently that the Mahul Creek area is thermally active, in terms of anomalous higher temperature than the surrounding sea water, with respect to a 5 km buffer zone off the shoreline. Mahul Creek mouth being situated in a bay area, is far from the influences of any deep sea warm water phenomenon and has shown consistent higher temperatures than the surrounding waters, an anomaly that can not be explained by anything but anthropogenic interference. In the month of March, Mahul area has shown quite high SST anomaly throughout the entire study period.

Objective 2) Monitoring the industrial outfall at Vashi Creek (CETP).

The Vashi Creek has also shown thermal anomalies similar to the Mahul Creek area, revealing possible human interference. This area has consistently shown higher SST than the 5 km buffer in January and March, though showing an anomaly in the month of December. In December, the surrounding water mass is reveals higher SST than the Creek outflow. However, in view of the warm water mass formation in the deep sea, the temperature is quite high during December and closer to the creek mouth; hence, a possibility of mixing during high tides can not be ruled out. It is proposed that further investigations should be carried out in this zone with detailed temporal studies to understand the coupled behavior of this thermally active area.

Further, it is found that the over-all temperature has been increasing in the coastal waters within the short span of 6 years (2004-2010). Apart from 2006, which was declared from various climatologic agencies abroad to be a La Nina year, the SST has increased from the year 2004 to 2010.

It is found that there is a need to modify the available global SST algorithm or generate a local algorithm to cater to the need of this specific area for different seasons. The current global algorithm which is widely used across the globe was mainly designed for temperate seas and fails to accurately estimate the true SST conditions of the study area. The output from this algorithm has consistently under-estimated the SST by 6-7 degree Kelvin, and as such, the algorithm should be modified according to local needs.

Objective 3) Study of the plume propagation pattern and the factors influencing the pollutant flow.

This objective was mainly to address the marine sewage outfall plumes at Bandra and Worli, and work is still going on in this area. According to the preliminary results, the chlorophyll-a algorithm known as Chlor_a_2 was found to be giving the most consistent results. On the other hand, MODIS data has been used for post-installation plume mapping with the help of satellite synchronous field data. The chlorophyll-a algorithm found to be best-suited for the area was Chlor_a_3. Further investigations are going on in terms of post-monsoon season mapping and monitoring of the outfall plumes.

To summarize, this study has been effective as a pioneering effort towards monitoring the coastal waters off Mumbai through satellite imagery and has proved the efficacy of remote sensing tools in such conditions. Keeping in view the optical, bio-physical and climatological variability of this area, further detailed studies are recommended. A major hurdle faced during this project was the availability and collection of sea-truth data from primary and secondary sources. The authors suggest that to address this problem, all relevant and active agencies working in this area should come together and share their data through a well-logged, documented and quality-controlled portal accessible to every interested organization. Collective efforts would not only minimize the replication of efforts, but also help to generate detailed, long-time ecological trends for the area which is severely lacking at present.

Annexure II: Scientific publications arising from the MME Project:

1) IDENTIFICATION OF BEST-SUITED CHLOROPHYLL ESTIMATION MODEL IN MUMBAI COASTAL WATERS DURING PRE-MONSOON SEASON

M. Bhattacharya, Y. Y.Y. Agarwadkar, S. Azmi, M. Apte, A. B. Inamdar*

CMR Lab, Centre of Studies in Resources Engineering, IIT Bombay, Mumbai, India, 400076 - (m_bhattacharya, agarwadkar, mugdhaapte, samiazmi, abi)@ iitb.ac.in

ABSTRACT:

This study attempts to find the best suited *chlorophyll* estimation model for the coastal waters off Mumbai, situated on the western coast of India. These waters are a part of the *Arabian Sea*, highly productive with optical characteristics of case-2 type. There are several diffuse and point sources of domestic and industrial sewage effluent outlets along the coast, apart from two major marine outfalls located around 3.5 km into the sea. The study attempts to use *MODIS* data for the pre-monsoon season and test several exiting *chlorophyll_*a estimation models for their site and season suitability for this area, with the help of synchronous sea-cruise data. The study area has been divided into various subgroups of ambient water quality difference, namely, highly sediment-laden water (outfall zones), high chlorophyll concentration zone and mixed water patches (high sediment + high chlorophyll concentration). The models are tested for each of these regions with the help of in-situ chlorophyll_a data, and their behaviour is analyzed through *regression* based analyses.

2) COASTAL WATER QUALITY ANALYSIS OF MUMBAI COAST USING PRE-MONSOON OCM IMAGES WITH SATELLITE-SYNCHRONOUS FIELD OBSERVATIONS

M. Bhattacharya*, Y.Y.Y. Agarwadkar, S. Azmi, M. Apte, A. B. Inamdar

Coastal & Marine Research Lab, CSRE, IIT Bombay, Mumbai, 400076, India

Abstract

This study aims to estimate water quality parameters such as concentrations of Chlorophyll-a and Suspended Particulate Matter (referred to further as Chl_a, and SPM) from pre-monsoon Ocean Colour Monitor (OCM) images of the Case-II type coastal waters of Mumbai for the year 2010. Mumbai, one of the largest and fastest growing coastal metropolises of the world, faces a dire sewage treatment and discharge problem. Two marine sewage outfall plumes located around 3.5 km from the coastline, commissioned in the years 2001 and 2003 are the major focus of the study for their impact on the ambient ecosystem and utility assessment. The OCM sensor is very effectively used for ocean colour interpretation, and is suitable for large scale oceanic colour and temperature analysis; however, the sensor is limited by the medium range spatial resolution (360m VNIR) for coastal areas and gives a lot of mixed pixels. However, the sensor is found to be just suitable for the study area in terms of spatial resolution. Radiance images were calculated from image DN values using gain and offset data after an initial atmospheric correction procedure. Remote sensing reflectance was calculated from band Radiance. Chl_a was estimated using OC-2, OC-4, Chlor_a_2 and Chlor_a_3 algorithms and output was correlated with satellite synchronous sea-truth data by regression analysis. SPM conc. was estimated by using Tassan (1994) algorithm. Results showed significant correlations between Chlor_a_2 and Chlor_a_3 algorithms for modeled Chl_a with in-situ measurements of chlorophyll for the study area, whereas OC-2 gave good performance in the nearing oceanic waters under cloud-free condition. Similarly, significant correlations were found for SPM. However, all the Chl_a algorithms tended to slightly over-estimate the chlorophyll conc.; hence Yellow Substances (YS) were modeled using Tassan's algorithm (1994). The study revealed that high SPM concentration nearing the marine outfall zone was interfering with the chl_a estimation. Hence, the co-variance of Chl_a and SPm were calculated for the modelled parameters. Though YS values could not be validated as field data was lacking, the study showed that there was also a significant relationship between Chl_a and YS in the offshore waters. To understand the complex nature of these relationships, further studies are recommended in the study area to model the ocean colour parameters with satellite synchronous data for the post monsoon season.

KEYWORDS: **OCEAN COLOUR MONITOR (OCM), CHLOROPHYLL_A, SPM, MUMBAI COAST, ARABIAN SEA**

Annexure III: Field & Lab Photographs

Phytoplankton and Zooplankton nets deployed on the trawler

On-board measurement of dissolved oxygen

Sea-gulls at the Bandra Outfall location

Water-sampler being deployed during cruise

Wet-lab procedures in the laboratory

Filtration assembly in the laboratory for Chlorophyll, CDOM and TSS estimation

Annexure-IV: New Lab Set-Up

Lab Set up			
Filtering Assembly (with pumping facility)	3 Sets	1 litre	TSS, Chlorophyll, TDS
Titration assembly	4 sets		DO, PP
Vaporising set up	1 set		TDS
Cold storage facility	1	- 2 to 5°C	Chlorophyll, TDS, TSS, NO$_3$, PO$_4$
Reduction column	3 set		NO^3
Light chamber	1		PP
Dark Chamber	1		PP
Reagents	List provided separately		
Distillation Assembly	1	6 litre per hour	
Electronic Weighing balance		0 - 120 gm	TDS, Reagents Preparation
Sampling			
Niskin Water Sampler	2	2.5 litre	Water samples Collection
Benthic soil grab	1	0.001 m3	Collection of Benthic Soil
Secchi disk	1		Euphotic Depth
Spectro radiometer	1	350 to 1050 nm	Visible & NIR reflectance readings
GPS	1	Handheld	Location of Sampling
Thermometer	2	-10 to 110°C	Temperature
Ice Boxes	2	78 litre	Chlorophyll, TDS, TSS, NO$_3$, PO$_4$
Light & Dark Bottles	60 each	175 ml	DO, PP